INFORMATION TO USERS

This manuscript has been reproduced from the microfilm master. UMI films the text directly from the original or copy submitted. Thus, some thesis and dissertation copies are in typewriter face, while others may be from any type of computer printer.

The quality of this reproduction is dependent upon the quality of the copy submitted. Broken or indistinct print, colored or poor quality illustrations and photographs, print bleedthrough, substandard margins, and improper alignment can adversely affect reproduction.

In the unlikely event that the author did not send UMI a complete manuscript and there are missing pages, these will be noted. Also, if unauthorized copyright material had to be removed, a note will indicate the deletion.

Oversize materials (e.g., maps, drawings, charts) are reproduced by sectioning the original, beginning at the upper left-hand corner and continuing from left to right in equal sections with small overlaps. Each original is also photographed in one exposure and is included in reduced form at the back of the book.

Photographs included in the original manuscript have been reproduced xerographically in this copy. Higher quality 6" x 9" black and white photographic prints are available for any photographs or illustrations appearing in this copy for an additional charge. Contact UMI directly to order.

UMI

A Bell & Howell Information Company
300 North Zeeb Road, Ann Arbor MI 48106-1346 USA
313/761-4700 800/521-0600

EQUILIBRIUM AND DYNAMIC SURFACE PROPERTIES OF AQUEOUS SOLUTIONS OF GEMINI SURFACTANTS; SUPERSPREADING OF SILICONE SURFACTANT SOLUTIONS

by

LI DONG SONG

A dissertation submitted to the Graduate Faculty in Chemistry in partial fulfillment of the requirements for the degree of Doctor of Philosophy. The City University of New York.

1996

This manuscript has been read and accepted for the Graduate Faculty in Chemistry in satisfaction of the dissertation requirement of the degree of Doctor of Philosophy.

2/22/96
Date

Chair of Examining committee

3/6/96
Date

Executive Officer

Supervisory Committee

Supervisory Committee

Supervisory Committee

The City University of New York

ABSTRACT

EQUILIBRIUM AND DYNAMIC SURFACE PROPERTIES OF AQUEOUS SOLUTIONS OF GEMINI SURFACTANTS; SUPERSPREADING OF SILICONE SURFACTANT SOLUTIONS

by

Li Dong Song

Advisor: Professor Milton J. Rosen

Two series of cationic gemini surfactants with rigid and flexible spacer, respectively, have been synthesized.

Some abnormal phenomena of the equilibrium surface tension and related surface properties have been explained by the premicellar aggregation of aqueous solutions of these gemini surfactants. The interactions of the synthesized cationic gemini surfactants with conventional anionic and nonionic surfactants in monolayer formation and micelle formation have been studied.

The dynamic surface tension of solutions of the synthesized cationic gemini surfactants and calculation of the dynamic surface tension parameters showed that the spacers affect the dynamic surface properties.

There is no correlation between superspreading of solutions of trisiloxane surfactants and Draves skein wetting test. The synergism of superspreading of trisiloxane surfactant with some additives on Parafilm surface has no relationship with the dynamic surface tension.

DEDICATION

To my lovely wife, Hai-Lan, for her love, support, and encouragement throughout my studies.

ACKNOWLEDGEMENTS

The author would like to express his sincere thanks:

to Professor Milton J. Rosen for his intellectual guidance and continual encouragement throughout this study;

to Professor Gary Mennitt, Professor David Locke, and Dr. Manilal Dahanayake, the members of my examining and advisory committee, for their advice and precious time;

to Professor Richard Pizer, the Executive Officer of the Department of Chemistry of The Graduate Center of CUNY for his advice and encouragement;

to the personnel of the Glass-blowing Shop, Machine Shop, Electronic Shop and Stock Rooms for their cooperation.

Contents

List of Tables

List of Charts

List of Figures

Abbreviations for Surfactants Stuydied

No.	Surfactant	Abbreviation
1	(p-Phenylene dimethylene) bis(alkyl-N,N-dimethyl ammonium dibromide)	$(C_nN)_2Ar$
2	1,3-bis(alkyl-N,N-dimethyl ammonium)-propanol dichlorides	$(C_nN)_2OH$
3	$C_{12}H_{25}(OC_2H_4)_7OH$	$C_{12}EO_7$
4	$C_{12}H_{25}(OC_2H_4)_8OH$	$C_{12}EO_8$
5	N,N-Dimethyl-1-tetradecane amine oxide	$C_{14}N(CH_3)_2O$
6	Double- or triple-chain surfactants with two sulfonate groups	$C_nC_nC_n$
7	$C_{12}H_{25}SO_4Na$	SDS
8	$C_{12}H_{25}(OC_2H_4)_2SO_4Na$	$C_{12}EO_2S$
9	Methoxy trisiloxane with eight oxyethylene units	L-77
10	Hydroxy trisiloxane with eight oxyethylene units	L-77OH
11	Linear hydroxy trisiloxane with eight oxyethylene units	L-77OH linear

12	Sodium di(2-ethylhexyl) sulfosuccinate	OT
13	Sodium di(hexyl) sulfosuccinate	MA
14	Sodium di(cyclohexyl) sulfosuccinate	A-196
15	Sodium di(amyl) sulfosuccinate	Ay
16	N-2-ethylhexyl-pyrrolidone	C2,6P
17	N-octyl-pyrrolidone	C8P
18	N-decyl-pyrrolidone	C10P
19	N-butyl-pyrrolidone	C4P
20	N-cyclohexyl-pyrrolidone	CHP
21	t-$C_{12}H_{25}S(OC_2H_4)_8OH$	SK

I. EQUILIBRIUM AND DYNAMIC SURFACE PROPERTIES OF AQUEOUS SOLUTIONS OF GEMINI SURFACTANTS

A. Introduction

Surfactants (surface-active agents) play a very important role in many industrial processes, e.g., dyeing of textiles, petroleum production, paper manufacture. In addition, they are important ingredients in many products, such as detergents, cosmetics, medicine, and food. Researchers are always trying to find new applications of surfactants or to develop new types of surfactants to meet the requirements of a wide variety of applications.

A.1. Equilibrium Properties

A surfactant is a compound that, when present at low concentration in a system, has the property of adsorbing onto the surfaces or interfaces of the system and altering to a marked degree surface or interfacial free energies of those surfaces (1a). For aqueous systems, a surfactant consists of a hydrophobic chain and a hydrophilic head group. A balance between the two parts is the cause of surface active properties. If the hydrophobic part of the surfactant is dissolved in the water, the hydrogen bonds between water molecules will be disrupted. In addition, the hydrophobic

group builds structure in the water around it, decreasing the entropy of the system. To prevent the hydrophobic chain from remaining in the aqueous phase, the surfactant molecule either adsorbs at the aqueous solution/air interface with the hydrophobic chain directed towards the air or aggregates to form micelles with the hydrophobic chains directed towards the interior of the micelles. On the other hand, the repulsion between similarly-charged head groups of each surfactant molecule and the loss of freedom are the forces opposing adsorption and micelle formation. Micelles form only when the concentration of the surfactant reaches a certain value called the critical micelle concentration (CMC).

There is increasing concern regarding the environmental impact of currently used chemicals. One method of minimizing this impact is to increase the efficiency and effectiveness of their action, so that less is needed. This decreases raw material, plant effluent, and product environmental impact.

In the case of surfactant utilization, there is a limit to the simple modification of the structure of conventional surfactants consisting of one hydrophobic chain and one hydrophilic head group. Increasing the length of the hydrophobic group increases the surface activity of the molecule (its tendency to adsorb at interfaces or to form micelles). However, if we improve the surface activity by

increasing the length of the alkyl chain, the water solubility will become worse.

In 1988, Okahara and co-workers (2-11) synthesized a new type of surfactant that has two hydrophilic and two or three hydrophobic groups per molecule gemini surfactants. These compounds possess greatly enhanced hydrophilicity because of the presence of the two ionic groups in the molecule, while their surface activity and micelle forming ability are greatly enhanced because of the presence of the two hydrophobic groups in the molecule. Rosen and co-workers (12), working with alkylated diphenylether sulfonate, showed that the dialkylated diphenyl ether disulfonate (gemini surfactant) had greater surface activity and better surface properties than the monoalkylated monosulfonated (conventional surfactant). Because of its greatly enhanced surface activity, this type of compound has great potential for industrial applications, since its environmental impact should be much smaller than that of a conventional surfactant. For a given level of performance, less chemical raw material would be required and less surfactant effluent would have to be treated. In addition, there are a number of interesting fundamental chemical structure/property relationships to determined, e.g., the effect of the gemini structure on molecular interaction with other surfactants, and on micellar aggregation

number and structure.

A.1.1. Previous Work

Okahara and co-workers (3) synthesized gemini surfactants by using the reaction of glycol diglycidyl ethers with long chain alcohols. The structures are shown in Chart I. They found that all these disulfates (series **III**) were readily soluble in water and the Krafft Point (T_{kp}, the temperature at which the solubility is equal to the CMC) of all compounds was below 0 °C. The CMC values were much smaller than those of conventional surfactants. They also observed that the γ_{CMC} value increased with increased bulkiness of the connecting group. The foaming ability and foam stability of these gemini surfactants are as good as those of conventional surfactants. The lime-soap dispersing requirement (about 6) of **III f-j** was greatly improved in comparison with conventional surfactants (for sodium dodecyl sulfate, SDS, this value is 30). The wetting out time (WOT) of **III g** is good (WOT was 9 seconds) but all the other gemini surfactants show poor wetting ability (WOT >50 s). Okahara and co-workers (4) also synthesized the gemini surfactants whose structures are shown in Chart II. They found that compound **3 a**, with the shortest connecting group, shows the lowest γ_{CMC} value

Chart I

Some Gemini Sulfates Synthesized by Okahara and Co-workers (ref.3)

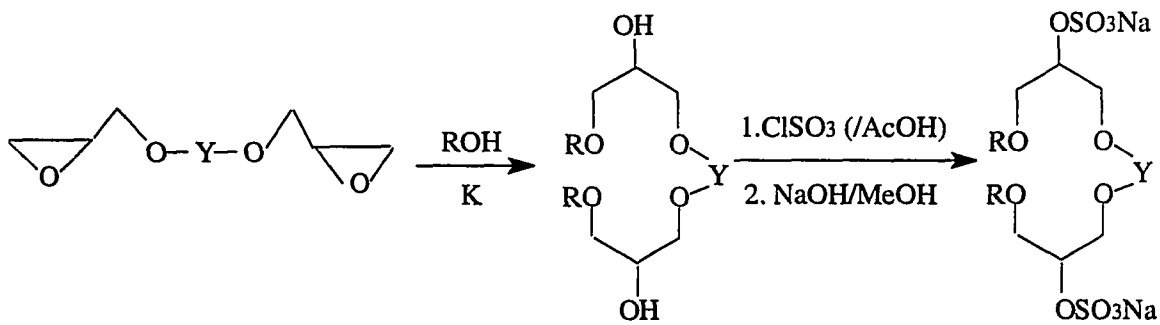

I II III

II, III	R	—Y—	II, III	R	—Y—
a	C_8H_{17}	$-CH_2CH_2-$	f	$C_{10}H_{21}$	$-CH_2CH_2-$
b	"	$-CH_2CH_2CH_2CH_2-$	g	"	$-CH_2CH_2CH_2CH_2-$
c	"	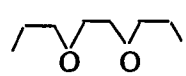	h	"	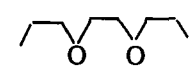
d	"	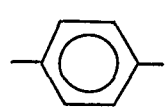	i	"	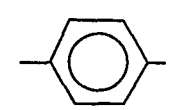
e	"	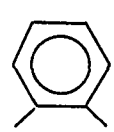	j	"	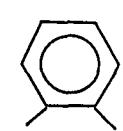

Chart II

Some Gemini Sulfonates Synthesized by Okahara and co-workers (ref.4)

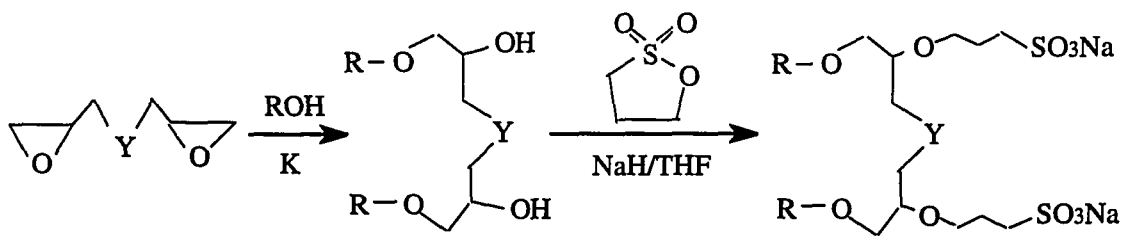

ethylene glycol diglycidyl ether

1 **2** **3**

2,3	R	-Y-	2,3	R	-Y-
a	$C_{10}H_{21}$	—O—	e	$C_{10}H_{21}$	$-O(CH_2)_4O-$
b	"	—O—O—	f	$C_{12}H_{25}$	—O—
c	"	—O—O—O—	g	$C_{14}H_{29}$	—O—
d	"	—O—O—O—O—			

(γ_{CMC}=28.0mN/m). By comparing the foaming ability and foam stability of the compounds, it appears compounds with a short connecting group (compound **3 a**) show good foaming ability and foam stability. Foam volume of compound **3 a** at 0 min and 5 min are 260 and 250 m m^3, respectively (comparing with the values of SDS: 215 and 130 m m^3). All compounds (except **3 g**) show good stability in hard water. Masuyama and co-workers (11) have studied the surface activity of gemini surfactants bearing three anionic head groups and three hydrophobic chains. The structures are shown in Chart III. They found the unusual behavior in which the CMC values in water for a homologous series increased with an increase in the number of carbon atoms in the alkyl chains. The CMC values of the series of compound 4 increased in the order: **4a > 4b > 4 c**. This result is contrary to the usual observation that the CMC for homologs of conventional single chain surfactants decrease with an increase in the number of carbon atoms in the alkyl chain (11).

The effect of the linkage (spacer) between the two hydrophobic groups on the surface activity and micellar properties of geminis has recently been studied by a number of investigators. Devinsky and co-workers (13-17) studied the relationship between properties (such as micellization and solubilization) and structures of many

Chart III

Some Trialkyl Geminis Synthesized by Masuyama and co-workers (ref.11)

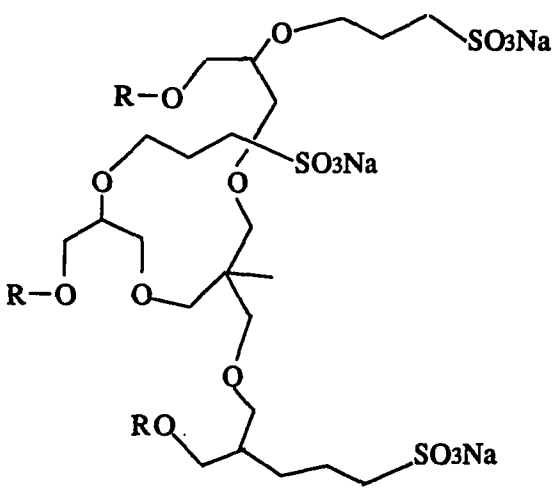

	R
4a	$C_{10}H_{21}$
b	$C_{12}H_{25}$
c	$C_{14}H_{29}$
d	$C_{16}H_{33}$

4a-d

bisquaternary ammonium gemini surfactants. One of their studies (13), using the du Nouy platinum ring method for measuring surface tension, was of the surface properties in water of gemini surfactants of the N,N'-bis(alkyl dimethyl)-3-X-1,5-pentane diammonium dibromides-type $[R(CH_3)_2N^+(CH_2)_2]_2X\cdot 2Br^-$, where X = CH_2, NCH_3, O, or S, and R = 6-18 carbon atoms. The substitution of X = CH_2 by the other atoms or groups was found not to affect the CMC values significantly. They attributed the deviations of some hexadecyl derivatives from linearity in the plot of log CMC vs. number of alkyl carbons in the chain to the experimental problems involved in the measuring of the surface tension of aqueous solution at very low concentrations (10^{-6}-10^{-7}M). But they also believed that the special rearrangements of the long-chain (hexadecyl, octadecyl) molecule in micelle formation played a significant role in the deviation.

Zana and co-workers(18-24) studied the relationship between the micellar structures and molecular structures of bisquaternary ammonium gemini surfactants. One of their studies (18) (using an electrical conductivity method) concerned the CMCs of a series of gemini compounds with flexible, hydrophobic spacers: C_sH_{2s}-α,ω-$((CH_3)_2N^+C_mH_{2m+1}Br^-)_2$. They found the CMC of the surfactant series with m=12 and 16 goes through a maximum of small amplitude for

s=5±1, irrespective of the length of the alkyl side chain. This may reflect the contribution of a change of conformation of the surfactant with increasing spacer chain length to the micellization process. They attributed the decrease of CMC with increasing s at s≥10 to a progressive penetration of the spacer into the micelle hydrophobic core. They also compared the free energy of transfer of a methylene group, $\Delta G°(CH_2)$, to the micelle of a gemini type with that of conventional type surfactants. They found that the $\Delta G°(CH_2)$ has the same value in the micellization process of both these two types of surfactants, i.e., the value of $\Delta G°(CH_2)$ depends only weakly on the structure of the surfactant.

Menger and Littau (24,25), using the du Nuoy ring method for measuring the surface tension studied the surface properties of three series of gemini surfactants with a rigid, hydrophobic, spacer. The structures are shown in Chart IV. They found for all the three series of compounds that the CMC values increased with increase in the alkyl chain length when it was over 16 carbons. Their explanation is that the geminis might form 1) submicellar aggregates, such as dimers or tetramers; or 2) self-coils, such as:

gemini→submicelle→micelle

gemini→self-coiling→uncoiling→micelle

Long chains would be adversely affected by the energy

Chart IV

Geminis Synthesized by Menger and Littau (ref.24)

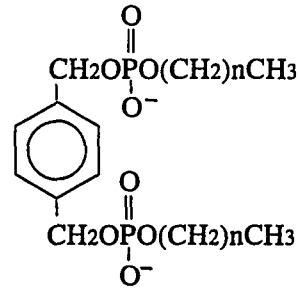

A. (p-Phenylenedimethylene)bis(alkyl hydrogen phosphate)

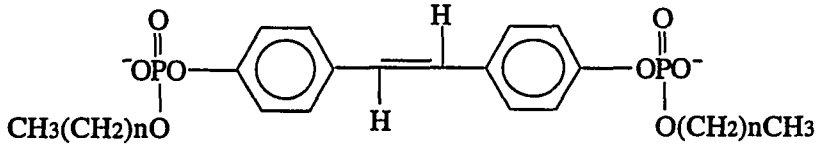

B. (Vinylenedi-p-phenylene) bis (alkyl hydrogen phosphate)

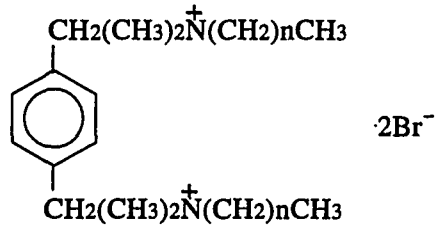

C. (p-Phenylenedimethylene)bis(alkyl dimethylammonium) Dibromide

requirements for uncoiling and reorganization prior to micellar assembly.

Rosen and co-workers (26) studied the interaction and synergism of some alkyl- and dialkyl-diphenylether mono- and disulfonates with conventional surfactants. They found the gemini type surfactant is more prone than the conventional type surfactants to show synergism in both surface tension reduction efficiency and effectiveness. This is probably due to increased chain-chain lateral interactions between the two types of surfactants as a result of the larger number of hydrophobic group per unit area at the aqueous solution/air interface. Gemini surfactants are less prone to show synergism in mixed micelle formation. They believed this is due to the greater steric inhibition of micelle formation by the gemini structure.

A.2. Dynamic Surface Properties

In many practical processing applications such as dyeing, foaming, painting, finishing, and resin-impregnation of fibrous material, the speed of the operation does not allow the surfactant molecules to reach equilibrium at the interface (27). Therefore, the dynamic surface tension–surface tension change with time of

interface formation is more relevant than the equilibrium surface tension to the description of the above processes. The maximum bubble pressure method (MBPM) can give precise and accurate values of dynamic as well as equilibrium surface tension (28). The MBPM has some advantages over the other dynamic surface tension measurement methods:

1) The results are more reliable in both accuracy and precision.
2) The operation of the MBPM is simple and not time consuming.
3) The MBPM has a broad time window. The time range of the instrument used in our labaratory for this study is 0.05 - 200 seconds.
4) It is capable of remote operation and is useful to measure the surface tension of melting metal.
5) The temperature range of operation is relatively broad. For aqueous solution this range could be 5 to 95°C.
6) Commercial instrumentation is available.

A.2.1. Previous work

The only paper published previously on the dynamic properties of gemini surfactant solutions is that of Rosen and co-workers (29). They used the maximum bubble pressure method to study the dynamic surface properties of some gemini surfactants

containing two sulfonate groups and two or three hydrophobic groups in the molecule, and of their mixtures with a nonionic or an amine oxide surfactant at 25°C in 0.1N NaCl. They found that the systems studied were all diffusion-controlled and that the apparent diffusion coefficient decreases with an increase in the number of alkyl chains and the bulkiness of the surfactant molecules. For the mixtures, when interaction between the two surfactant is weak, γ_t at short time (t<1s) is close to that of the component with the lower surface tension; at longer times, it is close to that of the component with the lower equilibrium surface tension. When interaction is strong, γ_t at short time is greater than that of either component.

B. Theoretical Background

B.1. Gibbs Adsorption Equation

The adsorption and desorption of surfactant molecules at the interface is a rapidly reversible process. The Gibbs equation (30) used for quantitative description of the process is in the form:

$$d\gamma = - \Gamma i d\mu i \qquad [1]$$

where γ is the surface tension of the solution, Γi surface excess concentration of solute i, and μi the chemical potential of solute i in

the system. For highly surface- active solutes (i.e., surfactants), Γ_i is essentially the concentration of surfactant at the interface. For dilute ($<10^{-2}$M) aqueous solutions containing only one nonionic surfactant (or ionic surfactant in the presence of a swamping, constant amount of a common non-surfactant counterion) the Eq. [1] can written as (1b):

$$d\gamma = -RT\Gamma_1 d\ln C_1 \quad [2]$$

$$= -2.3RT\Gamma_1 d\log C_1 \quad [3]$$

where C_1 is the surfactant molar concentration. When γ is in dyn/cm (=ergs/cm^2) or in mN/m (=mJ/m^2) , and R=8.3x10^{7}ergs/mol·K, then Γ_1 is in mol/cm^2; when R=8.3J/mol·K, then Γ_1 is in mol/1000m^2.

For dilute ($<10^{-2}$M) ionic surfactant of the 1:1 electrolyte type without the presence of a swamping, constant, amount of common non-surfactant counterion, Eq. [2] becomes:

$$d\gamma = -2RT\Gamma_1 d\ln C_1 \quad [4]$$

$$= -4.6RT\Gamma_1 d\log C_1 \quad [5]$$

From the experimental data, we can draw the γ vs. log C plot, from which the $d\gamma/d\log C$ and Γ_1 can be calculated. The area per molecule at the interface can be calculated from the relation: $a^s_1 = 10^{16}/(N\Gamma_1)$,

where N is Avogardo's number ($6.02x10^{23}$), Γ_1 is in mol/cm^2, and a^s_1 is in square angstroms ($Å^2$).

If the $d\gamma/d\log C$ is the maximum slope of the curve below the CMC, then the area per molecule will be equal to the minimum area per molecule (A_{min}).

B.2. The C_{20} Value (1c)

The "efficiency" of adsorption of the surfactant is measured by the concentration of surfactant in the solution phase required to produce a given amount of adsorption at the interface. When the surface tension of the solvent is decreased by 20 dyn/cm, the surface excess concentration (Γ_1) of the surfactant is close to its saturation value. So we can use the bulk concentration of the surfactant that can decrease the surface tension of solvent by 20 dyn/cm (C_{20}) as a measure of the efficiency of adsorption of the surfactant. The negative logarithm of the C_{20} value is symbolized pC_{20}.

B.3. The Γ_{MAX} and A_{min} values (1d)

The effectiveness of a surfactant in adsorbing at an interface is defined as the maximum surfactant concentration which can be

attained at the interface (Γ_{MAX}), i.e. the surface concentration of surfactant at surface saturation. The Γ_{MAX} is related to the minimum area per molecule adsorbed at the interface at surface saturation (A_{min}). The smaller the minimum cross-sectional area (A_{min}) of the surfactant at the interface, the larger the Γ_{MAX}. Usually the area occupied by a surfactant molecule at the surface appears to be determined by the area occupied by the hydrated hydrophilic group. For gemini surfactants, the portion between the two hydrophilic groups tends to lie flat in the interface, and the area occupied by the molecule is increased.

B.4. The γ_{CMC} and Π_{CMC} Values

The surface tension attained at the CMC (γ_{CMC}) or the surface pressure, $\Pi_{CMC}=\gamma_o-\gamma_{CMC}$), can be used for the measurement of effectiveness surface tension reduction (1d). Above the CMC, the concentration of monomeric surfactant molecule in the bulk phase remains virtually unchanged, so the amount of surfactant molecule adsorbed at the interface and the surface tension of the interface remains almost constant. If the surface is saturated when the surface tension of the solvent has been reduced by 20 mN/m, the Π_{CMC} can be expressed as:

$$\Pi_{CMC} = 20 + 2.3\ nRT\ \Gamma_{CMC} \log(CMC/C_{20}) \qquad [6]$$

where n is the number of ions whose surface concentration changes with change in the liquid phase concentration of the surfactant.

B.5. Thermodynamic Equations for Adsorption at the Interface

Rosen and Aronson (31) derived the following equations to calculate the standard free energy of adsorption of surfactant molecule at the aqueous/air interface ($\Delta G°_{ad}$). For nonionic surfactants at dilute concentrations ($<10^{-2}$M) the equation is:

$$\Delta G°_{ad} = 2.3RT\log(C_\pi/\omega) - 6.023\pi A_{min} \qquad [7]$$

where C_π is the concentration of surfactant ion in mol/L at a given value of π, π the surface pressure ($\pi = \gamma_o - \gamma$), ω the number moles of water per liter of water, A_{min} ($Å^2$) the minimum area per surfactant molecule.

When the surface tension of the solvent has been reduced by 20 dyn/cm. the relation becomes;

$$\Delta G°_{ad} = -2.3RTpC_{20} - 6.023x20A_{min} - 2.3RT\log\omega \qquad [8]$$

For ionic AB type surfactants in water solution the relation is:

$$\Delta G°_{ad} = 2.3RT[\log(C_\pi/\omega) + \log f_A + \log(C_B/\omega) + \log f_B] - 6.023\pi A_{min} \qquad [9]$$

where C_B is the concentration of the counterion B, of the surfactant

A, and f_A and f_B are the activity coefficients of A and B, respectively. The activity coefficients, f_A and f_B, can be evaluated by the Debye-Hückel equation (32):

$$\log f_{\pm} = \frac{-0.509|Z_+Z_-|I^{1/2}}{1 + 0.33\ \alpha\ I^{1/2}} \qquad [10]$$

$$\text{where} \quad I = (1/2)\Sigma\ CZ^2 \qquad [11]$$

where Z_+, Z_- are the charge number of cation and anion, α=0.3 for small ions(Na^+, K^+, Br^- Cl^-), 0.6 for the surfactant ion.

When a constant swamping amount of electrolyte (0.1N NaX) with common counterion of the surfactant is present, the terms $\log f_A$, $\log f_B$, $\log(C_B/\omega)$ are constant (=-1.74), so the Eq. [9] can be written as:

$$\Delta G^{\circ}_{ad} = 2.3RT[\log(C_{\pi}/\omega)-1.74]-6.023\pi A_{min} \qquad [12]$$

B.6. Empirical Equation for Micellization

For homologous straight-chain ionic surfactants, the relation between the CMC and the number of carbon atoms, n, in the alkyl chain can be described as (33):

$$\log CMC = A - B\ n \qquad [13]$$

where A and B are constants for a particular ionic head at a given temperature. Table 1 lists constants of A and B for conventional and

Table1 Constants for the Relation: log CMC = A - B n

Conventional Surfactants Series*	Temp (C°)	A	B
Na carboxylate (soaps)	20	1.85	0.30
K carboxylate (soaps)	20	1.92	0.29
Na (K) n-alkyl 1-sulfates	25	1.51	0.30
Na n-alkane-1-sulfonates	40	1.59	0.29
Na n-alkane-1-sulfonates	55	1.15	0.26
Na n-alkyl-1-sulfates	45	1.42	0.30
n-Alkyltrimethylammonium bromides	25	2.01	0.32
n-Alkyltrimethylammonium chlorides (in 0. 1 N NaCl)	25	1.23	0.33
n-Alkyltrimethylammonium bromides	60	1.77	0.29
n-Alkylpyridinium bromides	30	1.72	0.31
*Data from ref.1e			
Gemini Surfactants Series			
$(C_nN)_2OH$ (in 0.1 N NaCl)	50	3.80	0.70
$(C_nN)_2OH$ (in 0.1 N NaCl)	25	4.02	0.75
$(C_nN)_2Ar$ (in 0.1 N NaCl)	50	3.69	0.67
$(C_nN)_2Ar$ (in 0.01 N NaCl)	50	2.32	0.47

gemini surfactants. For conventional ionic surfactants, the CMC values are decreased to one half by increasing the alkyl chain by one methylene group (log2~0.3); to one third (log3~0.5), for conventional nonionics. For gemini ionic surfactants, the CMC values are reduced to one fifth (log5~0.7) by increasing by one methylene group each chain of the gemini surfactant (two methylene groups per molecule). This is somewhat smaller than the one quarter expected for conventional ionic surfactants (1/2x1/2)

B.7. Phase Separation Model for Micelle Formation:

The phase separation model considers micelle formation as analogous to a phase separation and the CMC is the saturated concentration of the surfactant monomeric state while the micelles constitute the separated pseudophase (34).

The free energy of micellization per mol of monomer, ΔG°_{mic}, is given by (35):

$$\Delta G^{\circ} = RT \ln X_{CMC} \qquad [14]$$

where X_{CMC} is the mol fraction of monomers. Zana and co-workers (18) have used this equation for calculating the standard free energy of micellization for cationic gemini surfactants in water.

B.8. Mass Action Law Model for Micellization (34):

The mass action law model postulates an equilibrium between monomers, (S), and a single micellar species of aggregation number, (x):

$$xS = S_x \qquad [15]$$

and

$$K_{eq} = (S_x)/(S)^x \qquad [16]$$

where K is the equilibrium constant. The standard free energy of micellization per mol of monomer, $\Delta G°_{mic}$, is given by:

$$\Delta G°_{mic} = -(RT/x) \ln K_{eq} \qquad [17]$$

For calculating the free energy to transfer one methylene group (CH_2) from aqueous solution to the micelle, we can use the following equation (36):

$$\Delta\Delta G°(CH_2) = \Delta G°(C_nH_{2n+1}\text{-}Y) - \Delta G°(C_{n-1}H_{2n-1}\text{-}Y)$$

$$= 2.303\ RT\ (\text{slope of log CMC vs. n}) \qquad [18]$$

B.9. Equations for Interactions in Mixed Surfactant Solutions

In 1979, based on regular solution theory, Rubingh (37) developed a method for calculating a parameter (β^m) that measures the interaction between two different surfactants in a mixed micelle in aqueous solution. In 1982, Rosen and Hua (38) extended this method to measuring the interaction (β^σ) between two different solutions at an interface forming a mixed monolayer.

The equations for calculating β^{σ} (for mixed monolayer formation) are:

$$\frac{(X_1)^2 \ln(\alpha_1 C_{12}/X_1 C_1^{\circ})}{(1-X_1)^2 \ln[(1-\alpha_1)C_{12}/(1-X_1)C_2^{\circ}]} = 1 \qquad [19]$$

$$\beta^{\sigma} = \frac{\ln(\alpha_1 C_{12}/X_1 C_1^{\circ})}{(1-X_1)^2}, \qquad [20]$$

where α_1 is the mole fraction of surfactant 1 in the total surfactant in the solution phase, C_1°, C_2°, and C_{12} are the molar concentrations of individual surfactants 1 and 2 and their mixture at a given value of α_1, respectively, required to produce the same surface tension value of the solution at a given temperature, and X_1 is the mole fraction of surfactant 1 in the total surfactant in the mixed monolayer. Eq. [19] can be solved numerically for X_1, when $a_1, C_1^{\circ}, C_2^{\circ}$ and C_{12} are known from experimental data.

Similarly, the interaction parameter β^{m} (for mixed micelle formation) can be calculated from the following equations:

$$\frac{(X_1^m)^2 \ln(\alpha_1 C_{12}^m/X_1^m C_1^m)}{(1-X_1^m)^2 \ln[(1-\alpha_1)C_{12}^m/(1-X_1^m)C_2^m} = 1 \qquad [21]$$

$$\beta^{\mu} = \frac{\ln(\alpha_1 C_{1\,2}^{m} / X_1^{m} C_1^{m})}{(1-X_1^{m})^2} \qquad [22]$$

where X_1^m is the mole fraction of surfactant 1 in the total surfactant in the mixed micelle and C_1^m, C_2^m, and $C_{1\,2}^m$ are the CMC values for surfactant 1, surfactant 2, and their mixture at mole fraction α_1, respectively. The larger the negative value of β, the stronger the attractive interaction between the different surfactant molecules.

B.10. Diffusion Equations for Dynamic Surface Tension Properties

When a fresh interface is created, an adsorption process starts, inducing a diffusion profile in the subsurface. If the adsorption time is much smaller than the diffusion time, the only time-dependent process is diffusion, expressing the instantaneous equilibrium of adsorption. This process can be described by Ward and Tordai equation(39-42), which is of the form:

$$\Gamma(t) = 2C_0\left(\frac{3Dt}{7\pi}\right)^{1/2} - 2\left(\frac{D}{\pi}\right)^{1/2} \cdot t^{-2/3} \int_0^{\sqrt{\tau}} C_s(\tau-t)\sqrt{\lambda} \qquad [23]$$

where $\Gamma(t)$ is the surface excess concentration of surfactant at time t, C_0 is the bulk concentration, D is the diffusion coefficient, C_s is the

subsurface concentration, τ is $(3/7)t^{7/3}$, λ is a dummy variable, t is surface age. In the very beginning of the adsorption process the subsurface concentration (C_s) is small and can be neglected, Eq. [23] becomes:

$$\Gamma(t) = 2C_o\left(\frac{3Dt}{7\pi}\right)^{1/2} \qquad [24]$$

From which: $$\ln t = 2\ln(\Gamma t/C) + \ln(1.8/D) \qquad [25]$$

At the end of the adsorption process, when the adsorption is close to the equilibrium value, Eq. [23] becomes (34):

$$\gamma_t = \gamma_e + \frac{RT\Gamma^2}{C_o}\left(\frac{7\pi}{12Dt}\right)^{1/2} \qquad [26]$$

where γ_t is the surface tension at time t, γ_e is the surface tension at infinite time, and Γ the surface excess concentration, obtained from the equilibrium surface tension vs. bulk concentration plot by use of the Gibbs adsorption equation, Eq. [3].

Dynamic surface tension data can be described very well by the following equation (43):

$$(\gamma_o-\gamma_t)/(\gamma_t-\gamma_m) = (t/t^*)^n \qquad [27]$$

where γ_t is the surface tension of the surfactant solution at surface age (time), t; γ_m is the meso-equilibrium surface tension (where γ_t shows only a small change with time); γ_0 is the surface tension of the solvent; t* and n are constants, t* has the dimension of time in the same units as t, and n being dimensionless.

The values of t* and n can be calculated by transforming equation [27] to its linear form:

$$\log [(\gamma_o-\gamma_t)/(\gamma_t-\gamma_m)] = n \log t - n \log t^* \qquad [28]$$

Eq. [27] can also be transformed into the following form (44):

$$\pi t = \pi m/[1+(1/a)\exp(-ny)] \qquad [29]$$

where $\pi t=(\gamma_o-\gamma_t)$ is the surface pressure at time t; $\pi m=(\gamma_o-\gamma_m)$ is the meso-equilibrium surface pressure, y = ln t and $a=(1/t^*)^n$. Some of these curves are shown in Fig.22. By using computer curve fitting of experimental data of πt vs. ln t, n and a and consequently, t* can be obtained. All the curves of γ vs. ln t show three regions (44): the induction region, the rapid increase region, and the meso-equilibrium region. The time ti, at the end of the induction period, (when the increasing rate of change in slope $d\pi t/d(\ln t)$ reaches a maximum value) and the surface pressure, πt, at ti can be calculated from the equations:

$$ti = (0.268/a)^{1/n} \qquad [30]$$

$$\text{and} \quad \pi_i = 0.211\ \pi_m \qquad [31]$$

For calculating the surface coverage, x_i, at the end of the induction period, we use the Davies equation (45) to calculate the area per surfactant molecule (A) occupied at the air/solution interface:

$$(\pi_i + 400M/A_{eq}^{3/2})(A_i - A_{eq}) = kT \qquad [32]$$

where M is the number of methylene groups ($-CH_2-$) in the surfactant alkyl chain (including the terminal methyl group), k is the Boltzman constant, T is the absolute temperature, A_i is the area per surfactant molecule at the end of the induction period, and A_{eq} is the area per surfactant molecule occupied at the aqueous/air interface at equilibrium, determined from the equilibrium surface tension-log C (molar surfactant concentration) curve by using the Gibbs adsorption equation, Eq. [3].

Therefore, $$x_i = A_{eq}/A_i \qquad [33]$$

For compounds with short alkyl chains, the induction times, t_i, are relatively small, so they should follow the assumption of the short-time Ward and Tordai equation. Therefore Eq. [25] can be written as:

$$\ln t_i = 2 \ln (\Gamma_i/C) + \ln (1.8/D) \qquad [34]$$

where Γ_i is the surface excess concentration in mol/cm^2, at the end of induction period. Values of Γ_i for used in Eq. [34] were calculated from values of A_i. The values of A_i were calculated from the value of π_i by use of the Eq. [32]. The values of π_i were calculated from the experimental values of π_m by use of the Eq. [31].

Differentiation of Eq. [27] (46) reveals that, at constant surfactant concentration, the rate of surface tension change with log time reaches a maximum:

$$|(d\gamma_t/d\log t)_{max.c}| = 0.576\ n\ \pi_m \qquad [35]$$

C. Experimental

C.1. Materials: Two series of bis (quarternary ammonium) surfactants were synthesized in our laboratory: one series with a rigid, hydrophobic spacer and the other with a flexible, more hydrophilic spacer, referred to as $(C_nN)_2Ar$ and $(C_nN)_2OH$, respectively. Their structures are shown in chart V.

1. (p-Phenylene dimethylene) bis(octyl-N,N-dimethylammonium) dibromide $(C_8N)_2Ar$. Dissolve 0.6g (2.3 mmol) of a,a'-dibromo-p-xylene (Fluka, purity > 98%) in 50 mL tetrahydrofuran (THF) in a 250 mL Erlenmeyer flask with magnetic

Chart V

Structures of Gemini Surfactants Being Studied

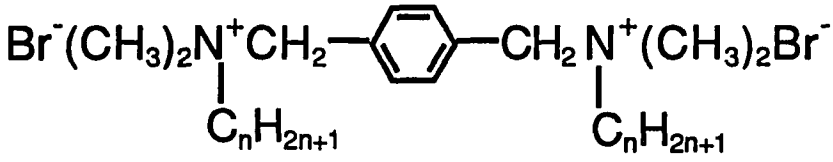

n=8,10,12,14,16,18 **(CnN)2Ar**

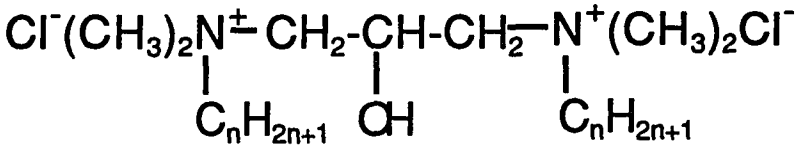

n=8,10,12,14,16,18 **(CnN)2OH**

stirring. Dilute 1.2 mL (0.9g, 5.8 mmol) octyl-N,N-dimethylamine (ADMA 8, Albemarle. purity 98%) with 25 mL THF and add this to the above solution. Stir for 4 hrs. Remove the solid by filtration and recrystallize the product twice from chloroform/acetone to obtain 1.1g $(C_8N)_2Ar$. Yield 83%. Melting point: 221.5-222.5°C.

^{1}NMR (250 MHz, D_2O): δ7.6 (s, 4 H), δ4.5 (s, 4 H), δ3.2 (t, 4 H), δ3.0 (s,12 H), δ1.3 (s, 4 H), δ1.2 (d, 20 H), δ0.8 (s, 6 H). Purity >98% as indicated by HPLC. In analogous fashion, the bis-decyl $[(C_{10}N)_2Ar]$, bis-dodecyl $[(C_{12}N)_2Ar]$, bis-tetradecyl $[(C_{14}N)_2Ar]$, bis-hexadecyl $[C_{16}N)_2Ar]$, and bis-octadecyl $[(C_{18}N)_2Ar]$ homologs were prepared. Elemental analysis for bis-octadecyl: Theory: C,67.15; H,11.08; N,3.26; Found: C,67.08; H,11.42; N,3.20.

2. 1,3-bis(dodecyl-N,N-dimethyl ammonium)-2-propanol dichloride $(C_{12}N)_2OH$. Add 1.8 mL (2.4g, 18.8 mmol) of 1,3-dichloro-2-propanol (Aldrich, purity 98%) to 10.8 mL (8.4g, 39 mmol) dodecyl-N,N-dimethyl-amine (ADMA 12, Albemarle. purity 98%) in a 50 mL round bottom flask. Add 20 mL 95% ethanol, reflux for 4 hrs. Pour the mixture into a 500 mL Erlenmeyer flask filled with 200 mL acetone, mix, and cool at 0°C for 2 hrs. Remove the solid by filtration and recrystallize the product twice from chloroform/acetone to obtain 7.8g $(C_{12}N)_2OH$, Yield: 78%, MP.78.0-79.0°C.

^{1}H NMR (250 MHz, D_2O): δ3.6 (m, 6 H), δ3.4 (d,12 H), δ2.3(s, 3 H), δ1.4 (s, 40 H), δ0.9 (t, 6 H). Elemental analysis: Theory for monohydrate: C, 65.52; H,12.32; N,4.83. Found: C, 64.89; H,12.30; H, 4.88.

In analogous fashion, the bis-octyl [$(C_8N)_2OH$], bis-decyl [$C_{10}N)_2OH$], bis-tetradecyl [$C_{14}N)_2OH$], bis-hexadecyl [$C_{16}N)_2OH$] and bis-octadecyl [$(C_{18}N)_2OH$] homologs were prepared. Their structures are shown in Chart V. Sodium 1-dodecanesulfonate ($C_{12}SO_3Na$, greater then 98% purity) was purchased from Research Plus (Bayonne, NJ); N,N-Dimethyl-1-tetradecaneamine oxide $C_{14}N(CH_3)_2O$, greater than 95% purity, was obtained from Ethyl Corporation (Baton Rouge, LA), courtesy of Kerry Hughes; $C_3C_1C_3$, $C_3C_3C_3$, $C_{10}C_1C_{10}$, $C_{10}C_3C_{10}$, research materials (8), courtesy of Dr. Masuyama (Osaka University, Japan); polyoxyethylenated n-dodecyl alcohol with a homogeneous head group of seven or of eight oxyethylene units ($C_{12}E_7$, $C_{12}E_8$), purity >98% by gas chromatography, was purchased from Nikko Chemical Co.(Tokyo, Japan).

C.2. Experiments

C.2.1. Equilibrium Surface Tension Measurements

These were made at 25±0.05°C and 50±0.2°C by the Wilhelmy plate technique, with a sand-blasted platinum blade of ca.5cm perimeter. When measurements were taken at 50°C, the sample container was covered with a larger plastic box placed in the thermostat, through which air at 50°C, saturated with moisture, was passed to decrease the evaporation of the sample solution. Instruments were calibrated against double-distilled water that had first been deionized and then distilled twice, the last time from alkaline permanganate solution through a one meter Vigreaux column with quartz condenser. All sample solutions were aged before taking measurements, the aging time varying from 10 to 40 min. at 50°C and from 2 to 24 hrs. at 25°C, depending upon the surfactant molar concentration.

When using the Wilhelmy plate technique for measuring surface tension, the surface tension is given by the down force upon the periphery of the plate. If the surfactant molecule is adsorbed with its head on the plate and its hydrophobic group towards the water, then the contact angle will not be zero. This will cause the measured surface tension to be lower than the true value. This can happen especially when dealing with cationic surfactants, where the surfactant molecule with positive charge is likely to adsorb on the surface with a negatively-charge platinum plate. To determine how

large an error can be caused by the above effect, two different techniques were used for the surface tension measurement. The first one was to keep the plate out of the solution (POS) and after the solution had been aged to reach equilibrium, to put the plate into the solution and take the first measurement. The other was to keep the plate in the solution (PIS), during the aging of the solution and to take the first measurement. For the POS method, the dropped plate will disrupt the organized array of molecules in the monolayer, which will cause higher surface tension. Figs. 1 and 2 show the differences of surface tension of some $(C_nN)_2OH$ series compounds measured by POS and PIS. From these plots we can draw the following conclusions:

1. The surface tension measured by the POS method is always higher than that measured by the PIS method.

2. The more dilute the solution, the larger the difference.

3. There is no significant difference between the CMC values obtained by both methods. Fig.3 shows the two methods used for measuring the surface tension of $(C_{12}N)_2Ar$ in H_2O at 50°C. This surfactant solution can reach equilibrium in 10 min.; the POS method gave almost constant surface tension value for a period of 150 min. The surface tension measured by the PIS method, on the other hand, continuously decreased with time. The absorption effect is

significant. In this research the POS method was used for all measurements.

C.2.2. Dynamic Surface Tension Measurements

In the maximum bubble pressure method instrument used in our laboratory, nitrogen gas is fed to a capillary tip which is immersed in a solution to a known depth. As the bubble grows, the pressure inside the bubble is sensed and displayed by a pressure transducer attached to an IBM microcomputer. With "notebook" software (Laboratory Technologies Corporation), both bubble frequency and maximum bubble pressure can be measured. The dynamic surface tension can be calculated by using the Laplace equation (47):

$$P_{max} = P\text{-}P_o = 2\gamma/R + \rho g h \qquad [36]$$

where P_{max} is the maximum pressure in the bubble, P_o is the atmospheric pressure, γ the surface tension, R the radius of the capillary, ρ the density of the liquid, and g the acceleration of gravity.

To obtain the empirical relation between γ and voltage (pressure has been converted into voltage), several pure compounds of known surface tension were used for calibration. The sensitivity of the pressure transducer is a 1.00 volt per inch of water pressure.

The calibration curves, using three different diameter capillaries and three pure compounds with known surface tension, are shown in Figs.4 and 5.

$$\gamma = K\ (Volt - f) \qquad [37]$$

where

$$f = \frac{\text{depth of immersion in cm}}{2.54\ \text{(cm/inch)}} \times 1.00\text{(volt/inch)} \qquad [38]$$

The Eq. [38] is based on the assumption that the density of the solution is 1.00g/ml.

C.2.3. Viscosity Measurement: Viscosity measurements were made by using an Ostwald viscosity meter which was calibrated with distilled water at 50°C. The viscosity of solution can be calculated by using the equation:

$$\eta / \rho = B\ t \qquad [39]$$

where η is viscosity, ρ is the density of solution, B is the instrument constant, and t is the flow time.

D. Results and Discussion

D.1. Equilibrium Surface Properties

D.1.1. Micellization Ability of Gemini Surfactants

To compare the surface properties of gemini surfactants with conventional surfactants, listed in Table 2 are their critical micelle concentrations (CMC), surface tension at CMC (γ_{CMC}), negative log of bulk concentration when surface tension decreased by 20 Nm/m (pC_{20}), and minimum area per molecule occupied at the interface of aqueous/air (A_{min}). The CMC of $C_{10}C_1C_{10}$ is lower than that of $C_{12}SO_3Na$ (both have similar numbers of carbon atoms per ionic group) by more than two orders of magnitude. The CMC range of conventional anionic surfactants is 10^{-2} to 10^{-3}M; for gemini anionic surfactants, this range is 10^{-5} to 10^{-6} mol/L. The increased ability to form micelles is probably the result of the increased distortion of water structure by the gemini surfactant. Table 3 lists the CMC values of cationic gemini surfactants with rigid, hydrophobic and with flexible, hydrophilic, spacers [$(C_nN)_2Ar$ and $(C_nN)_2OH$ series, respectively]. The CMC values of gemini surfactants with a flexible, hydophilic spacer are smaller than those of gemini surfactants with a rigid, hydrophobic spacer for the homologs with short alkyl chains C8-C12 (in 0.1 N NaCl at 25°C, CMC of C8OH: 1.07×10^{-2}M, C8Ar: 2.00×10^{-2}M; C10OH: 6.31×10^{-4}M, C10Ar: 1.15×10^{-3}M; C12OH: 2.29×10^{-5}M, C12Ar: 3.98×10^{-5}M). For longer alkyl chain homologs,

Table 2 Surface Properties of Anionic Gemini and Conventional Surfactant Solutions in 0.1N NaCl at 25°C

Compounds	CMC (M)	γ_{cmc} (mN/m)	Π_{CMC} (mN/m)	pC_{20}	Amin (Å^2)	CMC/C_{20}
$C_8C_1C_8$	2.19×10^{-4}	31.4	40.9	4.84	54	15.5
$C_8C_3C_8$	6.31×10^{-6}	29.0	43.3	7.40	89	158.5
$C_{10}C_1C_{10}$	7.24×10^{-6}	39.4	32.9	6.30	85	14.4
$C_{10}C_3C_{10}$	6.31×10^{-6}	28.0	44.3	8.30	111	125.9
$C_{12}EO_7$	8.71×10^{-5}	33.4	38.9	5.33	63	18.6
$C_{12}EO_8$	1.02×10^{-4}	34.0	38.4	5.25	64	18.1
$C_{14}N(CH_3)_2O$ pH=5.8	1.00×10^{-4}	29.5	42.8	5.20	50	15.8
$C_{14}N(CH_3)_2O$ pH=2.9	1.26×10^{-4}	29.6	42.7	4.90	41	10.0
$C_{12}H_{25}SO_3Na$	1.96×10^{-3}	35.0	37.3	3.56	52	7.1

the CMC values of both series show abnormal behavior (see following discussion). This is because the rigid spacer prohibits the intramolecular chain-chain interaction, thus decreasing the micelle formation ability. Table 4 lists the CMC values of conventional surfactants. Comparison of Table 3 with Table 4, shows that gemini surfactants always have smaller CMC values than conventional surfactants with the same number of alkyl chain carbon atoms per head group. Considering that most of the CMC values listed are measured in water, which would cause larger CMC values than when measured in a swamping amount of electrolyte, the difference usually is less than 1 order of magnitude. The other factor which affects the CMC is the temperature. The 25°C at which the CMCs of conventional surfactants were measured will give smaller values, because the minimum in the CMC-temperature curve appears to be around 25°C for ionic surfactants (48). Considering these two factors, it is obvious that the CMC values of gemini surfactants are still smaller than those of conventional surfactants. Although the goal of the investigation of these geminis is the study of the spacer effect on surface properties, rather than improvement of their micellar formation ability, some important interfacial phenomena, such as detergency and solubilization depend on the existence of micelles in solution. Therefore, it is expected that gemini surfactants will give

Table 3 Surface Properties of the Cationic Geminis Investigated

Compound	Media	Temp (°C)	CMC (mol/L)	pC_{20}	γ_{CMC} (mN/m)	A_{min} (nm^2x10^2)
$(C_8N)_2Ar$	0.01N NaCl	50	$3.16x10^{-2}$	1.90	41.2	124*
$(C_{10}N)_2Ar$	0.01N NaCl	50	$6.31x10^{-3}$	2.66	40.6	81*
$(C_{12}N)_2Ar$	0.01N NaCl	50	$4.57x10^{-4}$	3.93	40.2	78
$(C_{14}N)_2Ar$	0.01N NaCl	50	$1.38x10^{-5}$	5.44	40.0	72
$(C_{16}N)_2Ar$	0.01N NaCl	50	$8.71x10^{-6}$	5.98	38.4	98
$(C_{18}N)_2Ar$	0.01N NaCl	50	$3.80x10^{-6}$	5.62	43.8	44
$(C_8N)_2Ar$	0.1N NaCl	50	$2.00x10^{-2}$	2.20	42.0	112*
$(C_{10}N)_2Ar$	0.1N NaCl	50	$1.15x10^{-3}$	3.48	40.6	95*
$(C_{12}N)_2Ar$	0.1N NaCl	50	$3.98x10^{-5}$	5.08	38.4	68
$(C_{14}N)_2Ar$	0.1N NaCl	50	$7.24x10^{-6}$	5.62	37.8	47
$(C_{16}N)_2Ar$	0.1N NaCl	50	$5.37x10^{-6}$	5.74	37.4	46
$(C_{18}N)_2Ar$	0.1N NaCl	50	$2.09x10^{-6}$	5.90	43.2	45
$(C_8N)_2Ar$	0.1N NaBr	25	$1.20x10^{-2}$	2.80	39.4	75*
$(C_{10}N)_2Ar$	0.1N NaBr	25	$6.31x10^{-4}$	4.72	37.0	98
$(C_{10}N)_2Ar$	0.1N NaCl	25	$1.10x10^{-3}$	4.10	40.6	94*
$(C_{12}N)_2Ar$	0.1N NaCl	25	$3.31x10^{-5}$	5.60	39.6	95
$(C_8N)_2OH$	0.1N NaCl	50	$1.07x10^{-2}$	2.78	36.0	75*
$(C_{10}N)_2OH$	0.1N NaCl	50	$6.31x10^{-4}$	4.14	34.0	68
$(C_{12}N)_2OH$	0.1N NaCl	50	$2.29x10^{-5}$	5.62	32.2	55

continuated

continuation of Table 3

$(C_{14}N)_2OH$ 0.1N NaCl	50	$7.94x10^{-6}$	6.60	30.4	84
$(C_{16}N)_2OH$ 0.1N NaCl	50	$6.92x10^{-6}$	6.00	36.8	72
$(C_8N)_2OH$ 0.1N NaCl	25	$9.55x10^{-3}$	3.10	38.2	81
$(C_{10}N)_2OH$ 0.1N NaCl	25	$3.98x10^{-4}$	4.60	35.8	73
$(C_{12}N)_2OH$ 0.1N NaCl	25	$9.55x10^{-6}$	6.04	33.0	51
$(C_{14}N)_2OH$ 0.1N NaCl	25	$1.00x10^{-5}$	6.22	32.6	55
$(C_{16}N)_2OH$ 0.1N NaCl	25	$3.16x10^{-5}$	5.10	41.4	47

*Using Matijevic equation: $y=1 + C_{surf}/(C_{surf} + C_{NaCl(Br)})$, ref.82

Table 4 Critical Micelle Concentrations (CMC) of Conventional Cationic Surfactants*

Compounds	temperature (C°)	Media	CMC (M)
$C_{10}N(CH_3)_3Br$	25	H_2O	$6.5x10^{-2}$
$C_{12}N(CH_3)_3Br$	25	H_2O	$1.3x10^{-2}$
$C_{14}N(CH_3)_3Br$	25	H_2O	$3.3x10^{-3}$
	25	0.08 N NaBr	$3.9x10^{-4}$
$C_{16}N(CH_3)_3Br$	25	0.02 N NaBr	$8.2x10^{-5}$
$C_{16}N(CH_3)_3Cl$	25	H_2O	$1.4x10^{-3}$
$C_{16}N(CH_3)_3OH$	25	H_2O	$2.3x10^{-3}$
$C_{18}N(CH_3)_3Br$	30	H_2O	$2.9x10^{-4}$

* Data from ref.81

better results in these applications.

D.1.2. The Efficiency of Adsorption at the Aqueous Solution/Air Interface

The pC_{20} values of anionic gemini surfactants listed in Table 2 are larger than those of conventional anionic surfactants by 2 to 3 orders of magnitude. This means that the gemini surfactants have much greater tendency to adsorb at the aqueous/air interface and to reduce the surface tension. Rosen (49) has attributed this to the increased distortion of the water structure by the gemini double or triple chains. The distortion of the water structure by the hydrophobic group is the reason for surface activity of the surfactant molecule.

D.1.3. The Effectiveness of Surface Tension Reduction

As mentioned in the Introduction section, the "effectiveness" of surface tension reduction is determined by the maximum amount of surfactant adsorbed at the interface, Γ_{CMC}, and the CMC/C_{20} ratio (Eq.[6]). In Table 2 the A_{min} values of gemini surfactants are apparently larger than those of conventional surfactants. This is because the portion between the two head groups of gemini

surfactants makes the hydrated head group larger than conventional surfactants. The apparently large Π_{CMC} values of anionic gemini surfactants with three alkyl chains ($C_8C_3C_8$: 43.3 mN/m; $C_{10}C_3C_{10}$: 44.3 mN/m) were caused by their large CMC/C_{20} values ($C_8C_3C_8$: 158.5; $C_{10}C_3C_{10}$: 125.9). The Π_{CMC} and CMC/C_{20} values of the conventional anionic surfactant, SDS, are much smaller (37.4 mN/m and 7.1, respectively). Most of the γ_{CMC} values listed in Table 3 show that the gemini surfactants with a flexible, hydrophilic spacer have smaller γ_{CMC} ($\gamma_{CMC} = \gamma_o - \Pi_{CMC}$) values than those of gemini surfactants with a rigid, hydrophobic spacer. One of the reasons is that the $(C_nN)_2OH$ series have closer packing at the aqueous solution/air interface. It is confirmed by the smaller A_{min} values of the $(C_nN)_2OH$ homologs compared with those of the $(C_nN)_2Ar$ homologs in 0.1 N NaCl at 50°C (only valid for short alkyl chain homologs, see discussion in D.1.5. and D.1.7.).

D.1.4. Abnormal CMC and pC_{20} of Long Alkyl Chain Gemini Surfactants

Generally, surface tension measurements are best taken in solutions containing a swamping amount of electrolyte, in order to make unambiguous the value of the coefficient in the Gibbs

adsorption equation used to calculate the value of A_{min}. In a swamping amount of electrolyte, the value of the coefficient is 1 (1.b). In addition, there is no change in the ionic strength of the aqueous solution with change in the concentration of the surfactant when the surfactant is ionic, since change in ionic strength of the solution changes the effective charge of the hydrophilic group. This is particularly important when the surfactant, as in this case, has two ionic hydrophilic groups. Because of the low solubility of the members of the $(C_nN)_2Ar$ series in water at 25°C, only the C8 and C10 homologs could be measured at 25°C in 0.1 NaBr. The $(C_{12}N)_2Ar$ homologs could be measured at 25°C in 0.1 N NaCl, but not in 0.1 N NaBr, while the higher homologs could be measured, even in water, only at an elevated temperature (50°C).

Fig.6 shows the surface tension (γ) - log C plots for $(C_8N)_2Ar$ and $(C_{10}N)_2Ar$ in 0.1N aqueous NaBr at 25°C and of $(C_{10}N)_2Ar$ and $(C_{12}N)_2Ar$ in 0.1N NaCl at 25°C. It shows the expected increase in surface activity- lower CMC and higher pC_{20} (Table 3) with increase in alkyl chain length, and the expected decrease in surface activity with a less tightly bound counterion Cl^- (due to the greater hydration of Cl^-, compared to Br^-).

Fig.7 shows the γ - log C plots for members of the $(C_nN)_2Ar$ series in 0.01N aqueous NaCl at 50°C. The plots of the C8, C10, C12, and C14 homologs show the expected increase in surface activity with increase in the number of carbon atoms in the alkyl chain. However, the plots of the C16 and C18 homologs indicate anomalous behavior under these conditions—larger γ_{CMC} and/or larger CMC and smaller pC_{20} values than expected.

Fig.8 shows the γ – log C plots for the $(C_nN)_2Ar$ series in 0.1 N NaCl at 50°C. Here, the anomalous behavior is shown also by the C14 homolog. In Figs.9 and 10 , showing the γ – log C plots for members of the $(C_nN)_2OH$ series in 0.1 N NaCl at 50°C and 25°C, respectively, anomalous behavior is shown by the C14 and C16 homologs.

It is well known that there is a linear relationship between the log C_{20} value or the log CMC and the number of carbon atoms (n) in the alkyl chain of the hydrophobic group of conventional surfactant. Figs.11 and 12 show plots of log CMC versus n for the $(C_nN)_2Ar$ and $(C_nN)_2OH$ series, respectively. Figs.13 and 14 show plots of pC_{20} vs. n for the $(C_nN)_2Ar$ and $(C_nN)_2OH$ series, respectively. When the value of n exceeds a certain value, which varies with the electrolyte content and the temperature of the solution, the log pC_{20} and the log CMC values deviate from the expected linear relationship. They show

lower surface activity (smaller pC_{20} and larger CMC values) than expected, for the longer chain homologs.

D.1.5. Premicellar Self-Association Equilibrium Constants and Aggregation Numbers

The abnormally low surface activity of gemini surfactants with longer alkyl chains is probably the result of the formation of small premicellar aggregates (see Menger's work in Introduction section). Since, as we have seen in Figs.11-14, an increase in the alkyl chain length above a certain value results in a smaller increase in surface activity than expected for both the $(C_nN)_2Ar$ and $(C_nN)_2OH$ series, it can be assumed that any premicellar aggregates formed have little or no significant surface activity. Using this assumption, it is possible to calculate an equilibrium constant, K_{eq}, for the formation of these small aggregates and also to determine their aggregation number.

Based on a mass action law model, the self-association of monomeric surfactant molecules (S) to form small aggregates (S_x) can be described by equation [15]. The equilibrium constant, K_{eq}, for premicellar aggregation can be calculated using Eq. [16]. Values of $[S_x]$ and [S] for use in equation [15] are obtained in the following manner. We can estimate the values of CMC, C_{20} and γ_{CMC}, for the

higher homologs showing deviation from linearity pC_{20} vs. n and log CMC vs. n plots, in the absence of premicellar aggregation, by assuming that without premicellar aggregation they would fall on linear plots of pC_{20} or log CMC vs. n and estimating the value of γ_{CMC} from the values of the lower homologs. We can now construct the γ plots for the higher homologs that are expected in the absence of premicellar aggregation, from the values of C_{20} and γ_{CMC}, since the plot is linear between these two points. One such plot of $(C_{14}N)_2Ar$ in 0.1 N NaCl at 50°C is shown in Fig.8. Since the premicellar aggregates are assumed to have no surface activity, the observed γ values of the solutions at different surfactant concentrations must be due only to the monomeric S. The value of [S] can then be obtained at any value of γ from the γ – log C plot expected for that homolog in the absence of premicellar aggregation. The value of $[S_x]$ is the difference between the total surfactant concentration in the solution phase at any value (from the experimental γ – log C plot) minus [S] at the same γ value, divided by x. Different integral values of x can be taken and K_{eq} values calculated at different concentrations. Results are shown in Table 5. Since the units for K_2 are $(mol/L)^{-1}$; for K_3, $(mol/L)^{-2}$; and for K_4, $(mol/L)^{-3}$, in order to compare these values for constancy we have used $(K_3)^{1/2}$ and $(K_4)^{1/3}$. These are also listed in

Table 5 K_{eq} of Investigated Cationic Geminis at Four Different Surface Tensions

Compound	K_2	K_3	$(K_3)^{1/2}$	K_4	$(K_4)^{1/3}$
$(C_{14})_2OH$)	3.69×10^{6}	3.24×10^{12}	1.80×10^{6}	3.20×10^{18}	1.47×10^{6}
(0.1N Cl^-)	4.65×10^{6}	6.79×10^{12}	2.61×10^{6}	1.11×10^{18}	1.03×10^{6}
(50°C)	5.92×10^{6}	1.30×10^{13}	3.61×10^{6}	3.24×10^{19}	3.19×10^{6}
	6.70×10^{6}	2.14×10^{13}	4.63×10^{6}	7.67×10^{19}	4.25×10^{6}
range:	$3.7-6.7\times10^{6}$	$3.2-21.4\times10^{12}$	$1.8-4.6\times10^{6}$	$3.2-76.6\times10^{18}$	$1.5-4.2\times10^{6}$
$(C_{16})_2OH$	2.34×10^{10}	1.39×10^{18}	1.18×10^{9}	9.34×10^{25}	4.54×10^{8}
(0.1N Cl^-)	2.87×10^{10}	2.41×10^{18}	1.55×10^{9}	2.28×10^{26}	6.11×10^{8}
(50°C)	3.62×10^{10}	4.81×10^{18}	2.19×10^{9}	7.20×10^{26}	8.96×10^{8}
	4.99×10^{10}	1.05×10^{19}	3.24×10^{9}	2.50×10^{27}	1.36×10^{9}
range:	$2.3-5.0\times10^{10}$	$1.4-10.5\times10^{18}$	$1.2-3.2\times10^{9}$	$9.3-25.0\times10^{18}$	$4.5-13.5\times10^{8}$
$(C_{14})_2OH$	2.02×10^{8}	1.94×10^{15}	4.40×10^{7}	2.10×10^{22}	2.76×10^{7}
(0.1N Cl^-)	3.36×10^{8}	5.37×10^{15}	7.33×10^{7}	9.26×10^{22}	4.52×10^{7}
(25°C)	4.20×10^{8}	8.87×10^{15}	9.42×10^{7}	2.10×10^{23}	5.94×10^{7}
	4.81×10^{8}	1.28×10^{16}	1.13×10^{8}	3.82×10^{23}	7.26×10^{7}
range:	$2.0-4.8\times10^{8}$	$1.9-12.8\times10^{15}$	$4.3-11.3\times10^{7}$	$2.1-38.2\times10^{22}$	$2.8-7.2\times10^{7}$
$(C_{16})_2OH$	3.02×10^{12}	1.11×10^{21}	3.33×10^{10}	4.56×10^{29}	7.70×10^{9}
(0.1N Cl^-)	5.71×10^{12}	3.63×10^{21}	6.02×10^{10}	2.59×10^{30}	1.37×10^{10}
(25°C)	7.93×10^{12}	6.66×10^{21}	8.16×10^{10}	6.29×10^{30}	1.85×10^{10}
	9.97×10^{12}	1.05×10^{22}	1.02×10^{11}	1.25×10^{31}	2.32×10^{10}
range:	$3.0-9.8\times10^{12}$	$1.1-10.5\times10^{21}$	$3.3-10.2\times10^{10}$	$9.3-25.0\times10^{18}$	$7.7-23.2\times10^{8}$
$(C_{14})_2Ar$	2.44×10^{6}	1.63×10^{12}	1.28×10^{6}	1.22×10^{18}	1.67×10^{6}
(0.1N Cl^-)	3.21×10^{6}	1.79×10^{13}	4.23×10^{6}	8.89×10^{18}	2.08×10^{6}
(50°C)	4.01×10^{6}	2.12×10^{13}	4.60×10^{6}	1.28×10^{19}	2.34×10^{6}
	4.67×10^{6}	5.29×10^{13}	5.29×10^{6}	3.82×10^{19}	3.37×10^{6}
range:	$2.0-4.8\times10^{8}$	$1.9-12.8\times10^{15}$	$1.3-5.3\times10^{7}$	$1.2-38.2\times10^{18}$	$1.1-3.4\times10^{6}$

continued

continuation of Table 5

Compound	K2	K3	$(K3)^{1/2}$	K4	$(K4)^{1/3}$
$(C16)_2Ar$	$9.21x10^8$	$1.61x10^{16}$	$1.27x10^8$	$3.18x10^{23}$	$6.83x10^7$
(0.1N Cl^-)	$1.80x10^9$	$5.15x10^{16}$	$2.27x10^8$	$1.65x10^{24}$	$1.18x10^8$
(50°C)	$2.20x10^9$	$7.33x10^{16}$	$2.71x10^8$	$2.75x10^{24}$	$1.40x10^8$
	$3.64x10^9$	$1.71x10^{17}$	$4.14x10^8$	$9.06x10^{24}$	$2.08x10^8$
range:	$9.2-36.4x10^8$	$1.6-17.1x10^{16}$	$1.3-4.1x10^8$	$3.2-90.6x10^{23}$	$6.8-20.8x10^7$
$(C18)_2Ar$	$2.50x10^{11}$	$8.29x10^{19}$	$9.10x10^9$	$3.11x10^{28}$	$3.14x10^9$
(0.1N Cl^-)	$2.73x10^{11}$	$1.07x10^{20}$	$1.03x10^{10}$	$4.73x10^{28}$	$3.62x10^9$
(50°C)	$2.81x10^{11}$	$1.33x10^{20}$	$1.15x10^{10}$	$7.08x10^{28}$	$4.14x10^9$
	$5.21x10^{11}$	$3.16x10^{20}$	$1.78x10^{10}$	$2.15x10^{29}$	$5.99x10^9$
range:	$2.5-5.2x10^{11}$	$8.3-31.6x10^{19}$	$9.1-17.8x10^9$	$3.1-21.5x10^{28}$	$3.1-6.0x10^9$
$(C16)_2Ar$	$7.34x10^6$	$9.32x10^{12}$	$3.05x10^6$	$1.33x10^{19}$	$2.37x10^6$
(0.01N Cl^-)	$1.03x10^7$	$2.39x10^{13}$	$4.86x10^6$	$6.22x10^{19}$	$3.96x10^6$
(50°C)	$1.16x10^7$	$3.23x10^{13}$	$5.68x10^6$	$1.01x10^{20}$	$4.66x10^6$
	$1.35x10^7$	$5.70x10^{13}$	$7.55x10^6$	$2.70x10^{20}$	$6.46x10^6$
range:	$7.3-13.5x10^6$	$9.3-57.0x10^{12}$	$3.1-7.6x10^6$	$1.3-27.0x10^{19}$	$2.3-6.5x10^6$
$(C18)_2Ar$	$1.19x10^{10}$	$6.90x10^{17}$	$8.31x10^8$	$6.46x10^{25}$	$4.01x10^8$
(0.01N Cl^-)	$1.20x10^{10}$	$7.97x10^{17}$	$8.93x10^8$	$5.98x10^{25}$	$3.91x10^8$
(50°C)	$1.31x10^{10}$	$1.05x10^{18}$	$1.02x10^9$	$9.43x10^{25}$	$4.55x10^8$
	$1.43x10^{10}$	$1.55x10^{18}$	$1.24x10^9$	$1.89x10^{26}$	$5.74x10^8$
range:	$1.2-1.4x10^{10}$	$6.9-15.5x10^{18}$	$8.3-12.4x10^8$	$6.5-18.9x10^{25}$	$4.0-5.7x10^8$

Table 5. It is apparent that the values, compared in this manner, have the same degree of constancy, indicating that a series of oligomers is formed.

Although surface tension measurements and the above calculations are insufficient proof of premicelle existence, it is certain that the higher surface tension is caused by decreased monomer concentration at the aqueous/air interface. This means the equilibrium between monomer and aggregated monomer in equation [15] is moved considerably to the right with increased hydrophobic interaction.

D.1.6. Conditions that Facilitate Premicellization

It is to be expected in these premicellar aggregates that the molecules of geminis will be arranged with their similarly-charged hydrophilic groups at opposite ends of the structure and with their hydrophobic groups oriented towards each other in a manner somewhat similar to that in a very small bilayer or lamellar micelle (Chart VI). It is therefore to be expected that aggregation will be facilitated by the same factors that facilitate micellization, e.g., increase in the length of the alkyl hydrophobic groups, decrease in the charge on the hydrophilic group (larger ionic strength of the solution), and reduction in thermal motion (lower solution

Chart VI Schematic structure of dimers

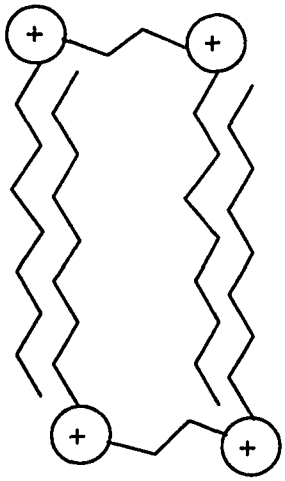

flexible spacer

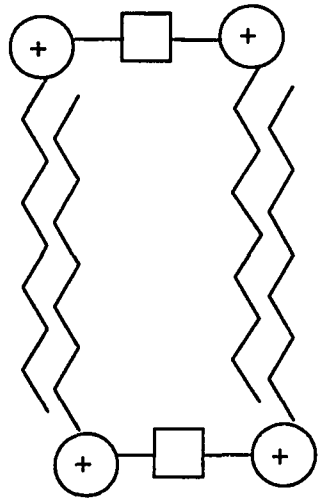

rigid spacer

temperature). All these factors should increase the value of K_{eq}. Inspection of the values of K_{eq} in Table 5 show that this is indeed the case. In 0.01 N NaCl at 50°C, where the charge on the hydrophilic groups is greater than in 0.1 N NaCl, and where thermal agitation is greater than at 25°C, we would expect that the K_{eq} values for a particular chain length would be smaller and that only for the longest chain homologs would the γ – log C plots deviate from their expected positions (Fig.11), while in 0.1 N NaCl at 25°C the K_{eq} values for a particular chain length would be greatest (Fig.12). This accounts for the positions of the γ – log C plots of the higher homologs, relative to the lower homologs in Figs. 8-10, and the chain length at which deviation of the pC_{20} and log CMC - n plots from linearity first appears (Figs.11-13).

D.1.7. Spacer Effect

Inspection of the K_{eq} values in Table 5 also reveals that there is stronger tendency to form premicellar aggregates in geminis with a flexible, hydrophilic spacer than in those with a rigid, hydrophobic one. This may be because the hydrophobic groups in the former molecules can pack together more closely than in the latter. This can be seen from the A_{min} values in Table 3 for the lower homologs of

the two different gemini types under similar conditions. In 0.1 N NaCl at 50°C, the $(C_8N)_2Ar$ has a A_{min} value of 0.96 n m^2, while for $(C_8N)_2OH$ the value is 0.68 n m^2; $(C_{10}N)_2Ar$ has a A_{min} value of 0.94 n m^2, while for $(C_{10}N)_2OH$ the value is 0.68 n m^2; for the C12 homolog, the values are 0.95 n m^2 and 0.51 n m^2, respectively. The energy for this closer packing (required to overcome the repulsion involved in bringing the two similarly-charged quaternary ammonium groups close together) may come from the energy released upon hydrogen bond formation between the hydroxyl group in the spacer and in the water molecules. This energy release would not be present for geminis with a hydrophobic spacer.

D.1.8. Standard Free Energies of Dimerization and Adsorption

Table 6 lists the values of standard free energy of dimerization of the $(C_nN)_2Ar$ and $(C_nN)_2OH$ series at different conditions, calculated from equation [17]. The free energy to transfer one methylene group ($-CH_2-$) from aqueous solution to premicelles (dimers), $\Delta\Delta G°_{di}(-CH_2-)$, were calculated using Eq. [18]. The data in Table 6 show that an increase in ionic strength facilitates transfer of a methylene group from aqueous phase to premicelle aggregates [for

Table 6 Standard Thermodynamic Parameters of Dimerization of Cationic Geminis [Calculated from K_2, $\Delta G°_{di} = -(RT/2)\ln K$]

Compound	Media	Temp(°C)	$\Delta G°_{di}$(kJ/mol)
$(C_{14}N)_2OH$	0.1N NaCl	50	-21.0
$(C_{16}N)_2OH$	0.1N NaCl	50	-32.5
$\Delta\Delta(CH_2)$*	0.1N NaCl	50	-4.3
$(C_{14}N)_2OH$	0.1N NaCl	25	-24.2
$(C_{16}N)_2OH$	0.1N NaCl	25	-36.4
$\Delta\Delta(CH_2)$*	0.1N NaCl	25	-4.3
$(C_{14}N)_2Ar$	0.1N NaCl	50	-20.2
$(C_{16}N)_2Ar$	0.1N NaCl	50	-28.8
$(C_{18}N)_2Ar$	0.1N NaCl	50	-35.7
$\Delta\Delta(CH_2)$*	0.1N NaCl	50	-4.1
$(C_{16}N)_2Ar$	0.01N NaCl	50	-21.7
$(C_{18}N)_2Ar$	0.01N NaCl	50	-31.2
$\Delta\Delta(CH_2)$*	0.01N NaCl	50	-3.4

*Calculated by Eq.[18]

$(C_nN)_2Ar$ series at 50°C, $\Delta\Delta G°_{di}(-CH_2-)$ = -4.1 kJ/mol in 0.1 NaCl and = -3.4 kJ/mol in 0.01 N NaCl]. Comparing the $\Delta\Delta G°_{mic}(-CH_2-)$ for conventional cationic surfactants, N-alkyl trimethyl-ammonium bromide, that value is -3.1kJ/mol in water at 25°C (37).

Gemini surfactants with a flexible, hydrophilic spacer can facilitate the transfer of a (-CH_2-) group from aqueous phase to premicelle (-4.3 kJ/mol and -4.1 kJ/mol, respectively) more than gemini surfactants with a rigid, hydrophobic, spacer.

The free energy of adsorption of gemini monomeric molecules at the aqueous solution/air interface ($\Delta G°_{ad}$) can be calculated from Eq. [12]. At the same temperature (50°C), the $\Delta G°_{ad}$ values of $(C_nN)_2Ar$ homologs in 0.1 N NaCl are more negative than those in 0.01 N NaCl [for $(C_8N)_2Ar$: $\Delta G°_{ad}$ values are -35.9 kJ/mol and -28.5 kJ/mol, respectively; for $(C_{10}N)_2Ar$: -43.6 kJ/mol and -34.2 kJ/mol; for $(C_{12}N)_2Ar$: -50.3 kJ/mol and -44.4 kJ/mol, see Table 7].

Comparing the $\Delta G°_{ad}$ values in 0.1 N NaCl at different temperatures (25°C and 50°C), the $\Delta G°_{ad}$ values of the $(C_nN)_2OH$ series are always more negative at the higher temperature [$\Delta G°_{ad}$ for $(C_8N)_2OH$ at 50°C and 25°C: -36.1kJ/mol and -35.5 kJ/mol, respectively; for $(C_{10}N)_2OH$: -44.5kJ/mol and -44.0kJ/mol; for $(C_{12}N)_2OH$: -52.1 kJ/mol and -50.0 kJ/mol; for $(C_{14}N)_2OH$: -61.6 kJ/mol and -52.0 kJ/mol]. This means increasing the temperature can facilitate the adsorption of gemini

Table 7 Standard Thermodynamic Parameters of Adsorption for Geminis at the Aqueous Solution/air Interface, Calculated by Eq.[12]

Surfactant	Media	Tem. (°C)	ΔG°_{ad} (kJ/mol)	$\Delta\Delta G^{\circ}(CH_2)$ (kJ/mol)	ΔS°_{ad} (kJ/mol K)
$(C_8N)_2Ar$	0.1N NaCl	50	-35.9		
$(C_{10}N)_2Ar$	0.1N NaCl	50	-43.6	-3.8	
$(C_{12}N)_2Ar$	0.1N NaCl	50	-50.3	-3.4	
$(C_{14}N)_2Ar$	0.1N NaCl	50	-51.1	-0.4	
$(C_8N)_2Ar$	0.01N NaCl	50	-28.5		
$(C_{10}N)_2Ar$	0.01N NaCl	50	-34.2	-2.8	
$(C_{12}N)_2Ar$	0.01N NaCl	50	-44.4	-5.1	
$(C_{14}N)_2Ar$	0.01N NaCl	50	-53.0	-4.3	
$(C_8N)_2OH$	0.1N NaCl	25	-35.5		
$(C_{10}N)_2OH$	0.1N NaCl	25	-44.0	-4.3	
$(C_{12}N)_2OH$	0.1N NaCl	25	-50.5	-2.8	
$(C_{14}N)_2OH$	0.1N NaCl	25	-52.0	-0.8	
$(C_8N)_2OH$	0.1N NaCl	50	-36.1	0.024	
$(C_{10}N)_2OH$	0.1N NaCl	50	-44.5	-4.2	0.020
$(C_{12}N)_2OH$	0.1N NaCl	50	-52.1	-3.8	0.064
$(C_{14}N)_2OH$	0.1N NaCl	50	-61.6	-4.7	0.384

monomers at the aqueous solution/air interface.

At the same temperature and ionic strength (50°C, 0.1 N NaCl), the ΔG°_{ad} values of $(C_nN)_2OH$ series are more negative than those of $(C_nN)_2Ar$ series. [For $(C_8N)_2OH$ and $(C_8N)_2Ar$: the ΔG°_{ad} are -36.1 kJ/mol and -35.9 kJ/mol, respectively; for $(C_{10}N)_2OH$ and $(C_{10}N)_2Ar$: -44.5 kJ/mol and -43.6 kJ/mol; for $(C_{12}N)_2OH$ and $(C_{12}N)_2Ar$: -52.1 kJ/mol and -50.3 kJ/mol; for $(C_{14}N)_2OH$ and $(C_{14}N)_2Ar$: -61.6 kJ/mol and -51.1 kJ/mol]. This means the flexible, hydrophilic spacer facilitates adsorption of monomeric gemini surfactants at the interface more than the rigid, hydrophobic spacer.

Comparison of Tables 6 and 7 shows that adsorption at the aqueous solution/air interface is favored more than dimerization (more negative ΔG°_{ad} than ΔG°_{di}).

D.1.9. Abnormal Behavior of $(C_{18}N)_2Ar$

Fig.15 shows the surface tension (γ) vs. log C plot of $(C_{18}N)_2Ar$ in 0.1 N NaCl at 50°C. There are two discontinuities in this plot. Only monomers exist at concentrations below the first discontinuity. At the first plateau, premicelles start to form and the monomer concentration remains constant, as evidenced by the constant surface tension. At the second discontinuity, micelles start to form. At the

second plateau, only micelles are formed and the monomer concentration is again constant. Lee and Woo (50), based on NMR measurements, showed that a second CMC exists at twice the value of the first CMC for aqueous solutions of conventional cationic surfactants. The two kinds of micelles show considerable differences in several physical properties, such as NMR parameters, solubilization sites of micelle-soluble probes, molar volumes, and spectroscopic properties, all of which reflect a transition of micelle structure. Aqueous micelles can transform into worm-like ones through micelle growth at a high surfactant concentration (the so-called worm-like transition), in which micelles have viscoelasticity (51). Based on conductivity measurements, Treiner and Makayssi (52) found that for conventional cationic surfactants with more than 16 methylene groups, there are two breaks in the conductivity versus concentration plot. They concluded that there are two CMCs in the system.

D.1.10. Some Other Abnormal Properties of Gemini Surfactants

(a) Fig.16 shows the surface tension (γ) vs. log C plots of the $(C_nN)_2Ar$ series in H_2O at 50°C. The parameters CMC and γ_{CMC}

obtained from plots C12, C14, C16 homologs are very close to those reported by Menger and Littau (18) for the same compounds under the same conditions (Du Nuoy method, using a platinum ring). But the plot of C18 is different from theirs (see Table 8). Menger and Littau's experiments were done with an ordinary vessel which we also used initially. We found it impossible to obtain surface tension measurements of any reliability at 50°C without the use of a plastic box with a supply of air saturated with water at 50°C, as described in the Experimental section. Without this apparatus, the solution, when uncovered, lost a significant amount of water by evaporation; when covered, water condensed on the cover that dripped back into the solution changed the surfactant concentration near the surface.

(**b**) Fig.17 shows the surface tension (γ) vs. log C plots of $(C_{18}N)_2OH$ in H_2O at 25°C and in 0.1 N NaCl at 25°C and 50°C. The increase in surface tension (γ) with increase in the surfactant bulk concentration has not been reported previously. The increase in surface tension means that the concentration of monomer decreases with increase in surfactant concentration, implying a very strong association with a non-surface active species. This phenomena does not occur at 50°C.

Table 8 Comparing Surface Active Parameters with Those of Menger and Littau (ref.24) for $(C_nN)_2Ar$ Series in H_2O at 50°C

Compound	CMC (M)*	CMC (M)**	γ_{CMC}* (mN/m)	γ_{CMC}** (mN/m)
$(C_8N)_2Ar$	3.16×10^{-2}	1.0×10^{-2}	41.2	38
$(C_{12}N)_2Ar$	1.10×10^{-3}	1.0×10^{-3}	39.4	39
$(C_{16}N)_2Ar$	7.94×10^{-5}	6.7×10^{-5}	40.6	41
$(C_{18}N)_2Ar$	1.74×10^{-6}	3.7×10^{-4}	46.6	38

* This work
** Menger and littau's work (24)

Table 9 Effect of pH on Interaction Between Anionic Geminis and Conventional Amineoxide Surfactants in 0.1N NaCl at 25°C

Mixture	pH	β^{σ}	β^{m}
$C_{10}C_1C_{10}$-$C_{14}N(CH_3)_2O_7$	5.8	-3.4	-0.9
$C_{10}C_1C_{10}$-$C_{14}N(CH_3)_2O_7$	2.9	-8.7	-5.9
$C_{10}C_3C_{10}$-$C_{14}N(CH_3)_2O_7$	7.9	-0.8	-1.0
$C_{10}C_3C_{10}$-$C_{14}N(CH_3)_2O_7$	7.2	-0.9	-2.1
$C_{10}C_3C_{10}$-$C_{14}N(CH_3)_2O_7$	5.8	-3.3	-4.3

D.2. Interactions Between Gemini and Conventional Surfactants

The interaction between surfactant molecules is influenced by many factors, such as type of charge on the head group, the length of alkyl chain, solution pH, and ionic strength. We will discuss the effect of changing some of these factors on the interactions between gemini and conventional surfactants.

D.2.1. Effect of pH on Molecular Interactions Between Gemini and Conventional Surfactants

When anionic gemini surfactants are mixed with the amine oxide surfactant ($C_{14}N(CH_3)_2O$), the absolute values of both β^{σ} and β^{m} increase with decrease in pH of the solution (Table 9). In neutral or alkaline solution, the amine oxide probably exists as an unionized hydrate and exhibits nonionic character. At low pH, the nitrogen atom appears to have some bonding tendency for protons and the molecule takes on a mildly cationic charge, the strength of which depends on the pH. When the pH reaches 2.9, the percentage of protonated amine oxide is 100% (53,54). Electrostatic attraction between anionic conventional and gemini surfactants and cationic protonated amine oxide dominates the interactions both in

monolayer formation at an interface and in micellar formation in bulk solution (55-61). The interaction in monolayer formation between anionic gemini and anionic SDS also increased with decrease in pH (Table 10). This is believed to be because the oxygens of the multiple ether linkages in the gemini molecules can also have some degree of combination with protons in acidic solution (62), thus imparting partial cationic properties to the geminis and with resulting increased interaction with the anionic SDS. Another explanation could be that the oxygen atoms of the multiple ether linkage of gemini surfactant can form stronger hydrogen bond with protonated water molecules in acidic solution and carry partial positive charge.

D.2.2. Effect of Chain Length on Molecular Interactions between Gemini and Conventional Surfactants

The effect of increase in chain length of the gemini surfactant on these interactions appears to be complex, especially when the gemini surfactant is capable of forming non-surface-active premicellar aggregates, either with itself alone or in a mixed aggregate with the conventional surfactant. Thus, one would expect, based upon data from conventional surfactant mixtures (1f), that

Table 10 Effect of pH on Interaction Between Anionic Geminis and Anionic Conventional Surfactants in 0.1N NaCl at 25°C

Mixture	pH	β^{σ}	β^{m}
$C_8C_1C_8$-$C_{12}H_{25}SO_3Na$	5.8	-0.7	+0.7
$C_8C_1C_8$-$C_{12}H_{25}SO_3Na$	2.9	-2.7	-0.9
$C_{10}C_1C_{10}$-$C_{12}H_{25}SO_3Na$	5.8	-1.8	---
$C_{10}C_1C_{10}$-$C_{12}H_{25}SO_3Na$	2.9	-3.0	---

Table 11 Effect of Alkyl Chain Length on Interaction between Anionic Gemini and Nonionic Conventional Surfactants in 0.1N NaCl at 25°C

Mixture	β^{σ}	β^{m}
$C_8C_1C_8$-$C_{12}EO_7$*	-1.5	-0.2
$C_8C_8C_8$-$C_{12}EO_7$*	-3.2	+0.7
$C_{10}C_1C_{10}$-$C_{12}EO_7$	-1.2	-0.3
$C_{10}C_8C_{10}$-$C_{12}EO_7$	-0.6	-2.8
$C_{10}C_1C_{10}$-$C_{12}EO_8$	-4.3	-5.3
$C_{10}C_8C_{10}$-$C_{12}EO_8$	-4.9	-7.5

*Data from ref.49

interaction strength would increase (more negative β values) with increase in the chain lengths of the gemini surfactant. Some data of this sort can be seen in Tables 11 and 12, particularly in the values of β^{σ}, e.g., $C_8C_1C_8$-$C_{12}EO_7$, β^{σ} = -1.5; $C_{10}C_1C_{10}$-$C_{12}EO_8$, β^{σ} = -4.3; $C_8C_8C_8$-$C_{12}EO_7$, β^{σ} = -3.2; $(C_8N)_2OH$-$C_{12}EO_2S$, β^{σ} = -15.6; $(C_{10}N)_2OH$-$C_{12}EO_7$, β^{σ} = -16.7. (The β^{m} values are complicated by the steric factors (55) involved in mixed micelle formation with geminis containing two alkyl and, even more so, three alkyl chains).

However, when the gemini surfactant has a tendency to form premicellar aggregates (which have no surface activity) with the conventional surfactant, the β values should become less negative (62). This accounts for the data in Table 12, showing a marked decrease in the |β| values of $(C_{12}N)_2OH$-$C_{12}EO_2S$ (β^{σ} = -5.5; β^{m} = -5.8) compared to $(C_{10}N)_2OH$-$C_{12}EO_2S$ (β^{σ} = -16.9; β^{m} = -12.3). For the $(C_{14}N)_2OH$-$C_{12}EO_2S$ system (Fig.20), the γ-log C plot is so far to the right that it is impossible to calculate the β interaction parameters from the curve.

D.3. Dynamic Surface Properties of Gemini Surfactant Solutions

As mentioned in the Introduction A.1., some studies have

Table 12 Effect of Alkyl Chain Length on Interaction Between Cationic Geminis and Anionic Conventional Surfactants in 0.1N NaCl at 25°C

Mixture	β^{σ}	β^{m}
$(C_8N)_2OH\text{-}C_{12}EO_2S$	-15.6	-13.0
$(C_{10}N)_2OH\text{-}C_{12}EO_2S$	-16.9	-12.3
$(C_{12}N)_2OH\text{-}C_{12}EO_2S$	-5.45	-5.81
$(C_{10}N)_2Ar\text{-}C_{12}EO_2S$	-16.1	-14.5

Table 13 Dynamic Surface Tension Parameters of $(C_nN)_2Ar$ Surfactant Solutions

compound	n	t_i (s)	A_i (Å^2)	π_m (mN/m)	π_{eq} (mN/m)	X_i
$(C_8N)_2Ar$ (Cx10^3M)						
H_2O 25°C						
24.0	0.14	4.1x10^{-9}	130	28	32	0.64
0.1N NaBr 25°C						
CMC: 12.6						
7.30	0.15	1.2x10^{-6}	114	30	31	0.65
3.65	0.15	3.1x10^{-6}	151	26	26	0.62
0.332	0.15	4.4x10^{-4}	244	15	15	0.59
$(C_{10}N)_2Ar$ (Cx10^4M)						
0.1N NaBr 25°C						

continued

continuation of Table 13

compound	n	ti (s)	Ai (Å^2)	π_m (mN/m)	π_{eq} (mN/m)	Xi
CMC> 4.00						
3.96	1.0	0.027	151	30	35	0.68
1.96	1.2	0.15	157	27	30	0.66
1.27	1.0	0.31	158	26	28	0.65
0.624	1.1	1.1	166	22	25	0.62
0.393	1.0	3.2	171	20	23	0.60
0.112	1.1	11	178	8	19	0.58
$(C_{12}N)_2Ar$ (Cx10^{5}M)						
0.1N NaCl 25°C						
CMC: 3.20						
3.93	1.3	1.9	119	30	32	0.66
1.12	1.5	8.3	143	25	27	0.62
0.862	1.5	16	147	25	26	0.62
0.1N NaCl 50°C						
12.7	1.4	0.14	137	29	30	0.67
$(C_{16}N)_2Ar$ (Cx10^{5}M)						
0.1N NaCl 50°C						
12.7	1.8	22	73	34	34	0.65
6.35	1.8	29	72	33	33	0.64
$(C_{18}N)_2Ar$ (Cx10^{5}M)						
0.1N NaCl 50°C						
12.7	2.1	80	69	25	25	0.68

investigated the effect of the hydrophobic chain length and of the structure of the linkage ("spacer") between the two hydrophilic groups on the equilibrium properties of aqueous solutions of some cationic gemini surfactants.

We have studied the effect of the spacer on the dynamic surface properties of the cationic gemini surfactants that we have synthesized.

D.3.1. Value of n:

Recall that the n is a constant in Eq.[27]. Figs.21 and 22 show π_t vs. ln t curves for the two series of gemini surfactants that we have synthesized. Values of n for the two different series, with a rigid hydrophobic and with a flexible, hydrophilic spacer, obtained by curve fitting (Kaleida Graph, Macintosh software, 1993) of Eq. [29] to dynamic surface tension data, are listed in Tables13-15, respectively, together with other dynamic surface tension parameters. Values of n for the two series under similar conditions are listed in Table 15. For both gemini series the n values increase linearly with increase in the alkyl chain length. This is consistent with previous results (61, 62) showing that n increases with increase in the hydrophobic character of the surfactant molecule, since n is related to the difference between the energies of adsorption and

Table 14 Dynamic Surface Tension Parameters of $(C_nN)_2OH$ Surfactant Solutions

	n	ti(s)	Ai ($Å^2$)	πm (mN/m)	πeq (mN/m)	X
$(C_{10}N)_2OH$(Cx10^4M)						
0.1N NaCl 25°C						
CMC: 3.98						
5.00	1.0	0.02	114	33	39	0.64
1.27	1.0	0.32	121	26	29	0.60
0.393	1.1	1.6	132	21	22	0.56
0.112	1.1	11	136	19	19	0.54
$(C_{12}N)_2OH$ (Cx10^5M)						
0.1N NaCl 25 °C						
CMC: 1.00						
12.7	1.8	1.3	79	38	39	0.65
3.93	1.8	9.5	79	38	39	0.65
1.12	1.8	37	79	38	39	0.65
0.316	1.8	126	80	32	33	0.62
0.200	1.8	360	83	25	26	0.58
0.1N NaCl 50°C						
12.7	1.7	0.56	80	35	---*	0.64
$(C_{14}N)_2OH$ (Cx10^5M)						
0.1N NaCl 25 °C						
CMC: 1.00						
12.7	3.1	49	81	40	40	0.69
3.93	3.2	108	82	38	40	0.68
1.12	3.2	210	83	36	40	0.67
0.1N NaCl 50°C						
12.7	3.1	8.8	86	35	---*	0.64

continued

continuation of Table 14

	n	ti(s)	Ai (Å^2)	πm (mN/m)	πeq (mN/m)	X
$(C_{16}N)_2OH$ (Cx10^{4}M)						
0.1N NaCl 50°C						
CMC: 2.85						
2.52	3.5	50	84	24	---*	0.63
1.27	3.6	80	84	24	---*	0.63

*no measurements

Table 15 Comparison of Surface Tension Parameters of the Two Series of Cationic Geminis under Similar Conditions (Data in parentheses are data for the $(C_nN)_2OH$ Series)

$(C_{10}N)_2Ar$ (Cx10^{4}M)	πm (mN/m)	n	ti (s)	t* (s)	0.57nπm
0.1N NaCl 25°C					
1.27	16 (26)	1.0 (1.0)	0.12 (0.32)	0.44 (1.2)	9.2(15.0)
0.393	13 (21)	1.0 (1.1)	0.88 (1.93)	3.28 (6.4)	7.5(13.3)
0.112	11 (19)	1.0 (1.0)	9.93 (11.3)	37.0 (42.0)	6.3(12.0)
$(C_{12}N)_2Ar$ (Cx10^{5}M)					
0.1N NaCl 25°C					
3.93	30 (38)	1.3 (1.8)	1.9(9.5)	5.2(20)	22.5(39.4)
1.12	25 (38)	1.5 (1.8)	8.3(37)	20(77)	22.5(39.4)
$(C_{16}N)_2Ar$ (Cx10^{5}M)					
0.1N NaCl 50°C					
12.7	34(24)	1.8(3.6)	22(80)	46(115)	35.3(49.8)

desorption of the surfactant. The increase in n with increase in alkyl chain length is larger for the gemini series with a flexible spacer than for the series with a rigid spacer (Fig.23). Values of n are essentially constant with concentration change for a specific compound, irrespective of whether the concentration is above or below the critical micelle concentration (CMC) of the surfactant (see Tables 13 and 14).

In the two cases (Table 14) where n values were obtained at 25°C and 50°C, there appears to be little effect on n in this temperature range.

D.3.2. Value of ti:

The values of the induction time (ti), the time when the surface tension starts to decrease significantly, also increase with increase in alkyl chain length in both systems. (Tables 13-15). However, here the increase is related to the increased packing of surfactant molecules with longer alkyl chains at the interface (44). For the $(C_nN)_2OH$ series, the ti values are larger than those of the $(C_nN)_2Ar$ compounds under the same conditions. This is rather unexpected, because it would be expected that the former, with a flexible spacer, would have a larger diffusivity and therefore smaller ti. Possible reasons for this unexpected observation are:

1) the hydroxyl group (-OH) in $(C_nN)_2OH$ can form hydrogen bonds with water molecules, and this hydration may decrease diffusivity; 2) because of the flexibility of the spacer, the long alkyl chains can interact to each other and combine to form large polymer-like (worm-like) aggregates in the $(C_nN)_2OH$ series. Evidence for this is the viscosity measurements of these solutions. (Measurements were made in H_2O because of the limited solubility of the C16 and C18 homologs of the $(C_nN)_2Ar$ series in NaBr or NaCl). Table 16 shows that, under the same conditions, the viscosity values of $(C_{18}N)_2OH$ and $(C_{16}N)_2OH$ are higher than those of the $(C_{18}N)_2Ar$ and $(C_{16}N)_2Ar$ compounds, the difference being larger with the longer alkyl chains.

D.3.3. Molecular Environment Effect on Dynamic Surface Tension Parameters

Table 16 lists the dynamic parameters of surfactant solutions of cationic gemini with rigid spacer. The t* is the time the surface tension drops to one half of the value of $(\gamma_o-\gamma_m)$, that is, the time of the maximum surface tension fall rate. From Eq.[27], when $(\gamma_o-\gamma_t) = (\gamma_t-\gamma_m)$, $t = t^*$. The smaller the value of t*, the faster the surface tension decrease. Table 16 shows that increasing the temperature of the solution (from 25°C to 50°C) will decrease the t_i and t* values

Table 16 Effect of Molecular Environment on Dynamic Surface Tension Parameters of Gemini Surfactant Solutions

		ti(s)	t* (s)	π_{eq}(mN/m)	π_m(mN/m)
Effect of Temperature					
$(C_{16}N)_2Ar$ 0.1N NaCl	25°C	160	333	---	32
C=6.35x10^{-5}M	50°C	29	60	35	33
Effect of Ionic strength					
$(C_{16}N)_2Ar$ 50 °C	H_2O	25	52	28	25
C= 1.27x10^{-4}M	0.1N NaCl	22	46	34	34
Effect of Counterion					
$(C_{10}N)_2Ar$ 25°C	0.1N NaCl	0.88	3.3	17	13
C=3.93x10^{-5}M	0.1N NaBr	3.2	8.7	23	20

Table 17 Relationship Between Induction Time (ti), Surfactant Concentration (C), and Surface Excess Concentration (Γi

Surfactant	Medium	Equation
$(C_{10}N)_2Ar$	0.1N NaBr (25 °C)	ln ti = 1.80 ln (Γi/C)+23.6
$(C_{12}N)_2Ar$	0.1N NaCl (25 °C)	ln ti = 1.78 ln (Γi/C)+22.8
$(C_{16}N)_2Ar$	0.1N NaCl (50 °C)	ln ti = 0.43 ln (Γi/C)+9.32
$(C_{10}N)_2OH$	0.1N NaCl (25 °C)	ln ti = 1.58 ln (Γi/C)+20.35
$(C_{12}N)_2OH$	0.1N NaCl (25 °C)	ln ti = 1.46 ln (Γi/C)+18.48
$(C_{14}N)_2OH$	0.1N NaCl (25 °C)	ln ti = 0.61 ln (Γi/C)+12.41
$(C_{16}N)_2OH$	0.1N NaCl (50 °C)	ln ti = 0.61 ln (Γi/C)+12.41

(160 s to 29 s and 333 s to 60 s, respectively). This means that the surface tension starts to drop and reaches the maximum fall rate faster when the temperature increases. Increase in the ionic strength of the surfactant solutions (H_2O to 0.1N NaCl) has the same effect, but the changes are relatively small (25 s to 22 s and 52 s to 46 s, respectively). The mesoequilibrium surface pressure (π_m), increases as ionic strength is increased (π_m increased from 25 to 34 mN/m), as would be expected from the known increase in equilibrium surface pressure, π_{eq}, with this change.

D.3.4. Adsorption Behavior at the Aqueous Solution/Air Interface

According to Eq. [32], when back-diffusion can be neglected at short times (for diffusion-controlled adsorption), it appears that ln t_i is a linear function of $\ln(\Gamma_i/C)$. As the alkyl chains become longer, the coefficients and intercepts decrease. According to Eq. [32], the decrease of the intercept means that the apparent diffusion coefficient increases with increase in the alkyl chain length of the surfactant. But usually, the diffusion coefficient decreases with increase in the alkyl chain length of the surfactant. This contradictory result probably results from Eq. [32] being based on the Ward and Tordai equation, simplified for short times only. Since

ti values increase greatly with increase in the alkyl chain length (see Table 13-15), Eq. [32] is not valid for the longer induction times. Table 17 and Figs.24 and 25 show that the ln ti vs. ln(Γ_i/C) plots are still linear as the alkyl chain lengths increase, the coefficients deviate more and more from the value of 2 of Eq. [32].

Another way of studying dynamic adsorption behavior is to use a long-time adsorption equation (Eq. [26]). If the adsorption process is diffusion-controlled, according to Eq.[26], the plot of γ_t vs. $t^{-1/2}$ should be linear. Figs.26 and 27 show that the plots of γ_t vs.$t^{-1/2}$ for all the compounds studied are linear. The intercept, γ_e, is the surface tension at infinite time, so γ_e should equal or be close to the equilibrium surface tension, γ_{eq}, obtained from equilibrium surface tension measurements. Table 18 shows the values of γ_e and γ_{eq}. In all cases studied, there is less than 10% deviation between the two values.

The diffusion coefficient can be calculated from Eq. [24]. In Table 19 are listed the values of the diffusion coefficient of the cationic gemini surfactants are studied. From these data, the following conclusion can be drawn. The diffusion coefficient decreases with:

1) increase in the bulk phase concentration of the surfactant;

Table 18 Equilibrium Surface Tension: Calculated from Eq.[26] (γ_e) and Measured by Wilhelmy Plate Method ($\gamma_{e\,q}$)

Compound	Media	γ_e (mN/m)	γ_{eq} (mN/m)
$(C_{10}N)_2Ar$ 25°C			
$1.12x10^{-5}M$	0.1N NaBr	54.4	54.4
$3.93x10^{-5}M$	0.1N NaBr	50.7	48.7
$1.27x10^{-4}M$	0.1N NaBr	45.2	44.0
$1.96x10^{-4}M$	0.1N NaBr	44.1	42.0
$1.12x10^{-5}M$	0.1N NaCl	62.4	60.5
$3.93x10^{-5}M$	0.1N NaCl	57.4	55.2
$1.27x10^{-4}M$	0.1N NaCl	53.6	51.3
$(C_{12}N)_2Ar$ 25°C			
$8.62x10^{-6}M$	0.1N NaCl	45.1	45.2
$1.12x10^{-5}M$	0.1N NaCl	44.6	44.4
$3.93x10^{-5}M$	0.1N NaCl	39.4	39.6
$(C_{12}N)_2Ar$ 50°C			
$6.64x10^{-4}M$	0.1N NaCl	44.3	45.0
$(C_{16}N)_2Ar$ 50°C			
$1.27x10^{-4}M$	0.1N NaCl	32.3	34.6
$(C_{10}N)_2OH$ 25°C			
$1.12x10^{-5}M$	0.1N NaCl	52.6	54.8
$3.93x10^{-5}M$	0.1N NaCl	50.5	49.2
$1.27x10^{-4}M$	0.1N NaCl	46.2	44.9

continued

continuation of Table 18

Compounds	Media	γ_e (mN/m)	γ_{eq} (mN/m)
$(C_{12}N)_2OH$ 25°C			
$1.12x10^{-5}M$	0.1N NaCl	30.1	33.0
$3.93x10^{-5}M$	0.1N NaCl	30.3	33.0
$1.27x10^{-5}M$	0.1N NaCl	31.4	33.0
$(C_{12}N)_2OH$ 25°C			
$1.27x10^{-4}M$	0.1N NaCl	31.1	32.0
$(C_{14}N)_2OH$ 50°C			
$1.27x10^{-4}M$	0.1N NaCl	28.1	28.0
$(C_{16}N)_2OH$ 50°C			
$1.27x10^{-4}M$	0.1N NaCl	26.5	28.0

Table 19 Apparent Diffusion Coefficients Calculated from Eq.[26]

Compound	Media	D x 10^6(cm^2/s)
$(C_{10}N)_2Ar$ 25°C		
$1.12x10^{-5}$M	0.1N NaBr	5.50
$3.93x10^{-5}$M	0.1N NaBr	0.49
$1.27x10^{-4}$M	0.1N NaBr	0.18
$1.96x10^{-4}$M	0.1N NaBr	0.17
$(C_{10}N)_2Ar$ 25°C		
$1.12x10^{-5}$M	0.1N NaCl	8.15
$3.93x10^{-5}$M	0.1N NaCl	3.74
$1.27x10^{-4}$M	0.1N NaCl	1.20
$(C_{12}N)_2Ar$ 25°C		
$8.62x10^{-6}$M	0.1N NaCl	3.89
$1.12x10^{-5}$M	0.1N NaCl	2.76
$3.93x10^{-5}$M	0.1N NaCl	0.62
$(C_{16}N)_2Ar$ 50°C		
$1.27x10^{-4}$M	0.1N NaCl	0.31
$(C_{10}N)_2OH$ 25°C		
$1.12x10^{-5}$M	0.1N NaCl	6.44
$3.93x10^{-5}$M	0.1N NaCl	2.55
$1.27x10^{-4}$M	0.1N NaCl	0.97
$5.00x10^{-4}$M	0.1N NaCl	0.33
$(C_{12}N)_2OH$ 25°C		
$1.12x10^{-5}$M	0.1N NaCl	2.56

continued

continuation of Table 19

3.93×10^{-5}M	0.1N NaCl	0.42
1.27×10^{-4}M	0.1N NaCl	0.11
$(C_{12}N)_2OH$ 50°C		
1.27×10^{-4}M	0.1N NaCl	2.63
$(C_{14}N)_2OH$ 50°C		
1.27×10^{-4}M	0.1N NaCl	0.08
$(C_{16}N)_2OH$ 50°C		
1.27×10^{-4}M	0.1N NaCl	0.01

Table 20 Relative Viscosities of Cationic Gemini Surfactant Solutions in water at 50°C

Compound	η/η^o
$C=3.25 \times 10^{-3}$M	
$(C_{18}N)_2OH$	3.13
$(C_{18}N)_2Ar$	1.03
$(C_{16}N)_2OH$	1.03
$(C_{16}N)_2Ar$	1.00
$C=6.55 \times 10^{-3}$M	
$(C_{16}N)_2OH$	1.23
$(C_{16}N)_2Ar$	1.02

2) increase in the alkyl chain length of the surfactant;

3) decrease in the temperature of the solution.

From the Stokes-Einstein equation (63):

$$D = (RT/N)(1/6\pi\eta r) \qquad [40]$$

where D is the diffusion coefficient, N the Avogadro constant, η the viscosity of medium, and r the radius of the particle.

Some of the above trends can be explained by this equation. Increase the alkyl chain length of the surfactant will increase the radius (r) of the molecule. The diffusion coefficients of the surfactants with a rigid, hydrophobic spacer are somewhat larger than those of the surfactants with a flexible, hydrophilic spacer. As explained above, this is probably because of the larger chain-chain interaction of the surfactant with flexible spacers, as evidenced by the higher viscosity of their solution (Table 20). It also appears that tighter binding of the counter-ion decreases the value of D, since the values in 0.1 N NaBr are smaller than in 0.1 N NaCl, but the data are too limited to determine whether this is generally true.

D.3.5. Surface Coverage (x_i) at t_i

The surface coverage at t_i was calculated by use of Eqs.[30-34]. The values of x_i, the ratio of surface coverage at t_i, the end of the

induction period, to the maximum equilibrium coverage are listed in Tables 13 and 14. The values are all in range 54-69%. This means that about two-thirds of the maximum possible coverage by surfactant molecules must be reached before the surface tension starts to be reduced significantly. Fig.28 shows that in both systems, the values of this ratio show little increase with relatively large increase in the surfactant bulk concentration.

D.3.6. Values of π_m, and π_{eq}

The meso-surface pressure, $\pi_m=\gamma_o-\gamma_m$, where γ_m is the surface tension, which does not change much with time, and γ_o is the surface tension of solvent, π_m must be smaller than or equal to the equilibrium surface pressure π_{eq}. Tables 13 and 14 show that the values of π_m and π_{eq} for both gemini series are equal or close to each other. In no case is π_m larger than π_{eq}. These data can be used for checking the accuracy of dynamic and equilibrium measurements.

D.3.7. Value of $|(d\gamma_t/d\log t)_{max.c}|$

The value of the product of n and π_m determines the maximum rate of reduction of surface tension in the fast reduction region, Eq. [35]. Table 15 lists data for both gemini series investigated under

similar conditions. Although the π_m values show a maximum for the optimum alkyl chain length, the continued increase in the value of n with increase in chain length causes the longer chain compounds to show a faster rate of surface tension change in the fast reduction region, Eq. [37]. In all cases, the geminis with a flexible hydrophilic spacer show a faster surface tension reduction rate than those with a rigid, hydrophobic one.

II. SUPERSPREADING OF SILICONE SURFACTANT SOLUTIONS

A. Introduction

A wetting agent is a surfactant which, when dissolved in a solvent, lowers the advancing contact angle and surface tension between the solid surface and the wetting liquid, and aids in displacing the air phase at the surface of the solid. The superspreading behavior is significant in several technologically important areas, including coatings and agrochemical formulations (64,65). Various kinds of sprays, such as insecticidal sprays, which should wet the waxy surface of leaves or the epidermi of insects; animal dips, where wetting of greasy hair is desired; inks, which should wet the paper properly; scouring of textile fibers, including the removal of unwanted natural oils and the subsequent wetting of the fibers by desirable solutions; and the laying of dust, where a fluid must penetrate between dust particles such as on roads or in coal mines (66). The wetting power of aqueous surfactant solutions is often measured by some dynamic method such as the Draves skein wetting test (67). On the other hand, wetting power can also be measured by the rate and extent of the spreading of the solution on some non-porous planar substrate (68). There is often a significant difference in the behavior of an aqueous solution of a particular

surfactant as measured by these two types of tests, even when both substrates are hydrophobic. Most noteworthy is the much better spreading behavior of aqueous solutions of certain surfactants containing trisiloxane hydrophobic groups, compared to aqueous solutions of surfactant containing alkyl hydrophobic groups on hydrophobic substrates such as Parafilm, even when the latter show somewhat better wetting behavior on hydrophobic cotton skeins in the Draves test. Because of this superior behavior of the trisiloxane derivatives on Parafilm, it has been named "superwetting" or "superspreading" by a number of investigators of the phenomenon (68, 70-74).

A.1. Previous Work:

Structures of some of the compounds studied are shown in Chart VII.

Various theories have been advanced for this superspreading behavior of the trisiloxane derivatives. Ananthapadmanabhan and co-workers (68) studied the wetting properties of three silicone surfactants, of which only the L-77 shows superspreading properties on a low energy surface (polyethylene). They believe this is the result of the compact nature, efficient adsorption and packing of L-77 molecules are readily adsorbed to the polyethylene interface

Chart VII

Structures of compounds used for spreading study

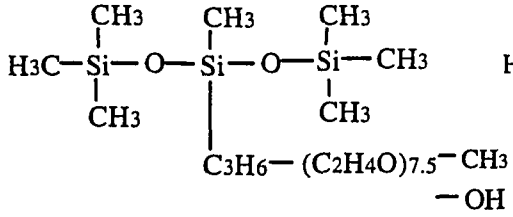

SILWET L-77

SILWET L-77 OH

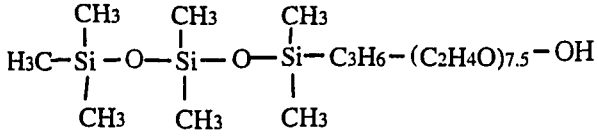

SILWET L-77 OH linear

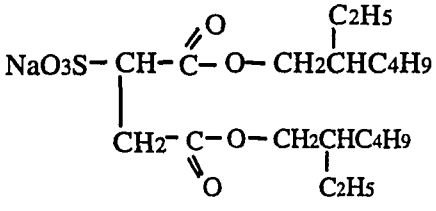

Di(2-ethylhexyl) sulfosuccinate)
(Aerosol OT-100)

Aerosol MA: Di (hexyl)
Aerosol A-196: Di (cyclohexyl)
Aerosol AY: Di (amyl)

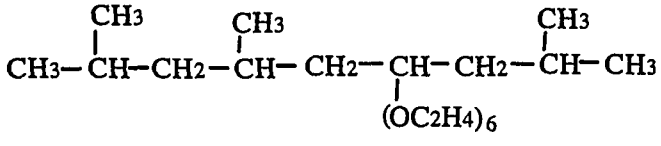

TMN-6

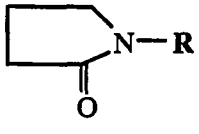

N-alkyl pyrrolidones

R	
C4P	$-C_4H_9$
C8P	$-C_8H_{17}$
C10P	$-C_{10}H_{21}$
C2,6P	$-CH_2-CH(C_2H_5)-(CH_2)_3-CH_3$
CHP	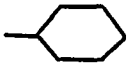

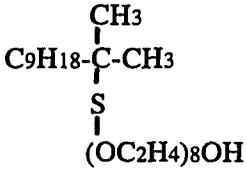

Alcodet SK

facilitating progressive advance of the liquid film in a manner like a "zipper". Fluorocarbon surfactants, which can lower the surface tension of water even further, do not wet polyethylene as efficiently. This is caused by to the fluorocarbon chain not being compatable with the hydrocarbon surface of Parafilm. The fluorocarbon chain not only repels water but also repels oil (69).

Ward and co-workers (73) used the quartz crystal microbalance (QCM) for the measurement of wetting rates of aqueous solutions of trisiloxane surfactant. This method provides for convenient measurement of spreading rates under a variety of conditions such as surfactant concentration, substrate surface energy, and humidity. They found the spreading velocities were greatest on surfaces of moderate hydrophobicity. Superspreading was observed on rough surfaces of high hydrophobicity but was negligible on smooth ones.

Davis and co-workers (74) have studied the spreading of aqueous solutions of six different silicone surfactants (the structures are shown in Chart VI) on Parafilm (low energy, hydrophobic surface). They found that only the four that are dispersed, rather than dissolved, spread in water and that the presence of water vapor is necessary for spreading. The presence of vesicles and finely-divided surfactant particles that act as reservoirs of the

superspreading agent at the spreading front was linked to superspreading. The initial spreading area wetted by the drop of solution was proportional to the surfactant concentration. They also reported that superspreading was not observed in dry air, but in supersaturated air spreading was even faster than the spreading observed in saturated air. The molecular geometry (whether the molecule is hammer-like or linear) of the trisiloxane is not critical factor for superspreading. However, the reason for superspreading behavior still remains unclear (74).

B. Theoretical Background

If a liquid (L) is spread over a substrate (S) and displaces the air (A) from its surface, the spreading coefficient ($S_{L/S}$) is defined as:

$$S_{L/S} = \gamma_{SA} - (\gamma_{SL} + \gamma_{LA}) \qquad [41]$$

where γ_{SA} is the interfacial tension between substrate and air, γ_{SL} the interfacial tension between substrate and liquid, and γ_{LA} the interfacial tension between liquid and air. If $S_{L/S}$ is positive, the spreading can occur spontaneously. One of the major roles of a surfactant lowers the surface tension of the solution (decreasing γ_{LA}), and thus increasing the $S_{L/S}$ value. For spontaneous spreading on a low free energy solid, the surface tension of the solution must be

lower than a specific value called the critical surface tension (75,76). Typical values are 43, 39, and 31 mN/m for polyethylene-terephthalate, PVC, and polyethylene, respectively (77).

The difficult problem of measuring the interfacial tension between solid and air (liquid) can be solved by using Young's equation (78), which is in the form:

$$\gamma_{LA} \cos\theta = \gamma_{SA} - \gamma_{SL} \qquad [42]$$

where θ is the contact angle between liquid and solid. By measuring the contact angle (θ) and surface tension of the solution (γ_{LA}), the spreading coefficient can be calculated by the equation:

$$S_{L/S} = \gamma_{LA} (\cos\theta - 1) \qquad [43]$$

This equation also shows that only when θ is zero, $S_{L/S}$ is ≥ 0 and the spreading is complete.

The current investigation is an attempt to provide some insights into the phenomenon of superspreading and its relationship to skein wetting.

C. Experimental Section

C.1. Materials: SILWET L-77, Tergitol TMN-6, 2-Et-1,3-hexanediol,

all commercial products, were supplied by Union Carbide Corp. L-77OH (-OH group instead of -OMe group in L-77), L-77OH linear (linear structure) both research compounds, were supplied by Dow Corning Corp. Alcodet SK, supplied by Rhone-Poulenc, Inc. 2-Me-2,4-pentanediol and 2-Me-butanol, were purchased from Eastman Kodak Co. The sodium di(2-ethylhexyl) sulfosuccinate (Aerosol OT), di(hexyl) sulfosuccinate (Aerosol MA), di(cyclohexyl) sulfosuccinate (Aerosol A-196), di(amyl) sulfosuccinate (Aerosol AY), all commercial products, were supplied by American Cynamid Co. The N-2-ethylhexyl-(C2,6P), and N-octyl-(C8P), N-decyl-(C10P), N-butyl-(C4P), N-cyclohexyl-(CHP), pyrrolidones, were supplied by GAF Corp. All compounds were used without further purification. Gemini surfactant, $(C_8N)_2OH$, was synthesized and purified in our lab. (See section C.1.).

C.2. Experimental:

C.2.1. Spreading Wetting (69): A 50 µl drop of the solution was placed, using a micro syringe, on a clean sheet of Parafilm stretched across an optically flat glass plate resting upon the horizontal mouth of a glass bottle. The diameter of the spread drop was measured as a

function of time for a total period of 5 minutes, using a metric ruler. The spreading factor (SF) is the ratio of the average diameter of the surfactant solution drop to that of a distilled water drop. An SF value of 6 or more in 4 minutes with an aqueous solution of 0.1% total surfactant concentration is considered "superwetting".

C.2.2. Draves Skein Wetting Test (79)**:** Standard skeins of gray, unwaxed cotton, folded to form 9 inch loops, each skein weighing 5.0g, were purchased from Testfabrics, Inc. (Middlesex, NJ.). Wetting times were done in duplicate. Wetting-out time (WOT) was measured on the cotton skein which were weighted with a 3g steel hook. Test solutions were prepared from deionized, distilled water. All measurements were made at room temperature (21±2°C).

C.2.3. Dynamic Surface Tension Measurements: Dynamic surface tension measurements were made using the maximum bubble pressure apparatus described previously. All measurements were made at 25±0.2°C.

C.2.4. Absorbance Measurements: The solution clarity was measured with a Beckman, Model DU quartz spectrophotometer, at 600 nm, at 21±2°C.

Table 21 Skein Wetting Out Times (WOT) and Spreading Factor (SF) of 0.1% Aqueous Surfactant Solutions at 21±2°C

Surfactant	WOT (s)	SF (5min.)
L-77	9.9	8.6
L-77 (after 72 hrs.)		2.2
L-77OH	9.5	8.5
L-77OH linear	6.5	7.4
Aerosol OT 100	2.0	1.6
Tergitol TMN-6	2.7	2.2
Alcodet SK	7.6	1.8

Table 22 Absorbance (A) of 0.1% aqueous surfactant solutions at 600 nm

Surfactants	% additive	A	% additive	A
L-77	0	0.081	after 72 hrs	0.035
L-77OH	0	0.222		
L-77OH linear	0	0.069		
AOT in L-77	1	0.031	2	0.014
	3	0.010	5	0.000
	100	0.000		
MA in L-77	3	0.078	5	0.068
	10	0.056	20	0.050
	30	0.032	50	0.015
	60	0.014	80	0.011
	100	0.000		

continued

continuation of Table 22

Surfactant	% additive	A	% additive	A
A196 in L-77	10	0.064	20	0.054
	40	0.034	60	0.025
	80	0.011	100	0.000
AY in L-77	20	0.056	30	0.048
	40	0.041	60	0.028
	80	0.012	100	0.000
C4P in L-77	10	0.071	20	0.058
	30	0.049	40	0.034
	50	0.025	60	0.020
	70	0.007	100	0.000
C2,6P in L-77	10	0.071	20	0.060
	30	0.052	40	0.041
	50	0.030	60	0.021
	70	0.012	80	0.004
	100	0.000		
C8P in L-77	10	0.088	30	0.070
	50	0.053	100	0.000
TMN-6 in L-77	20	0.058	30	0.050
	50	0.031	70	0.000
SK in L-77	10	0.061	30	0.046
	100	0.000		

D. Results and Discussion:

D.1. Skein Wetting and Superspreading:

The lack of any relationship between spreading wetting on Parafilm and Draves skein wetting is apparent from the data shown in Table 20. Here, the alkyl chain derivatives show better skein wetting behavior then the trisiloxane derivatives. One reason may be the partial solubility of the trisloxane derivatives in water (Table 21). It has been shown previously (80), that surfactants that are not completely soluble in water at the concentration used show longer Draves wetting times, even when they are capable of reducing the equilibrium surface tension of water to a low value. Another reason may be the higher surface tension values (Fig.29) of the trisiloxane derivatives at short times (< 1s).

Typical superspreading behavior (SF>6 in 4 min.) is shown in Fig.30, for three trisiloxane derivatives at 0.1% (w/w) concentration. The alkyl chain surfactants, which have excellent skein wetting times, have SF values of about 2.

D.2. Dynamic Surface Tension

The dynamic surface tension data shown in Fig. 29 sheds some

light on the differences in skein wetting and spreading behavior. Although the alkyl chain containing surfactants in Fig.29 reach lower surface tension values at shorter times (≥0.2s) than the trisiloxane derivatives, which make the former faster skein wetters, these values do not change much with time. Consequently, the SF values for these compounds remain almost unchanged with time (Fig.30). On the other hand, although the trisiloxane derivatives show higher surface tension values than the alkyl chain surfactants at very short times (≤ 0.2s), the surface tension values of the former continue to decrease with time and reach values below those of the latter (Fig.29). Since spreading increases with decrease in the surface tension of the solution, Eq. [41], the SFs of the trisiloxane derivatives continue to increase during the first few minutes of the test and reach higher values than attainable by the alkyl chain surfactants.

This reduction of the surface tension to about 21 mN/m consequently appears to be a necessary condition for superspreading. However, it appears not to be a sufficient property for optimum superspreading. The three trisiloxane derivatives all show rather similar dynamic surface tension behavior (reaching about 21 mN/m values in 10 s), but show rather different SF values. In fact the linear L-77OH shows the lowest dynamic surface tension values (Fig.29) at all times up to 10 s, but gives the lowest SF value

of the three trisiloxanes (Fig.30). Additional evidence for the necessary but not sufficient relationship between dynamic surface tension values and optimum superspreading is seen in Figs. 31 and 32. It shows that SF values for the mixture of L-77 with TMN-6 were less than that of L-77 by itself but the dynamic surface tension values of the mixture were at least as low as that of the latter. Fig.33 shows that there is no significant difference between the dynamic surface tension of the solutions of L-77 with additive C2,6P and L-77 itself.

D.3. Mixtures of Superspreader and Other Surfactants

In an effort to further determine the importance of the presence of dispersed surfactant particles in superspreading, a surfactant that could solubilize these dispersed particles (Aerosol OT) was added to aqueous solutions of the L-77. Data are shown in Table 21. The replacement of over 5% of L-77 by Aerosol OT yielded a clear solution. The SF values of the 5% Aerosol OT and L-77 mixture are not very different from those of L-77 by itself, indicating that the absence of dispersed particles did not decrease the SF value of the L-77 appreciable.

Further investigation of the replacement of a portion of L-77 by non-superspreading surfactants (Aerosol series, sulfosuccinate),

showed that the SF values for the mixtures could be larger than that of L-77 by itself (See Fig.35). That is, the mixtures exhibit synergism in superspreading. In each case, the addition of the non-superspreading synergistic surfactant resulted in an increase of the SF value of the mixture to that greater than that of L-77 alone, with a maximum being reached at a L-77: additive ratio that varied with the length of the alkyl chain of the additive. In the case of sulfosuccinate additives, the amount of L-77 that could be replaced in the mixture at the maximum SF value increased with decrease in hydrophobic chain length in the order: di(2-ethylhexyl) $\ll$dihexyl $\ll$ diamyl, dicyclohexyl. On the other hand, the SF value at the maximum increased in the order: di(2-ethylhexyl) < diamyl < dicyclohexyl < dihexyl.

In order to find the relationship between enhancement of superspreading and the structure of the additive, the following compounds have been tested as additives: nonionic surfactants: N-alkylprrolidones (Fig.36); non/low surface active agents, 2-Et-1,3-hexanediol and 2-Me-butanol (Fig.37); and cationic surfactants, $(C_8N)_2OH$ and $C_8H_{17}N(CH_3)_3Br$ (Fig.38). From all the above results, the following conclusions can be drawn:

1) The additive can be a non or low surface active agent. This means the enhancement of superspreading is not caused by the further

lowering the surface tension of the solution. This also showed in the dynamic surface tension study. Fig.29 shows that the surface tension is the same for the solution with additive as that of the L-77 by itself.

2) The type of head group of the additive has no effect on the enhancement of superspreading. The enhancement effect depends only on the length of the alkyl chain of the compound.

3) The optimum amount of additive which gives the maximum SF values is about 30%.

4) Maximum enhancement appears to be achieved by using a compound with an eight carbon atom branched chain. For example, by adding 30% 2-Et-1,3-hexanediol to L-77, the SF value for a 0.1% total solute concentration aqueous solution can be increased by 270%.

Fig.39 shows the dynamic spreading (SF value change with time) data for mixed solutions with and without spreading synergism. The spreading rate is correlated with the equilibrium SF value, that is, the larger the equilibrium SF value, the faster the spreading.

- END-

Figure 1 Surfaec tension vs. logC of (C12N)2OH in 0.1N NaCl at 50°C, measured by POS and PIS

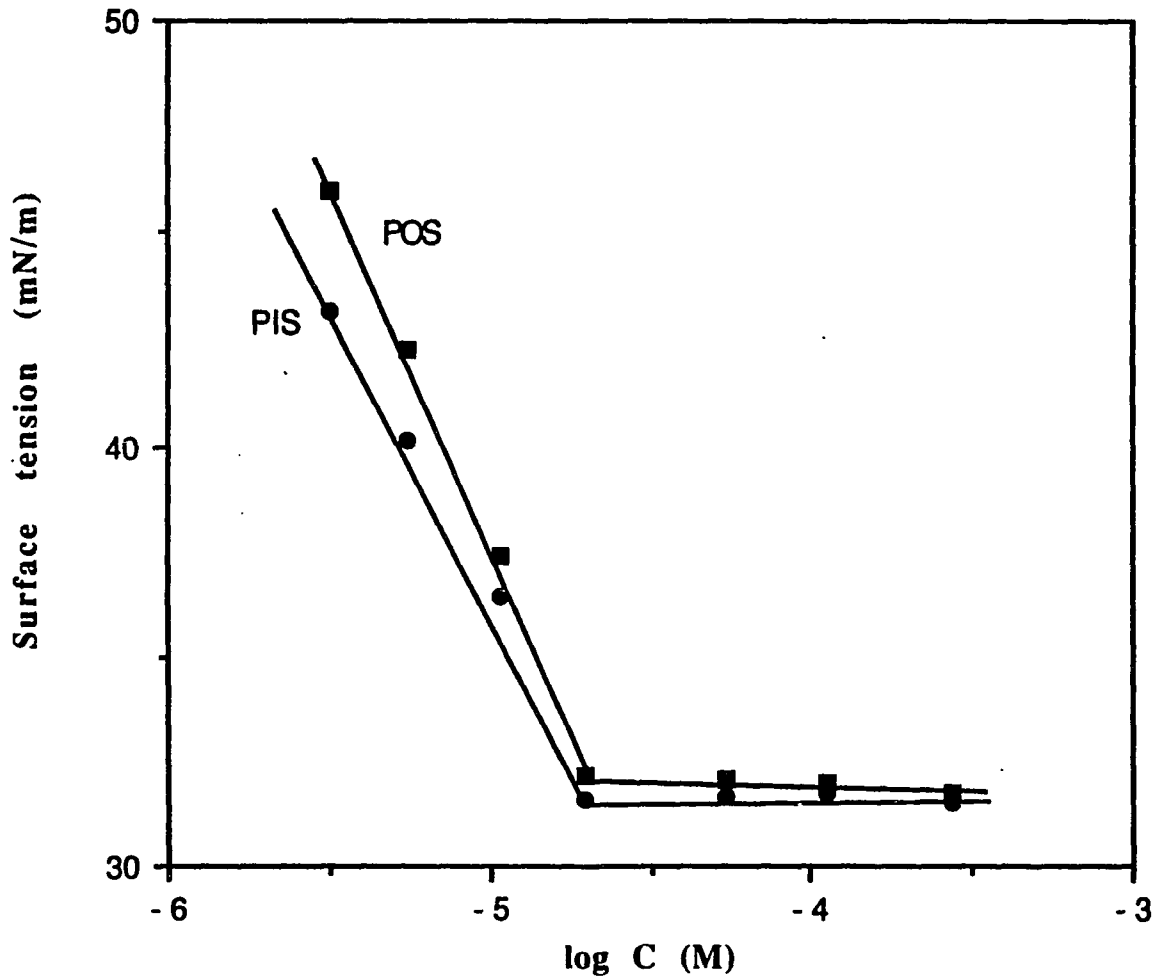

Figure 2 Surface tension vs. logC (C14N)2OH and (C16N)2OH in 0.1 N NaCl at 25°C

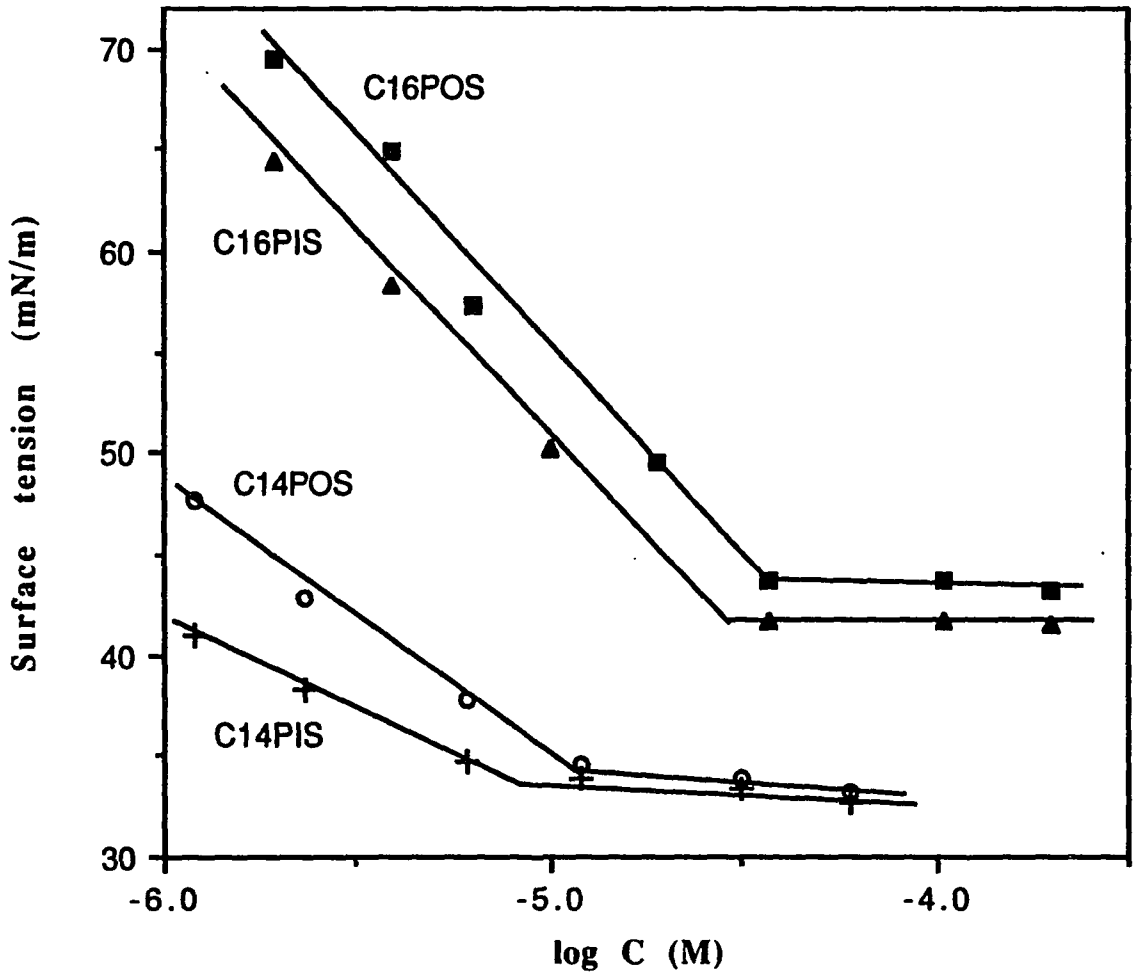

Figure 3 **Surface Tension vs. Time for (C12N)2Ar in H2O at 50°C Measured by POS and PIS**

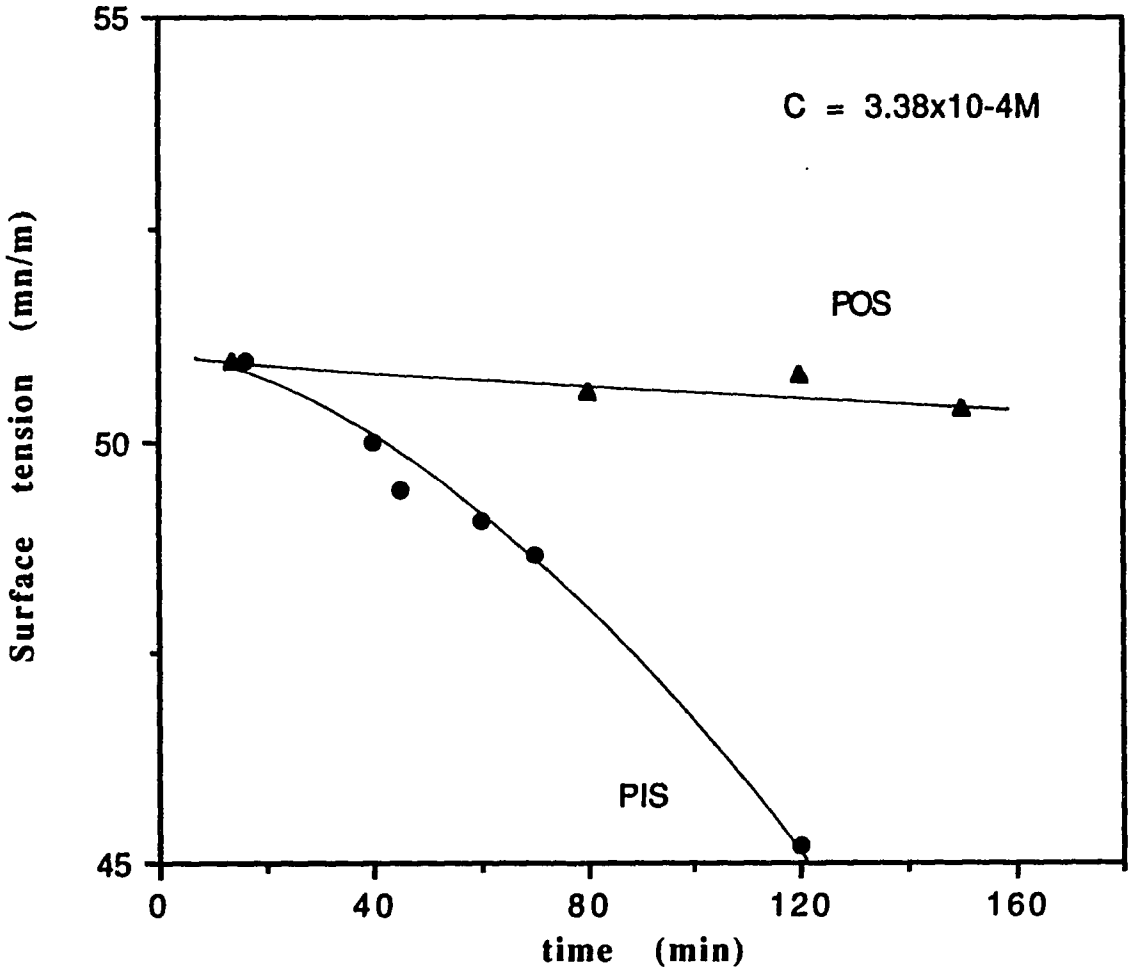

Figure 4 Calibration curve of transducer without correction for density of acetone, nitrobenzene, and water

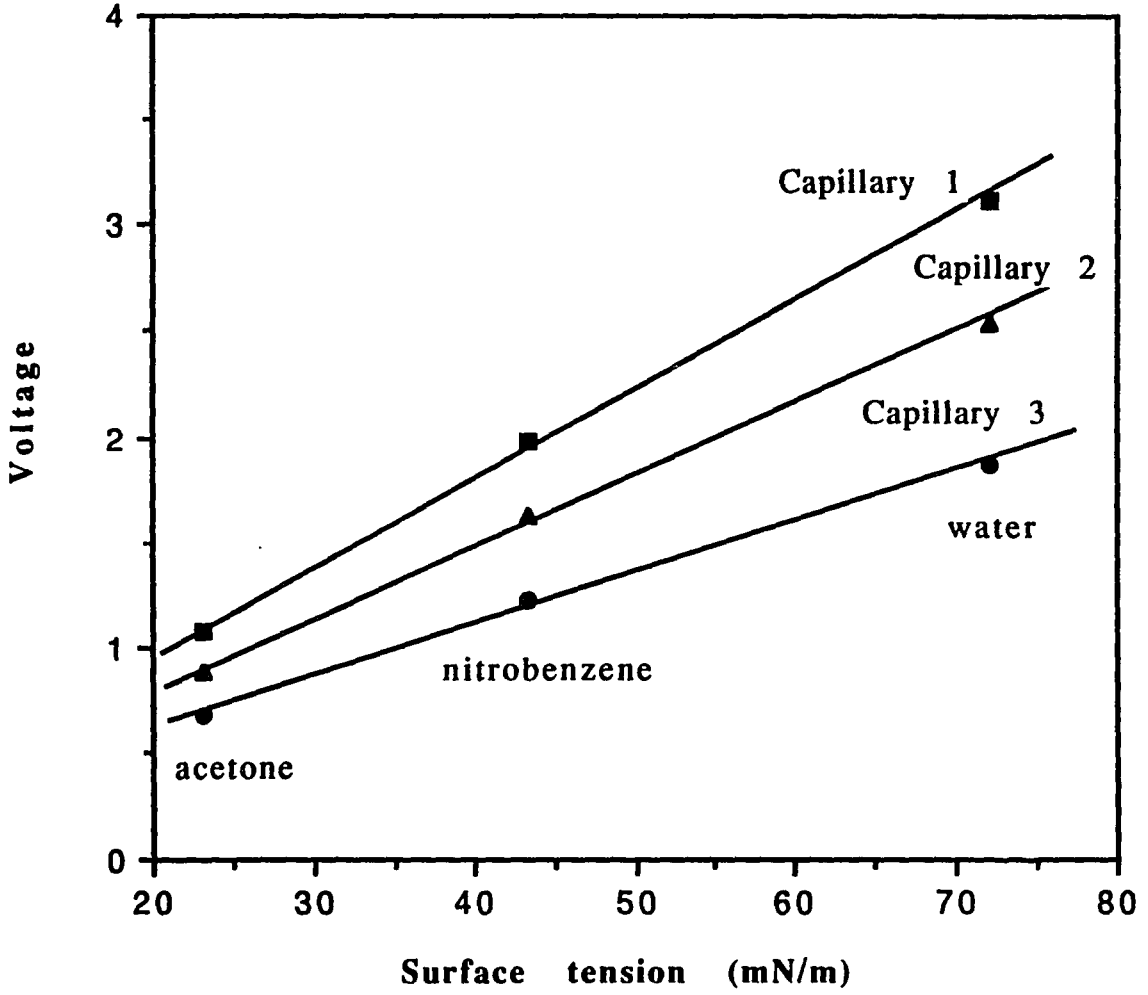

Figure 5 Calibration curve of transducer with correction for density of acetone, nitrobenzene, and water

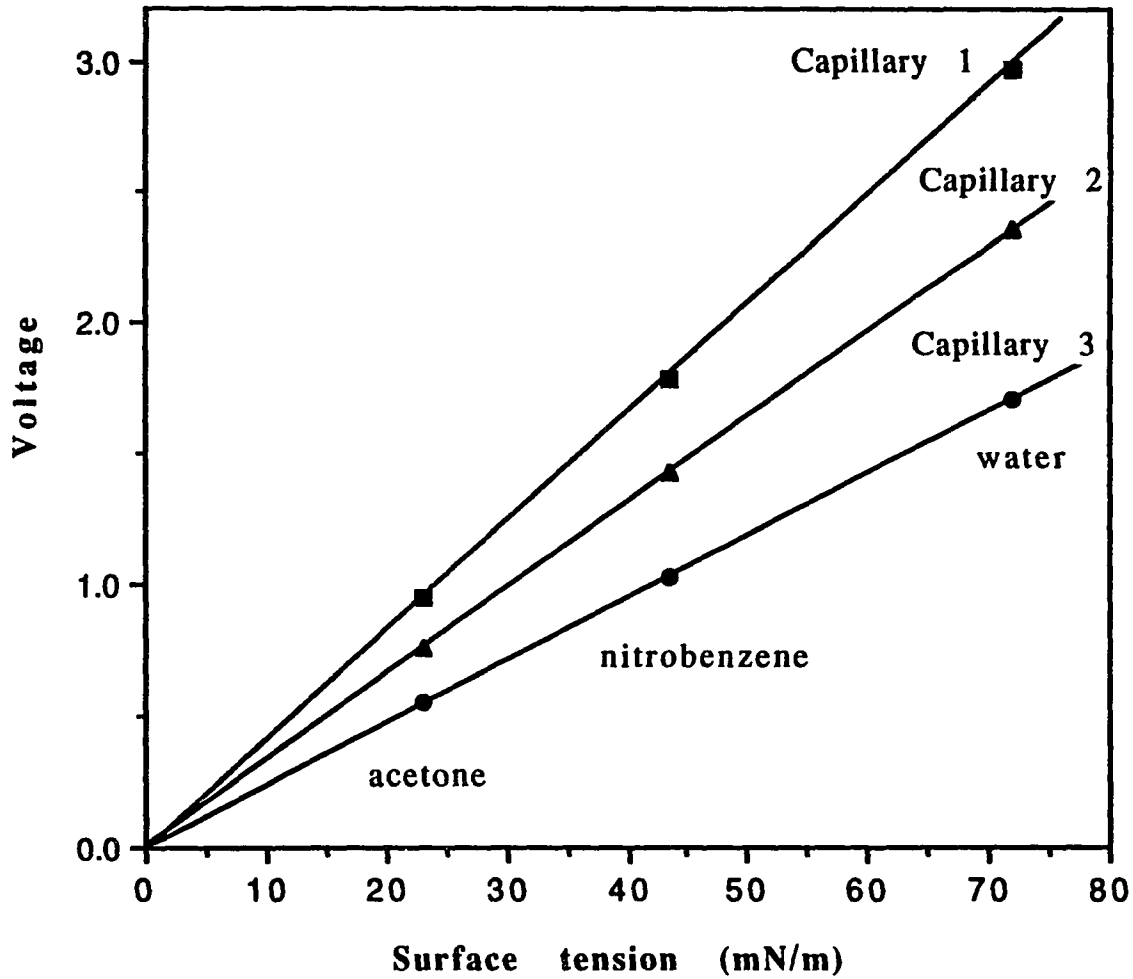

Figure 6 Counterion effect on the surface-activity, (CnN)2Ar series at 25°C

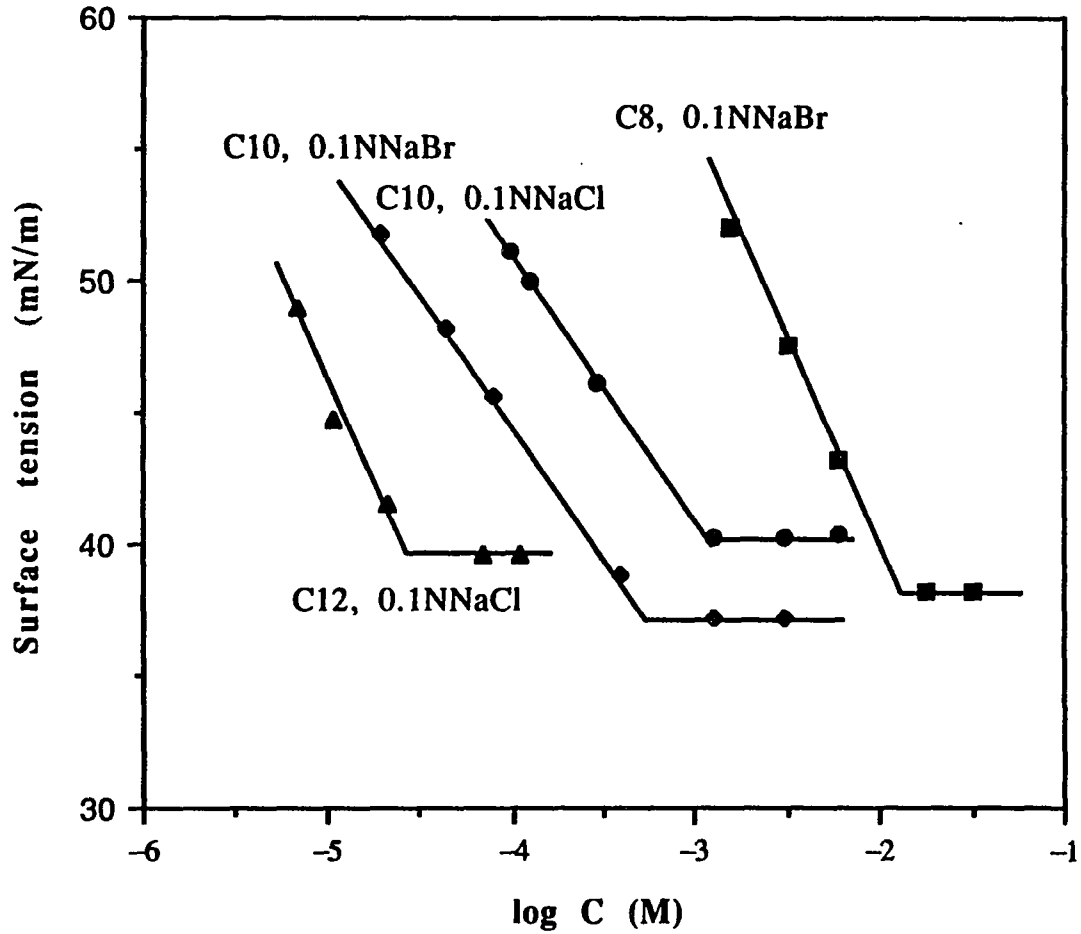

Figure 7 Surface tension vs. log C of (CnN)2Ar series in 0.01N NaCl at 50°C

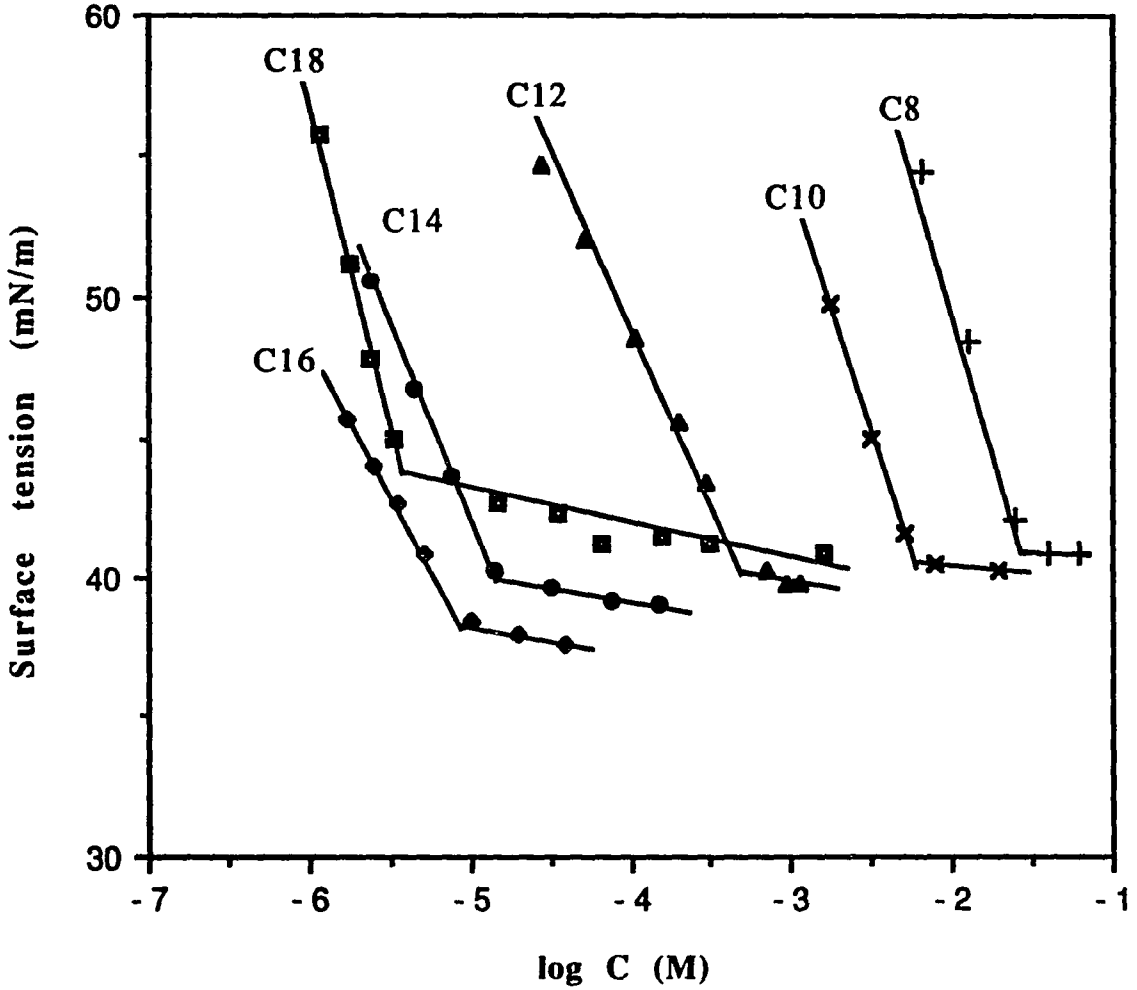

Figure 8 Surface tension vs. logC of (CnN)2Ar in 0.1N NaCl, at 50°C, plus calculated expected curve for C14 in absence of self-aggregation

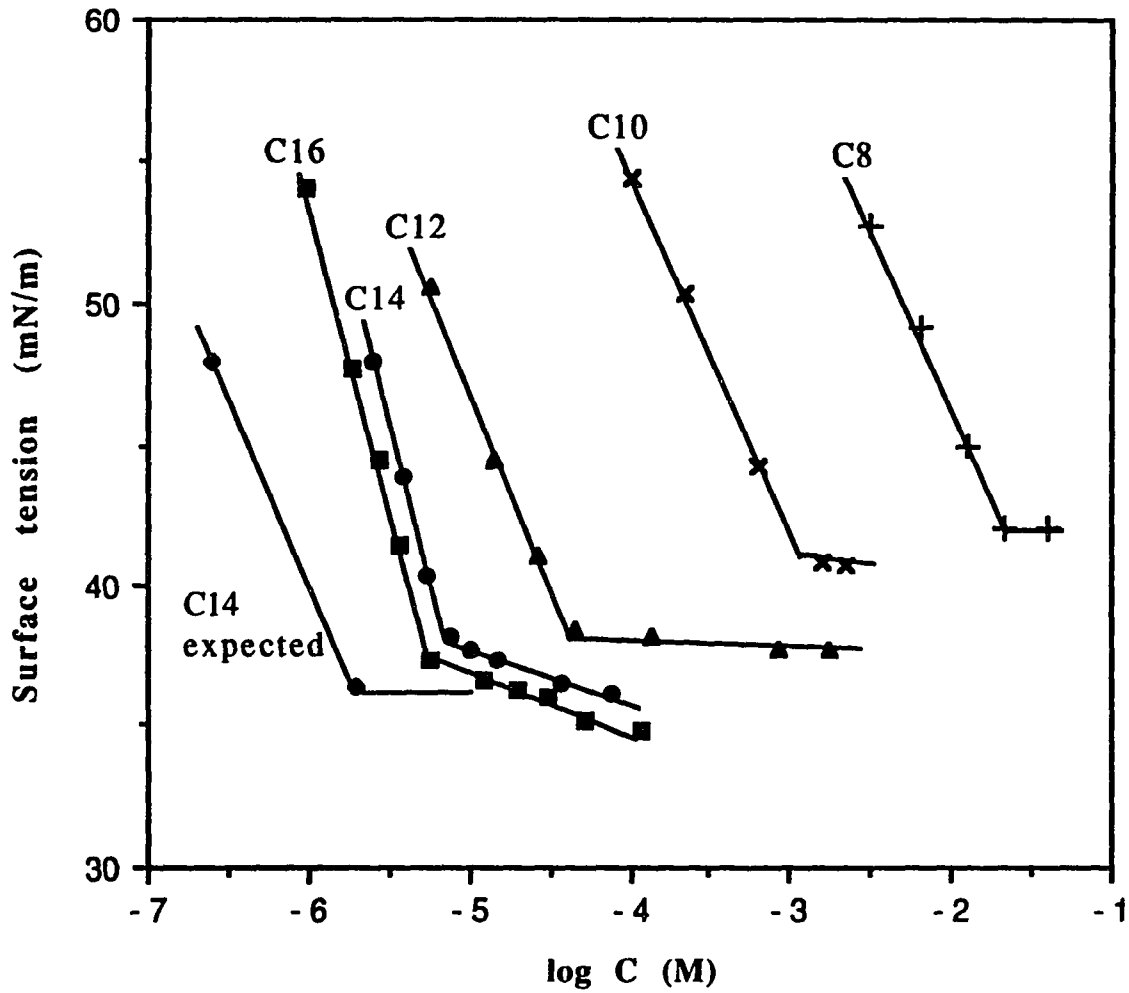

Figure 9 Surface tension vs. logC of (CnN)2OH in 0.1N NaCl at 50°C

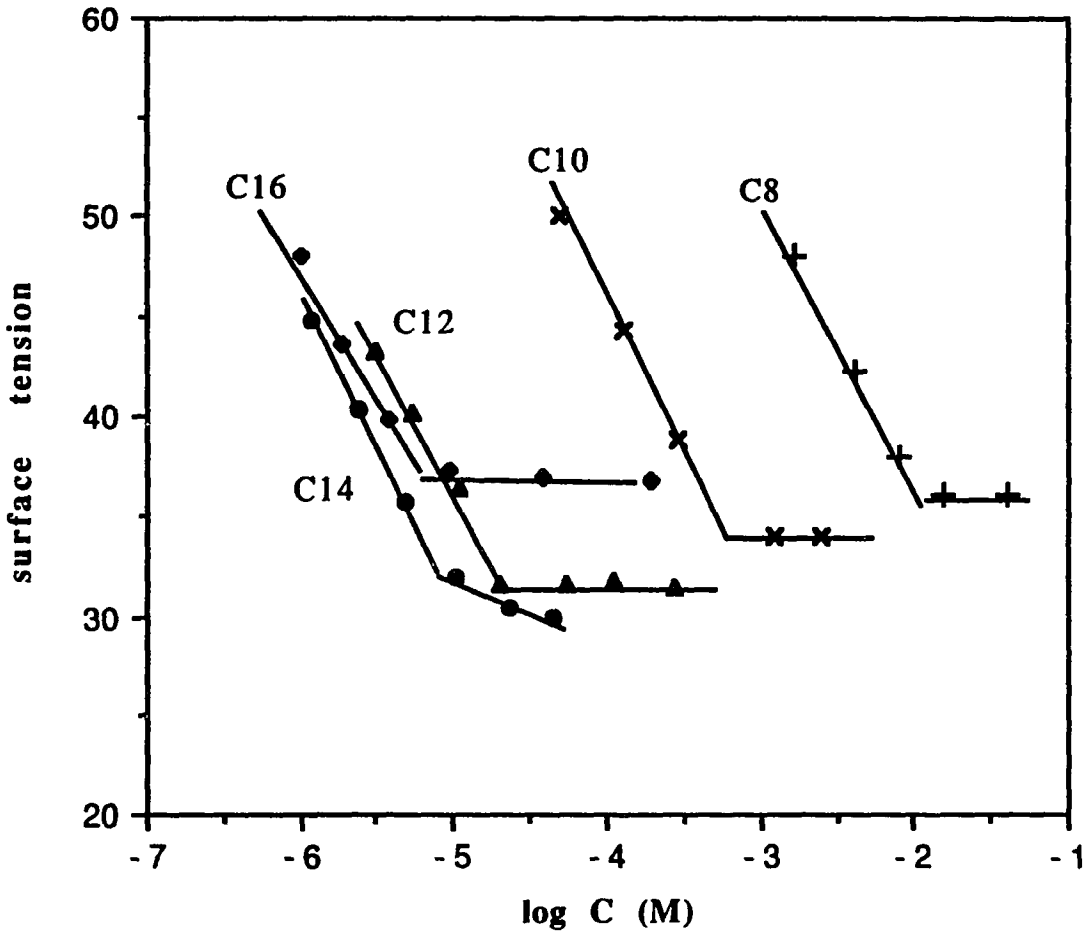

Figure 10 Surface tension vs. logC of (CnN)2OH in 0.1N NaCl at 25°C

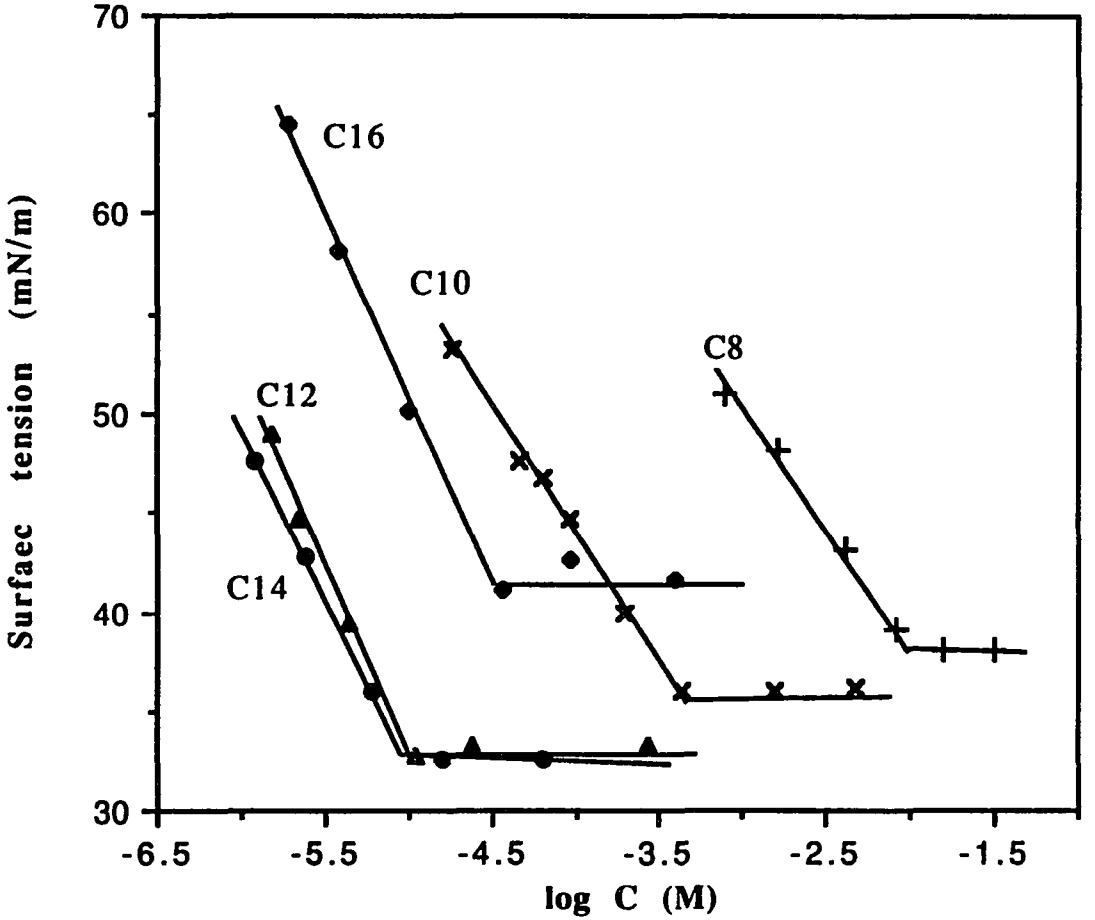

Figure 11 log CMC vs. carbon number (n) for (CnN)2Ar series in 0.1 and 0.01 N NaCl at 50°C

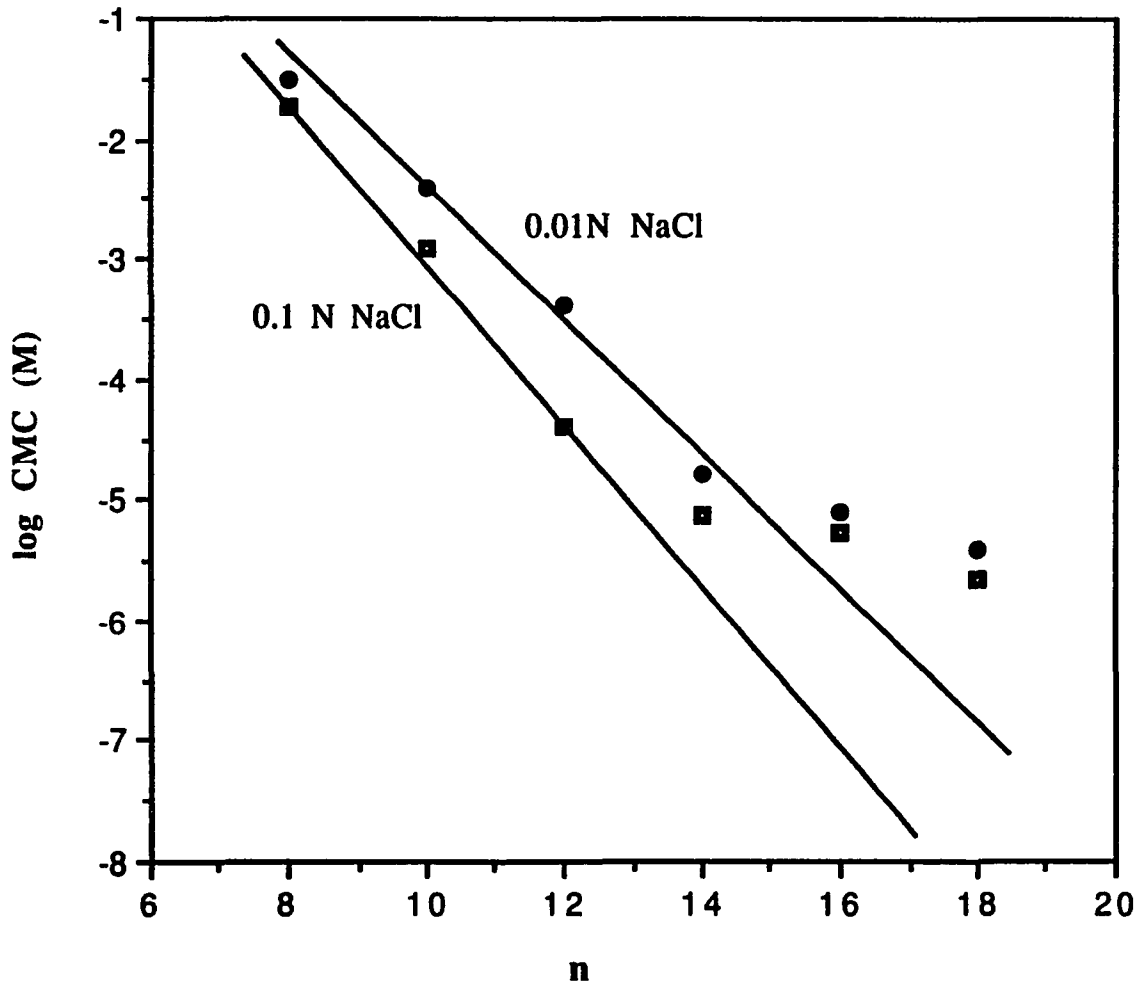

Figure 12 log CMC vs. carbon number (n) of (CnN)2OH series in 0.1 N NaCl at 25°C and 50°C

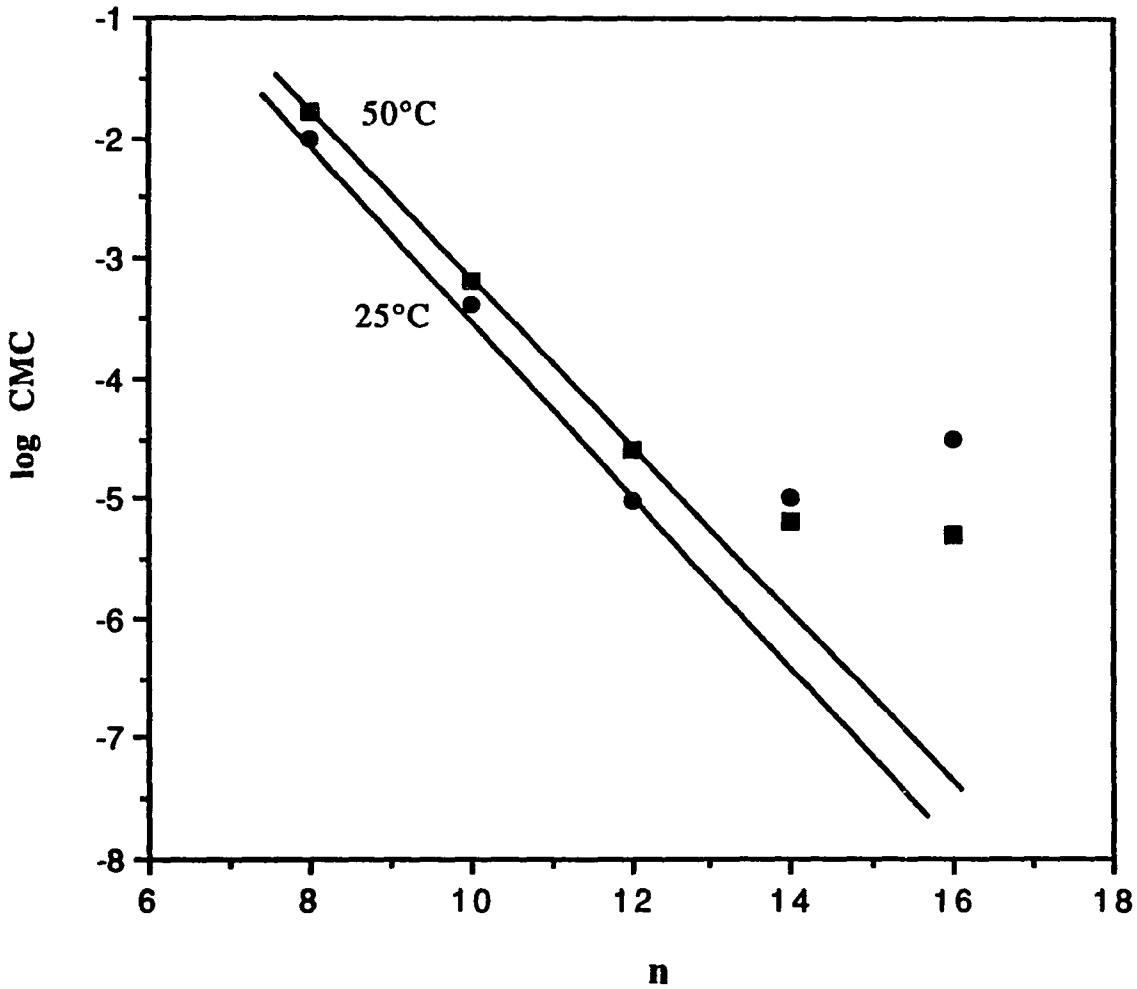

Figure 13 pC20 vs. carbon number (n) of (CnN)2Ar in 0.1 and 0.01 N NaCl at 50°C

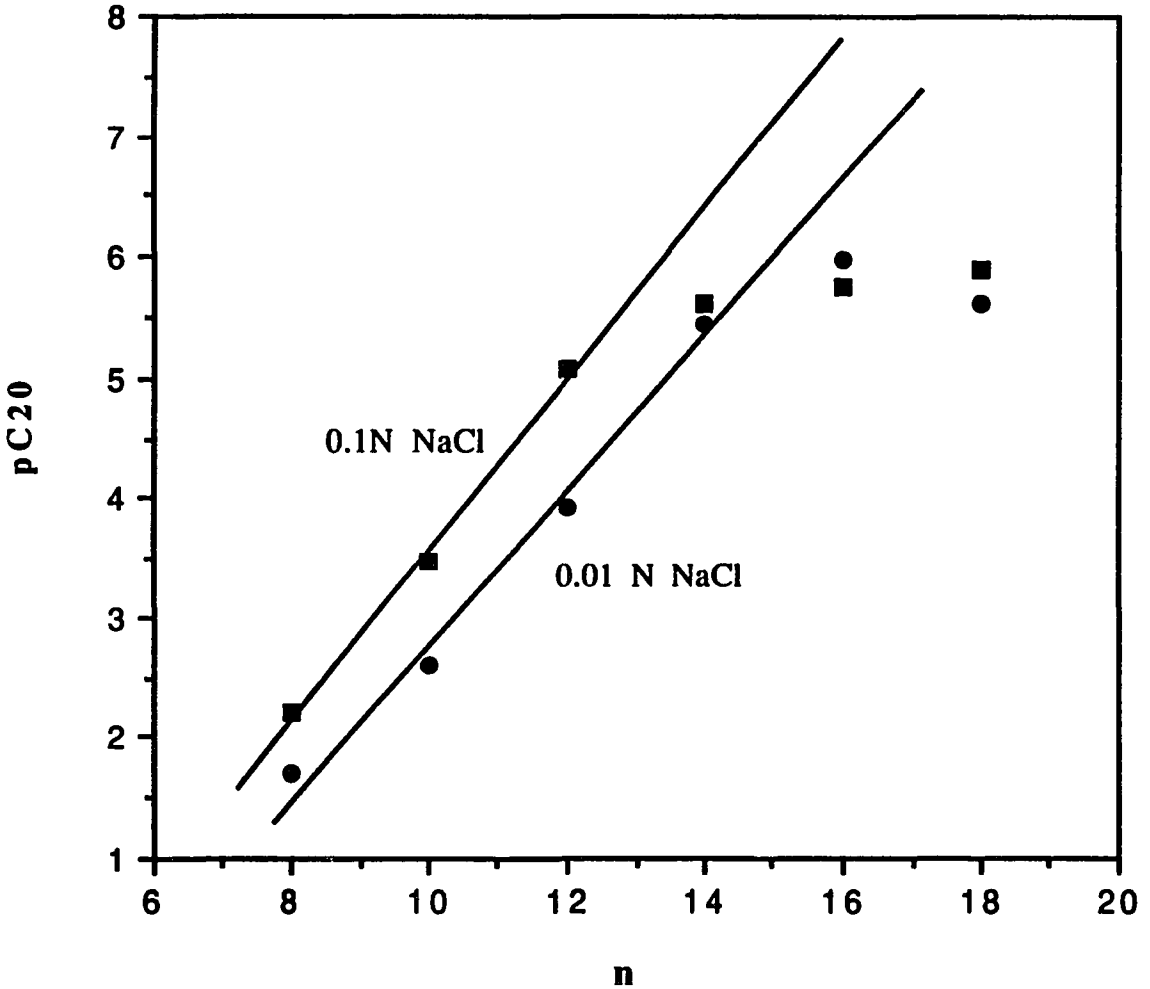

Figure 14 pC20 vs. carbon number (n) of (CnN)2OH in 0.1N NaCl at 25°C and 50°C

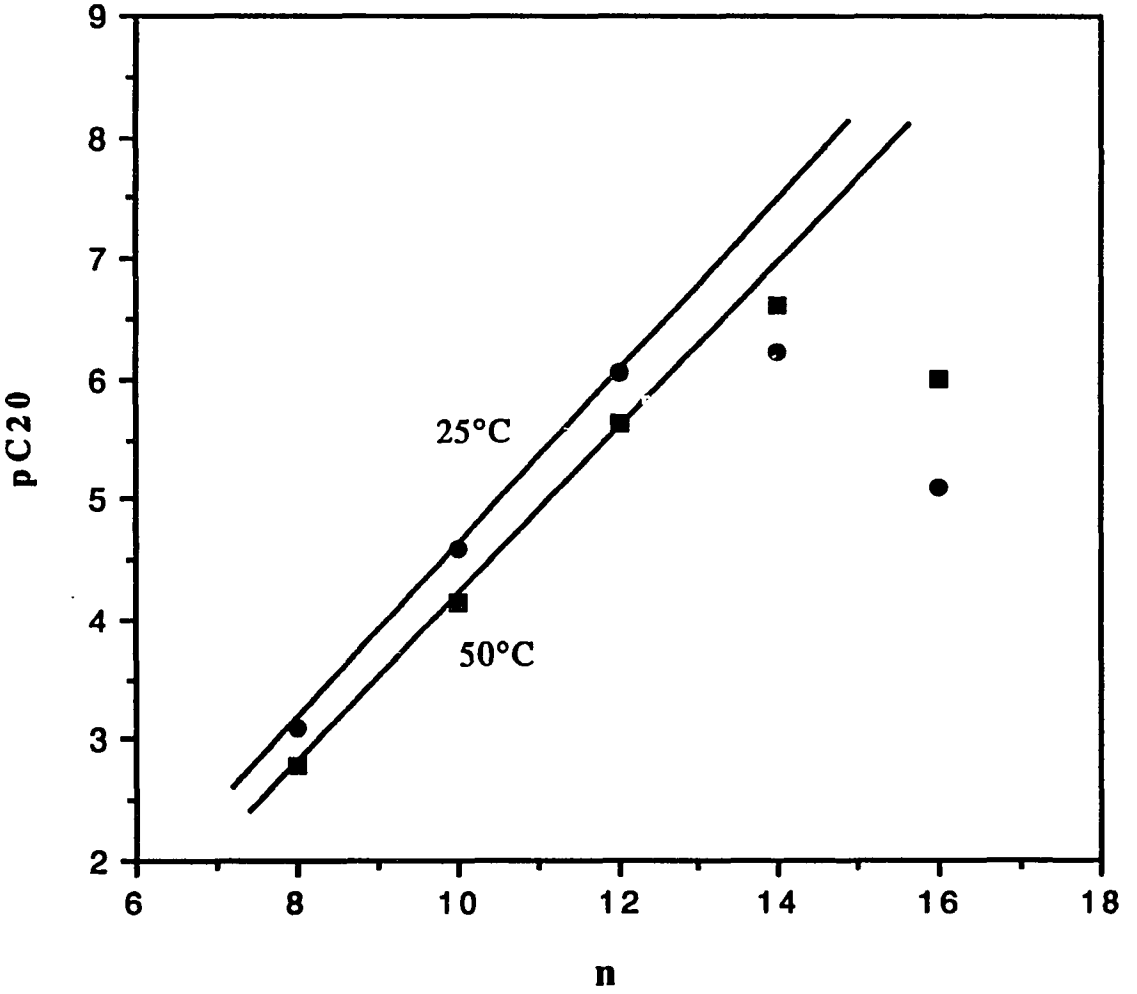

Figure 15 Surface tension vs. log C of (C18N)2Ar in 0.1 N NaCL at 50°C

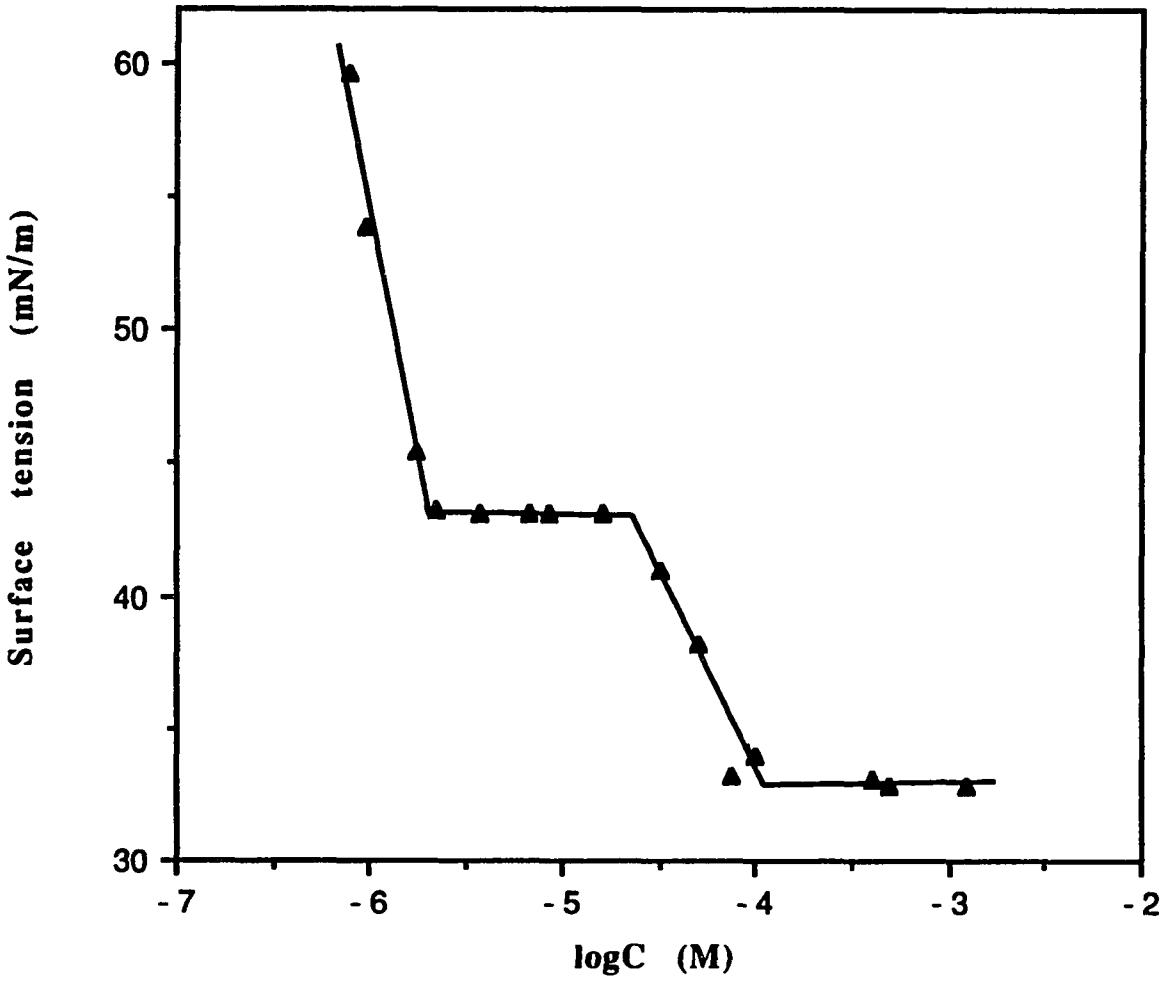

Figure 16 Surface tension vs. log C of (CnN)2Ar series in water at 50°C

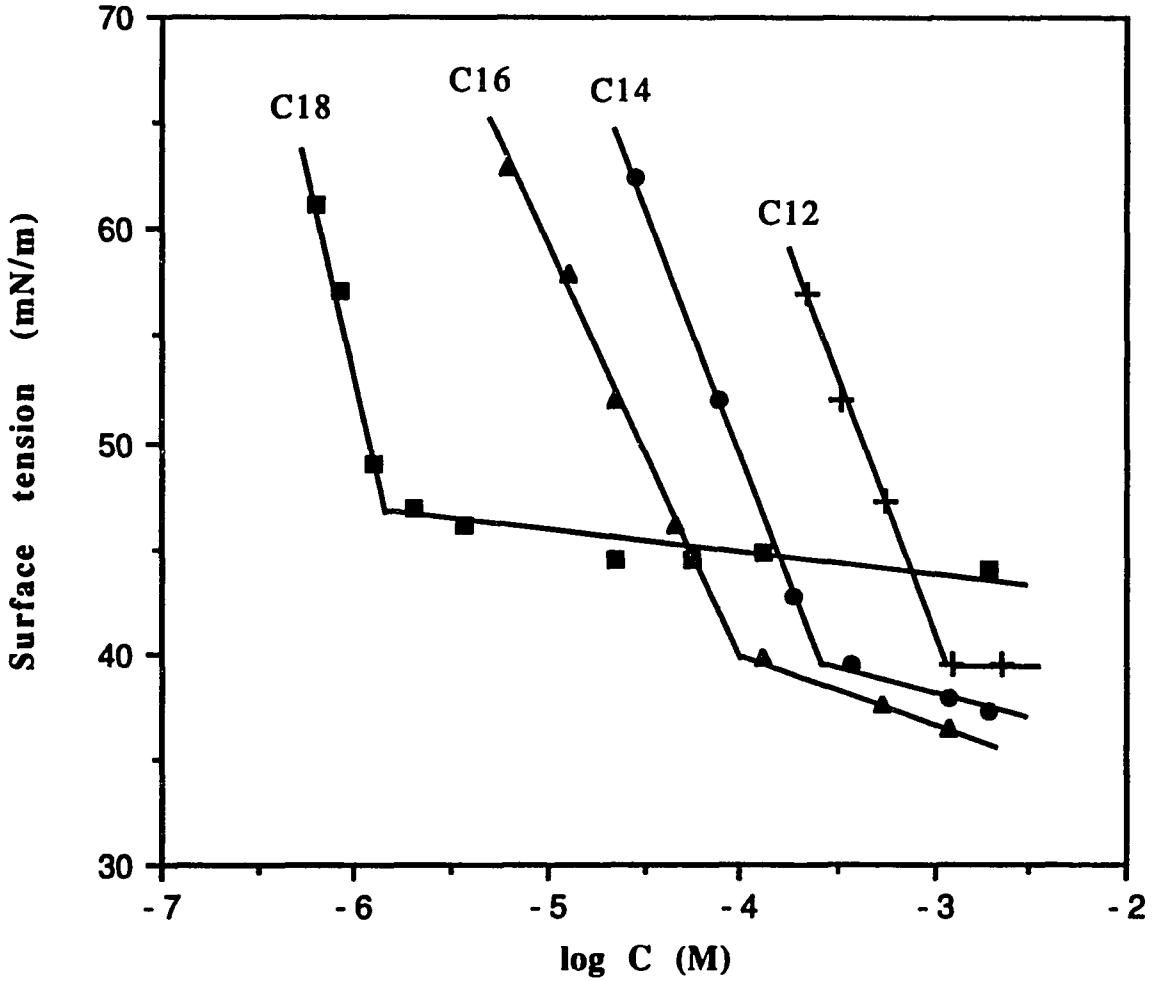

Figure 17 Surface tension vs. logC of (C18N)2OH in H2O and 0.1N NaCl at 25°C and 50°C

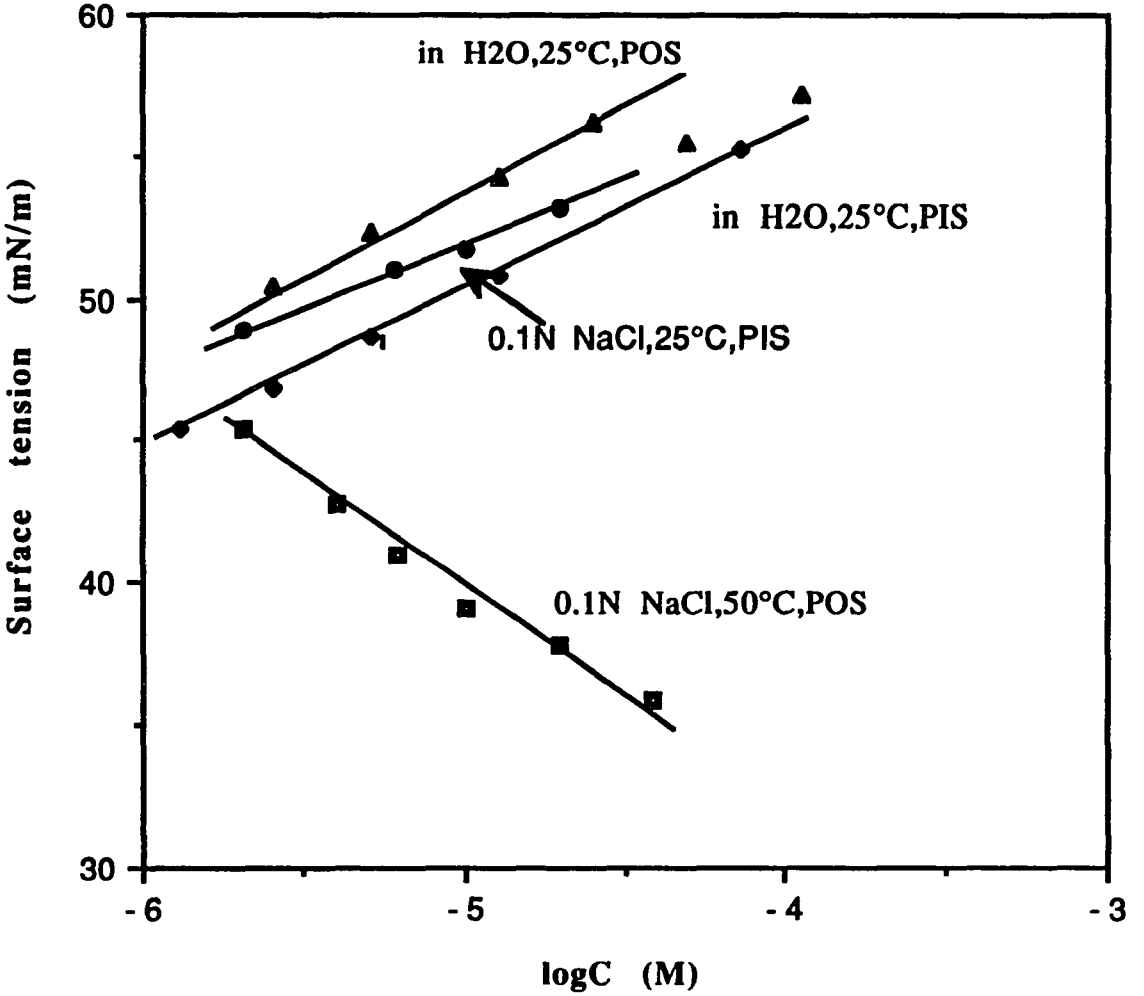

Figure 18 Surface tension vs. logC of (C8N)2OH and (C10N)2OH and their mixtures with C12EO2S in 0.1NNaCl at 25°C, α=0.17

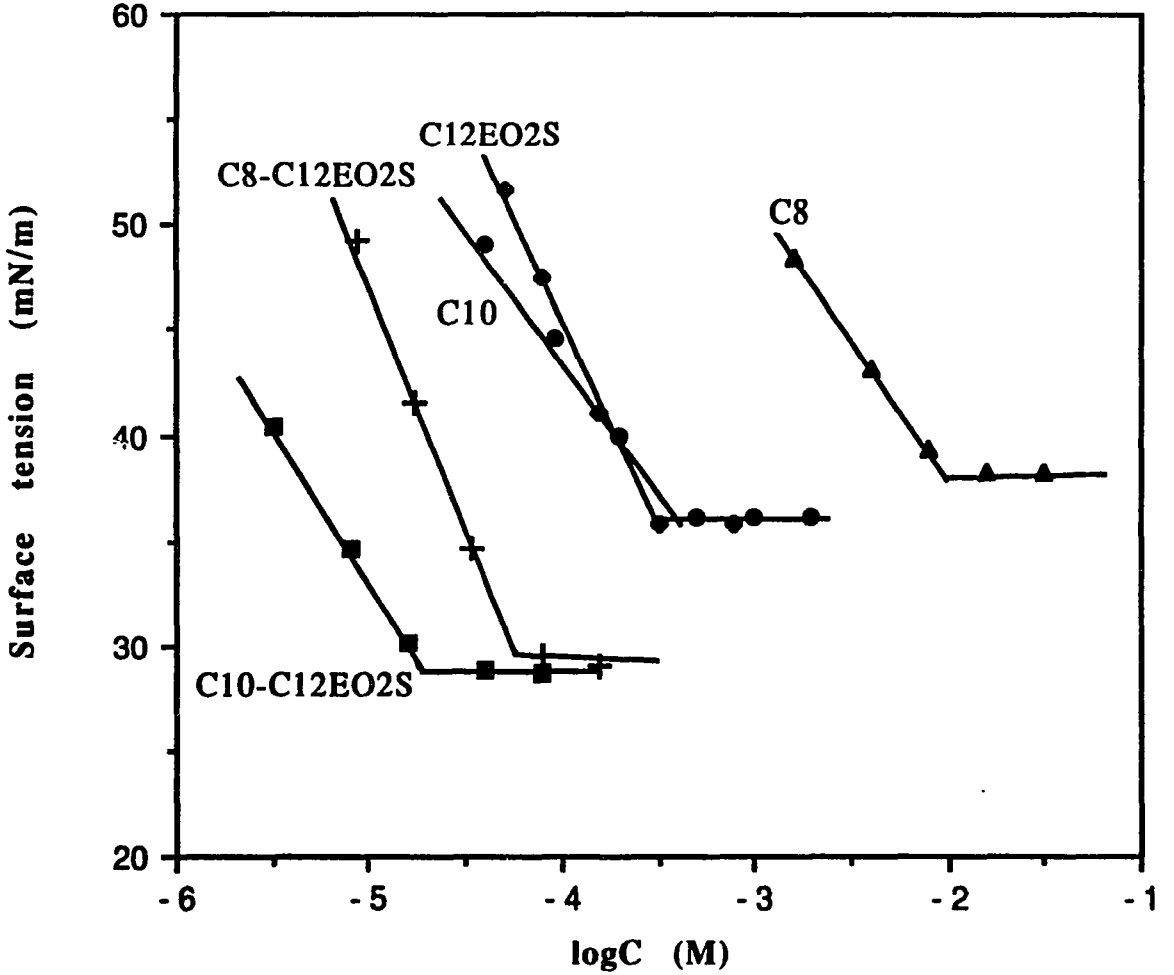

Figure 19 Surface tension vs. logC of (C10N)2OH, (C10N)2Ar and their mixture with C12EO2S in 0.1NNaCl at 25°C, α =0.17

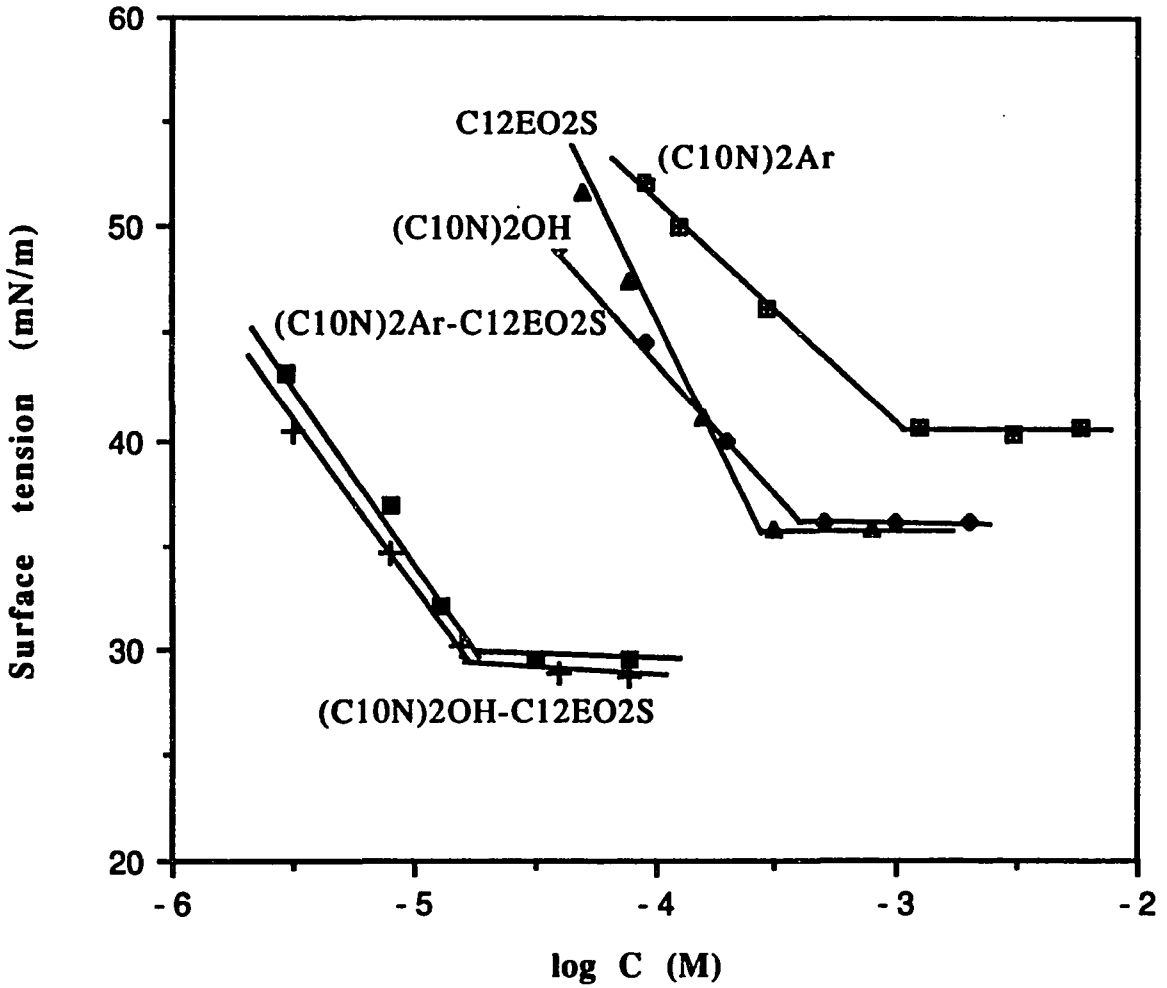

Figure 20 Surface Tension vs. log C of (C12N)2OH and (C14N)2OH and their Mixtures with C12EO2S in 0.1NNaCl at 25°C, α=0.17

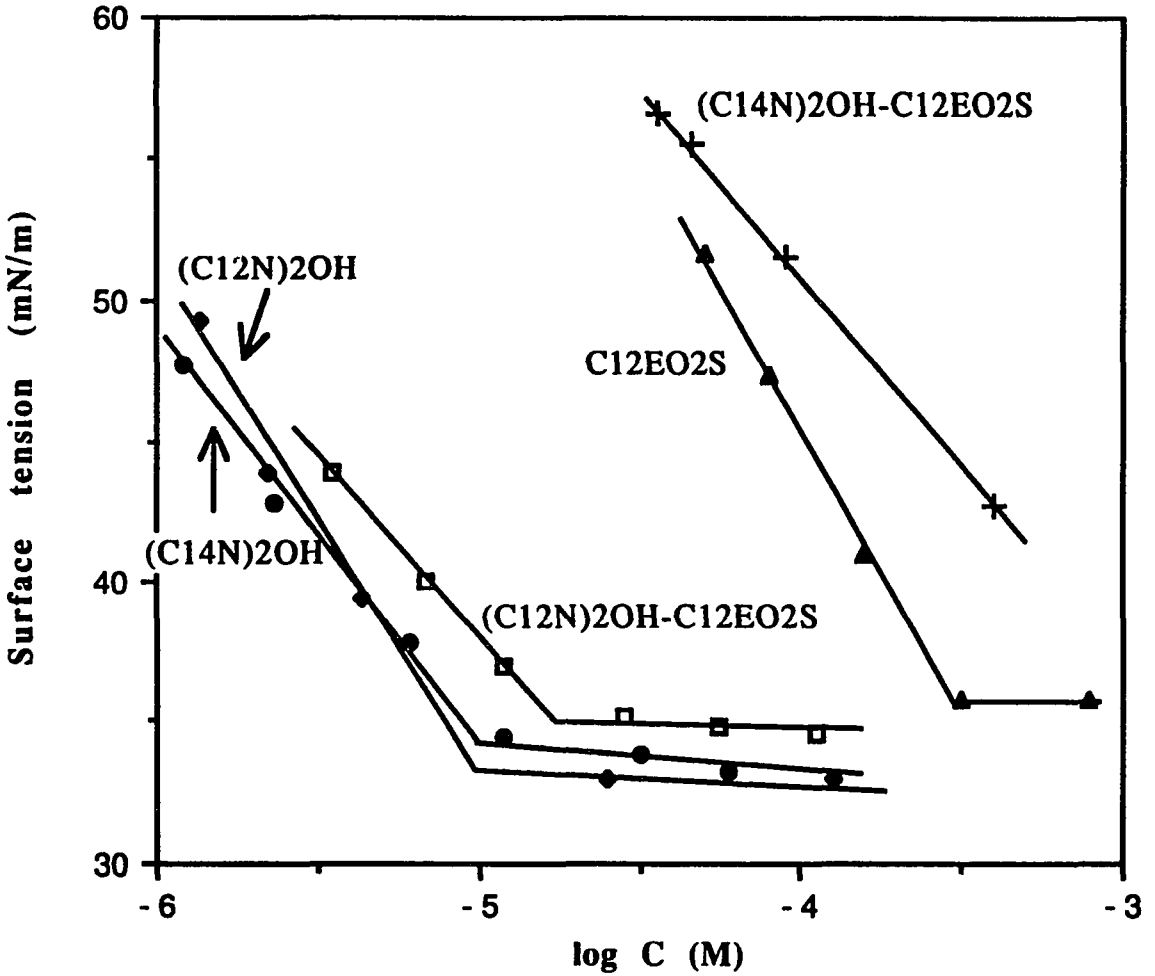

Figure 21 Dynamic surface tension vs. time of (C10N)2Ar and (C12N)2Ar in 0.1 NaCl at 25°C

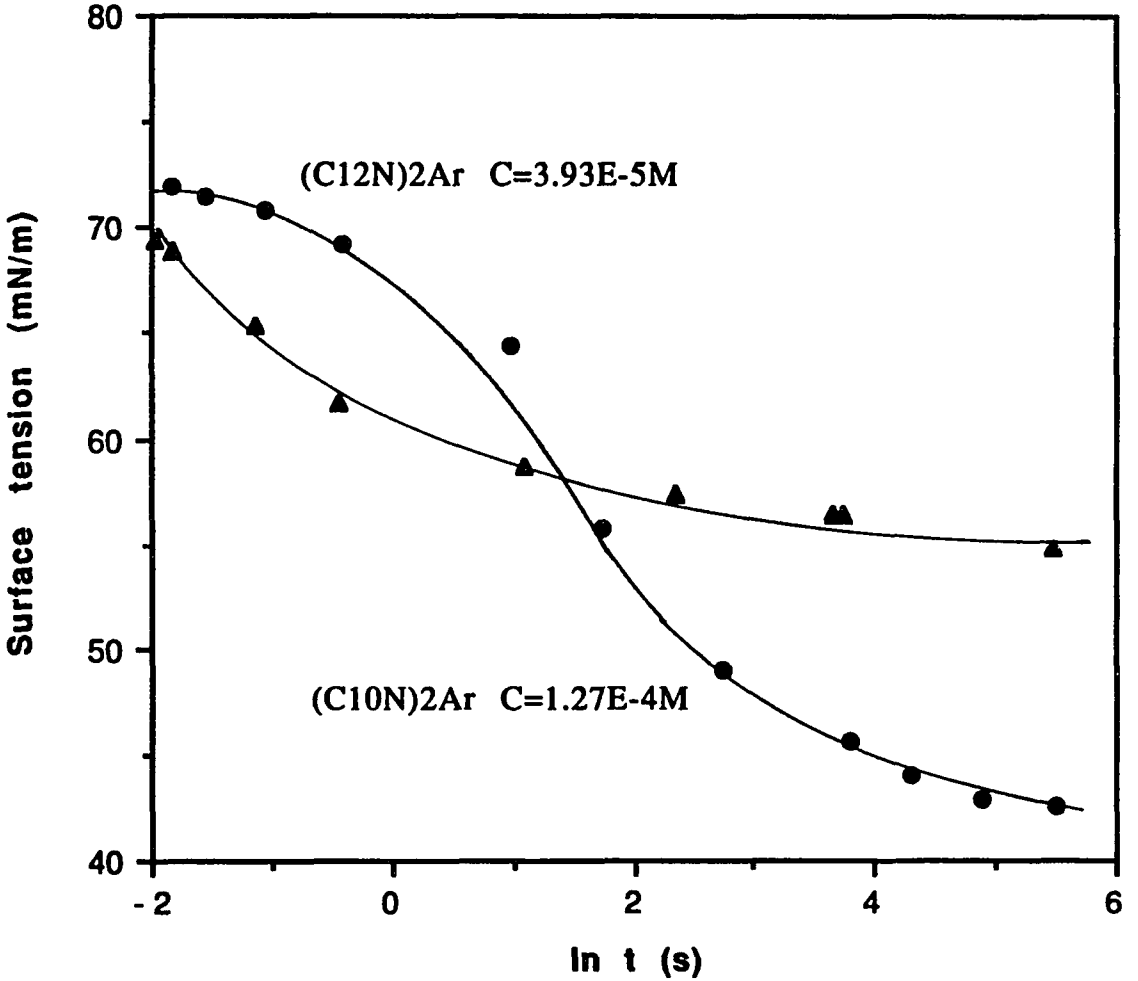

Figure 22 Surface pressure vs. ln t (s) of (C14N)2OH in 0.1 NNaCl at 25 °C γ_0=72.3mN/m and 50°C γ_0=68.0mN/m

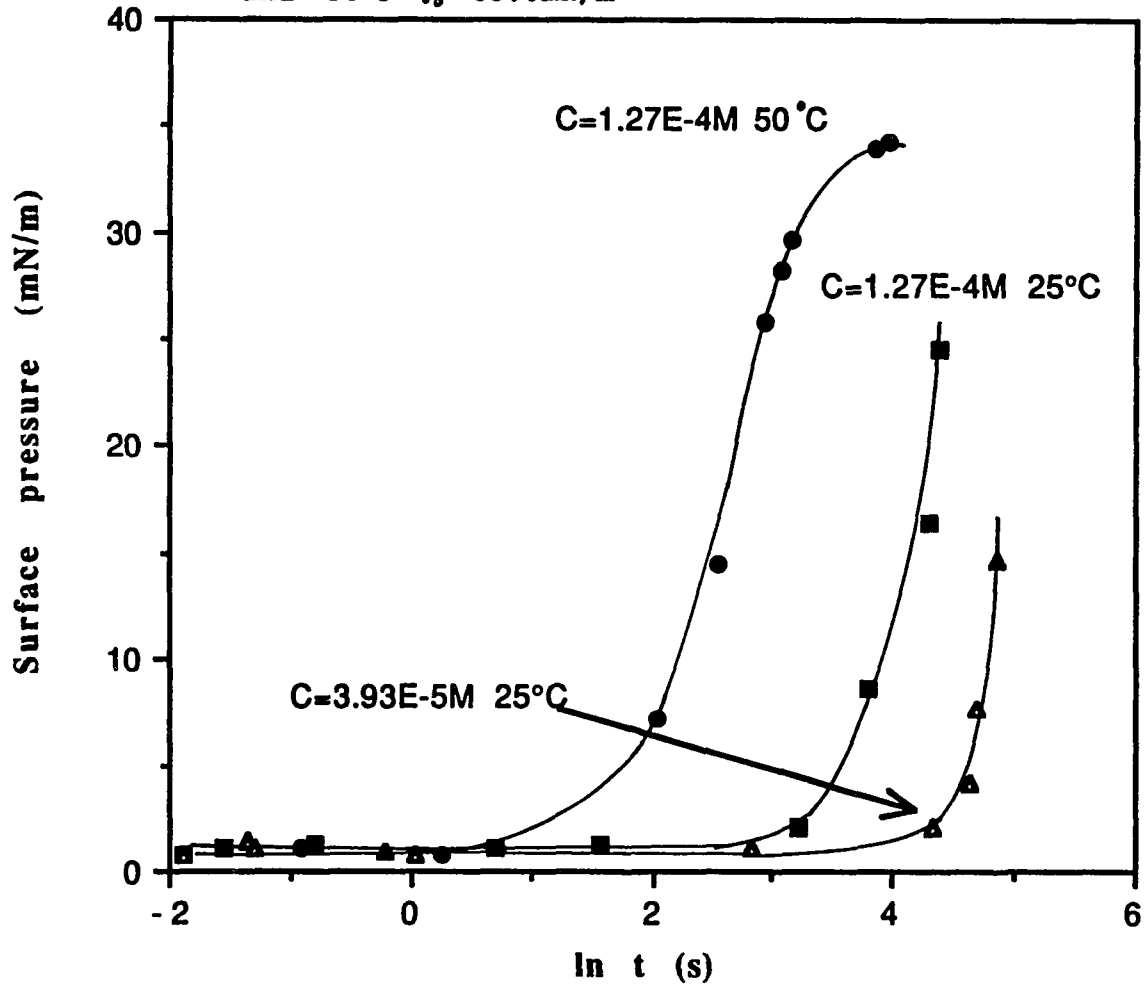

Figure 23 Dynamic parameter (n) vs. carbon number (Cn) of two series of gemini surfactants in 0.1 N NaCl at 50°C

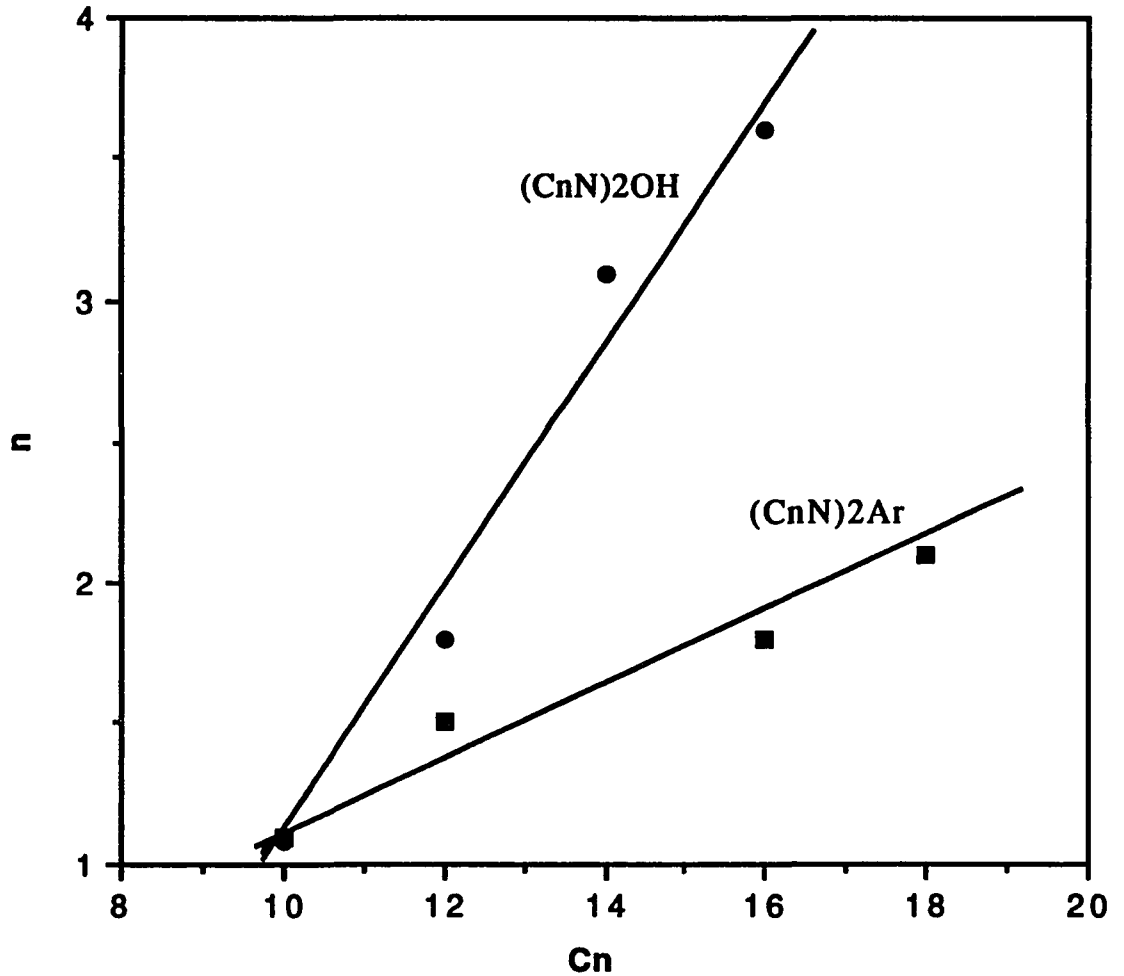

Figure 24 ln Γi/C vs. ln ti of (CnN)2OH series in 0.1 N NaCl at 50°C

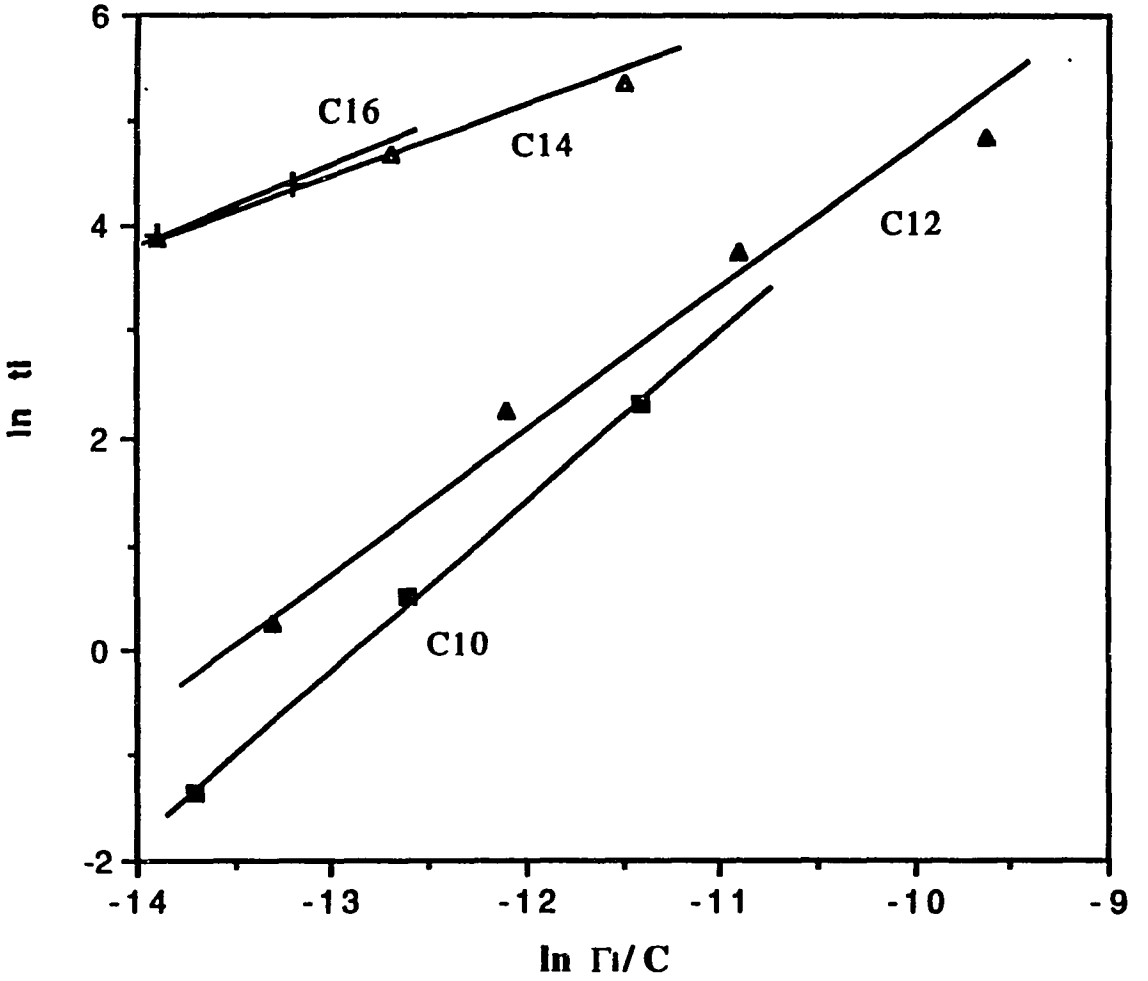

Figure 25 **ln Γi/C vs. ln ti of (CnN)2Ar series in 0.1 N NaCl at 50°C**

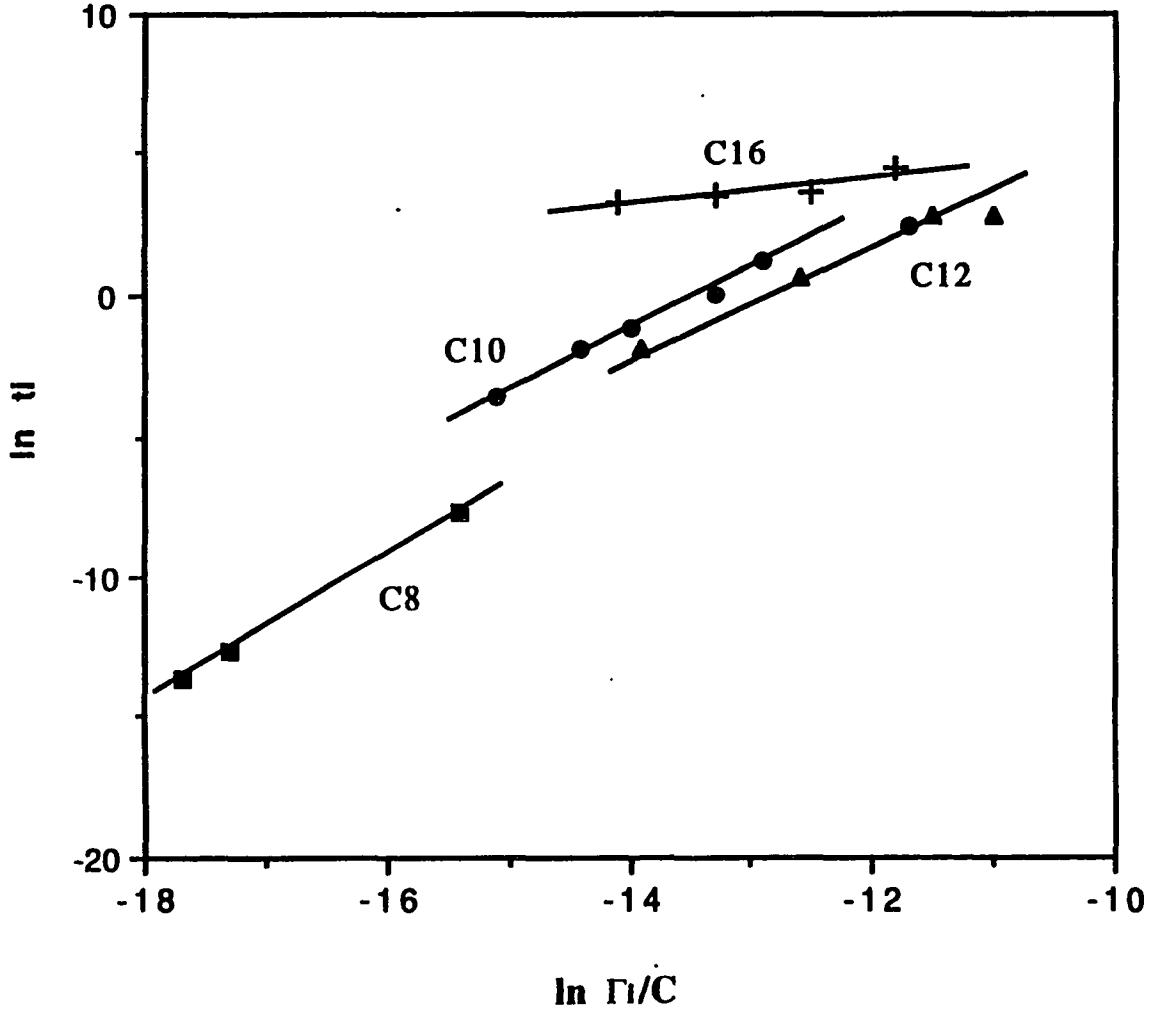

Figure 26 Dynamic surface tension vs. $t^{-1/2}$ of (C10N)2Ar in 0.1 N NaBr at 25°C

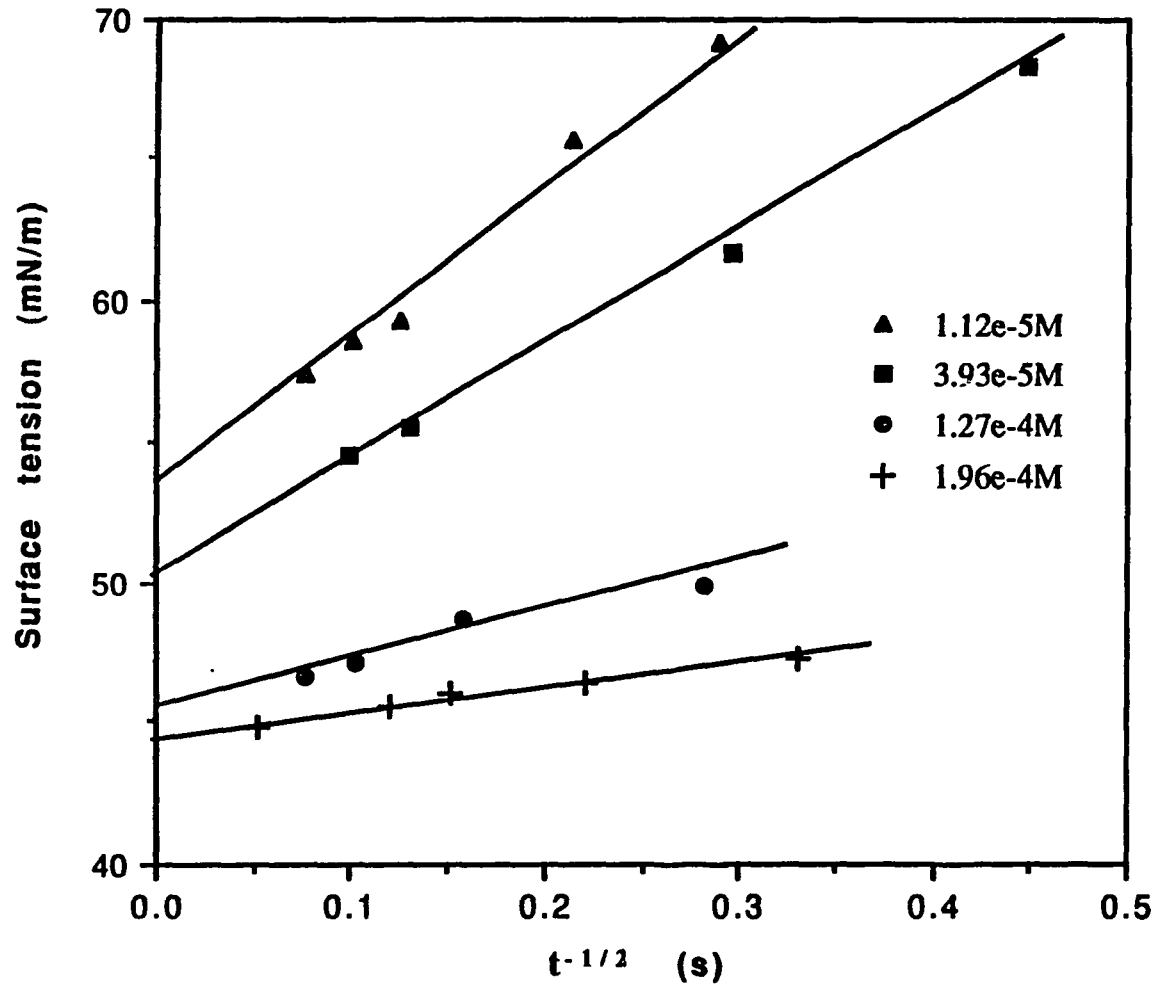

Figure 27 Dynamic surface tension vs. $t^{-1/2}$ of (C12N)2OH in 0.1 NaCl at 25°C

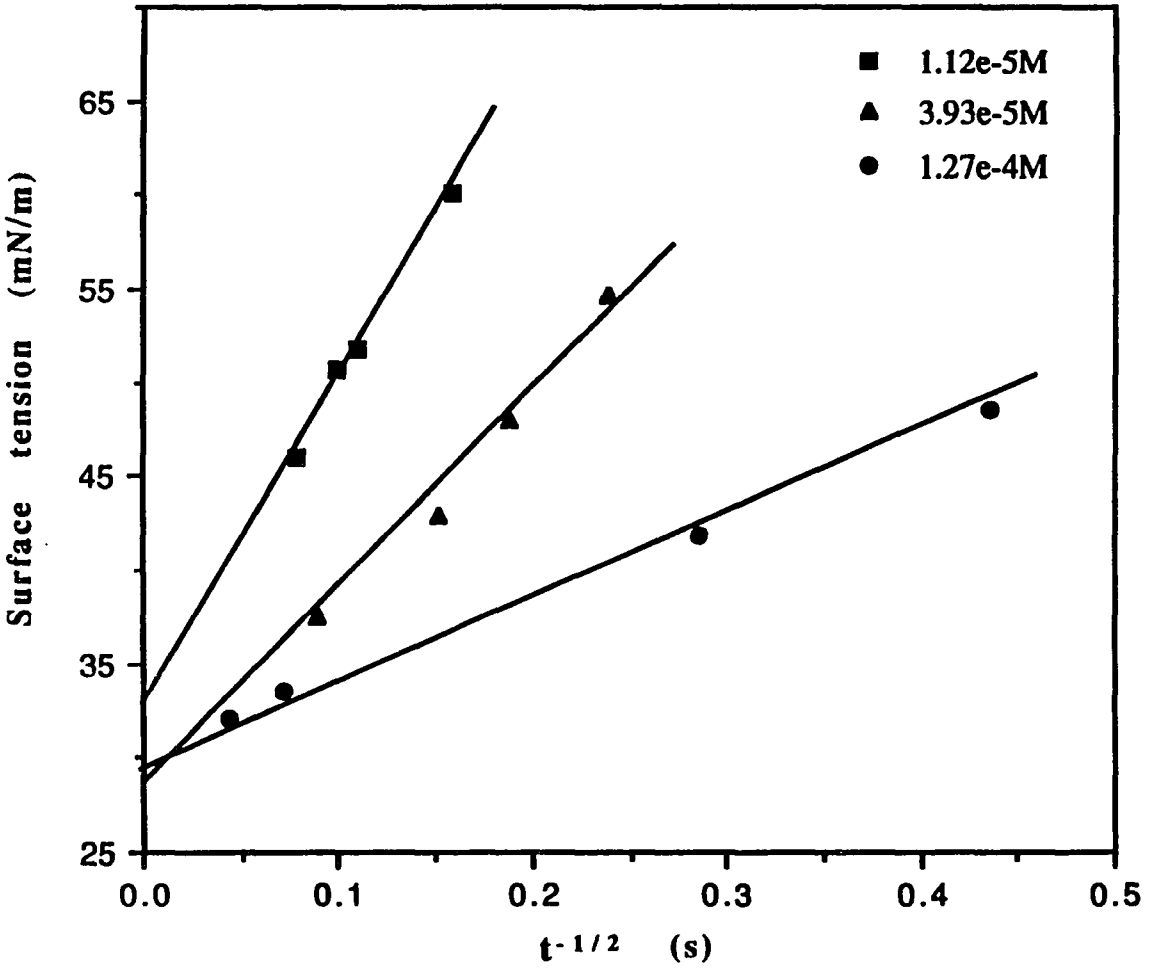

Figure 28 Surface coverage (xi) at the end of induction period (xi) vs. concentration (C) at 25°C

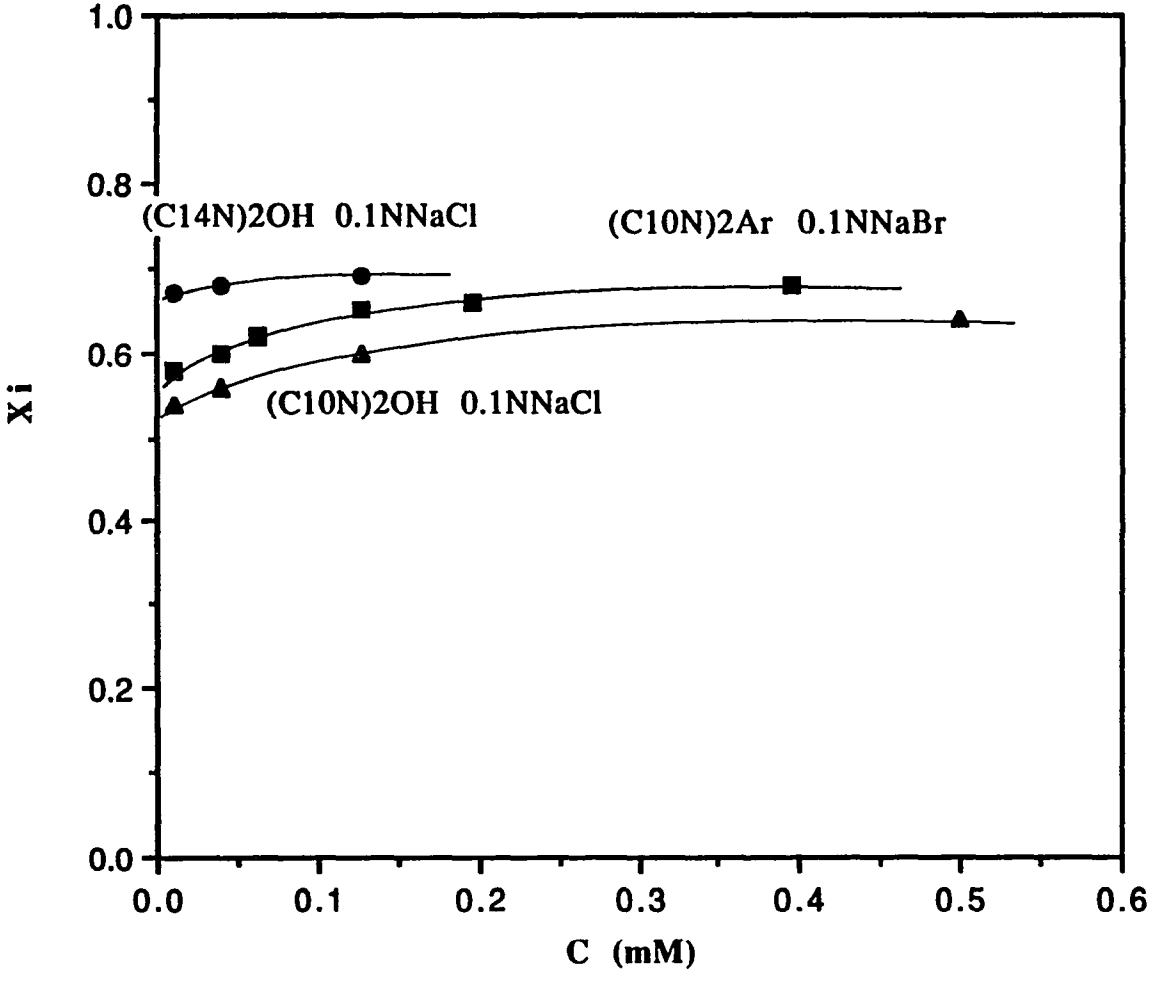

Figure 29 Dynamic surface tension of 0.1(w/w) at 25°C surfactants with/without superspreading character

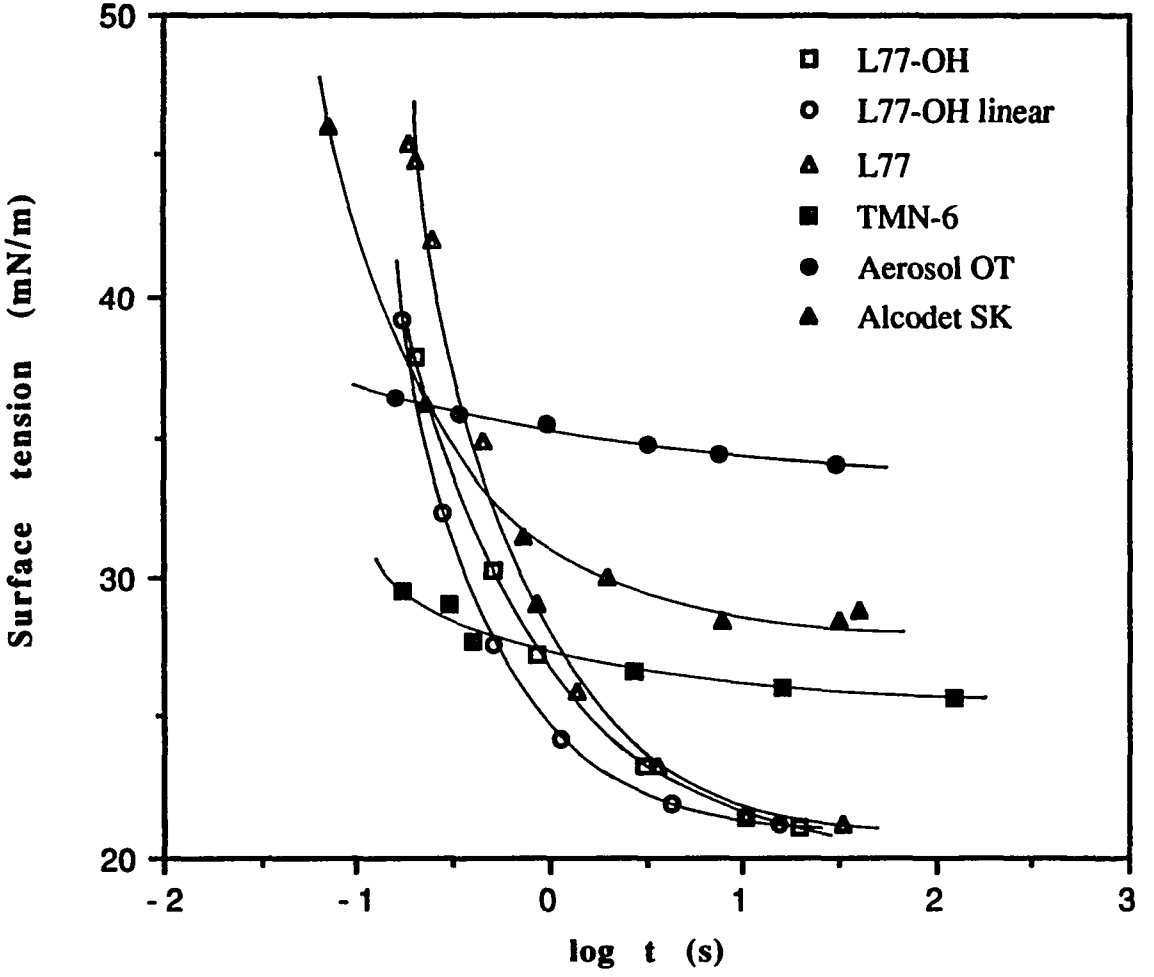

Figure 30 Spreading factor vs. time of surfactants (0.1w/w) at 22°C with/without superspreading character

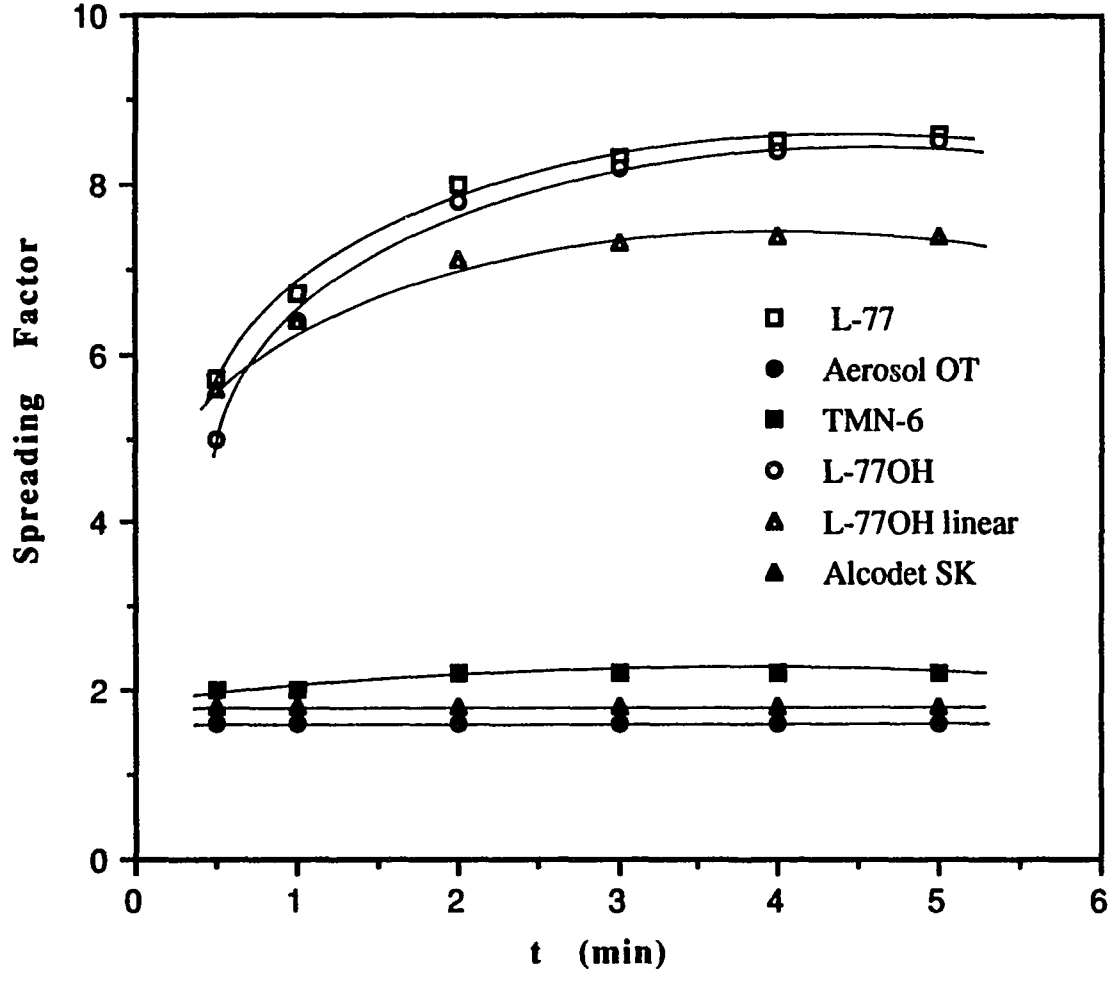

Figure 31 Spreading behavior of L-77 with additives: OT and TMN-6, 0.1% 22°C

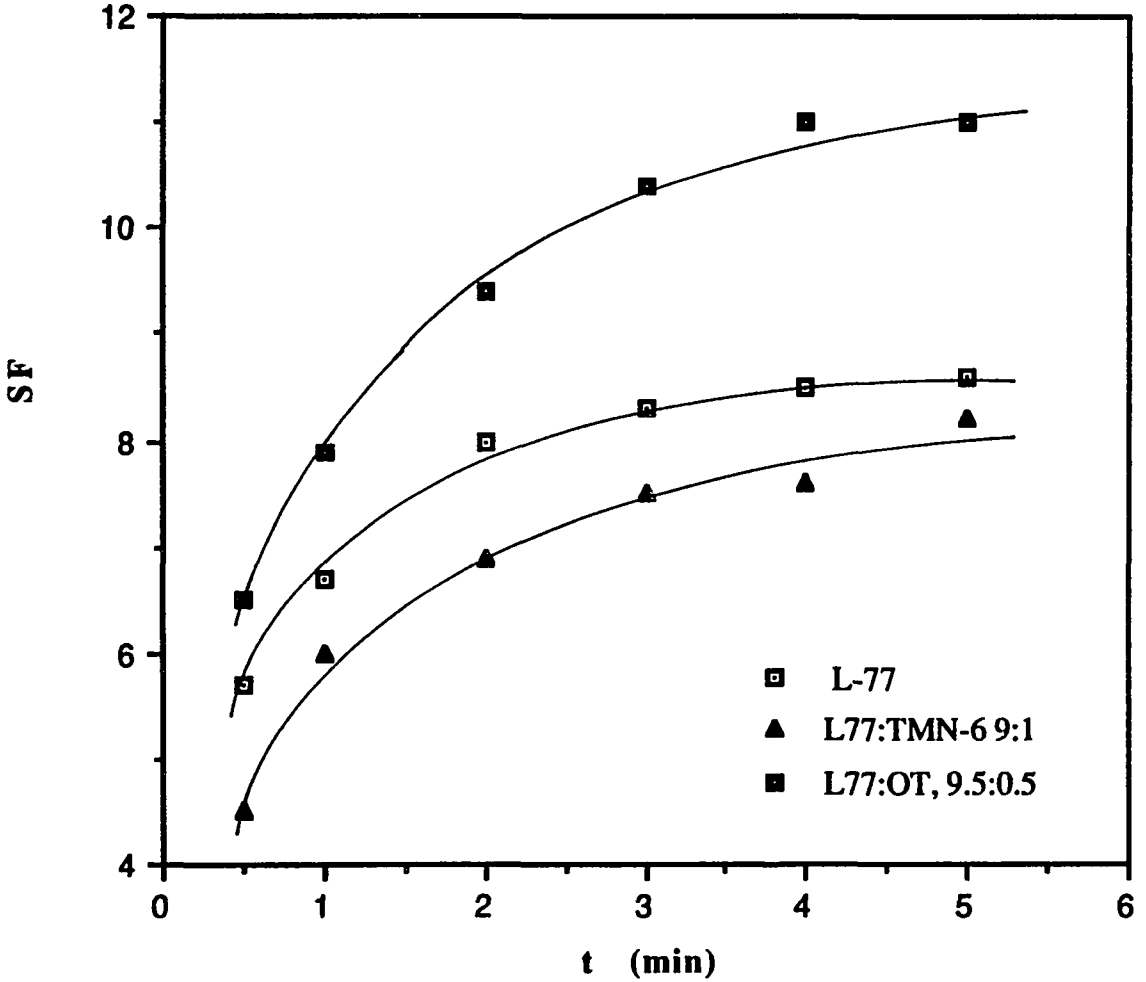

Fig. 32 Dynamic surface tension vs. log t(s), % of TMN-6 in L-77, total concentration: 0.1% (w/w)

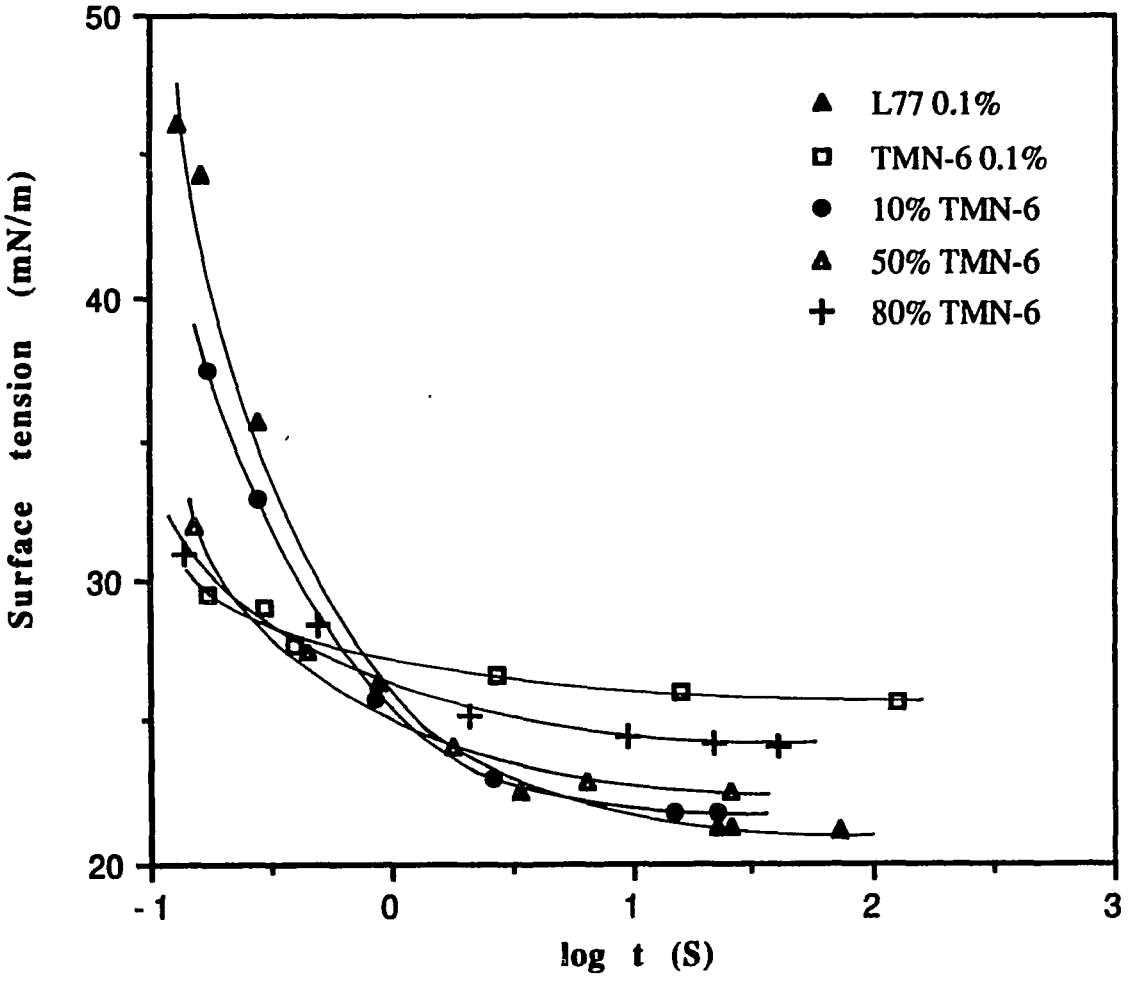

Figure 33 Dynamic surface tension vs. log t(s) of L-77 with additives and their mixtures, total concentration: 0.1% (w/w)

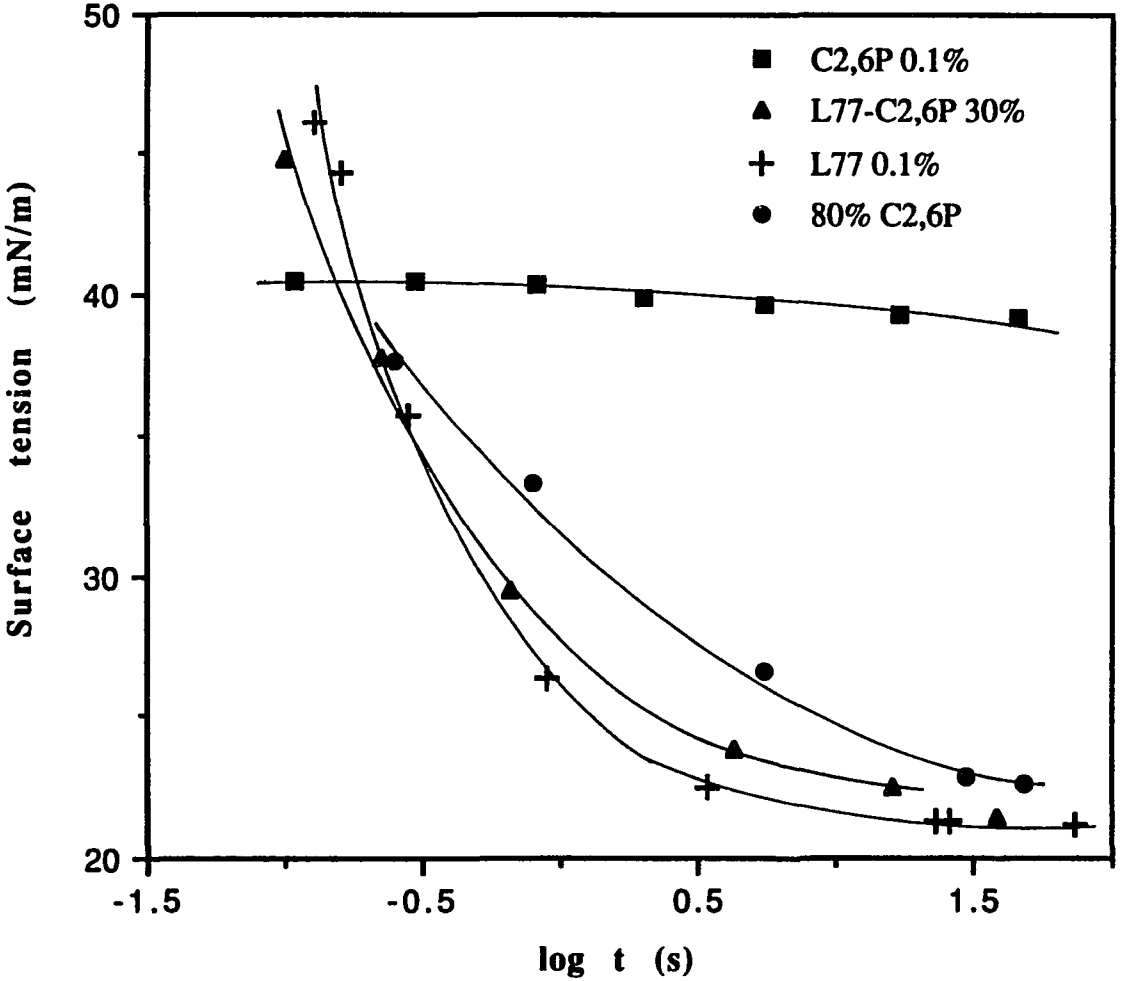

Figure 34 Dynamic surfacetension vs. log t(s) of L-77 (0.1w/w) after standing for 72 hrs

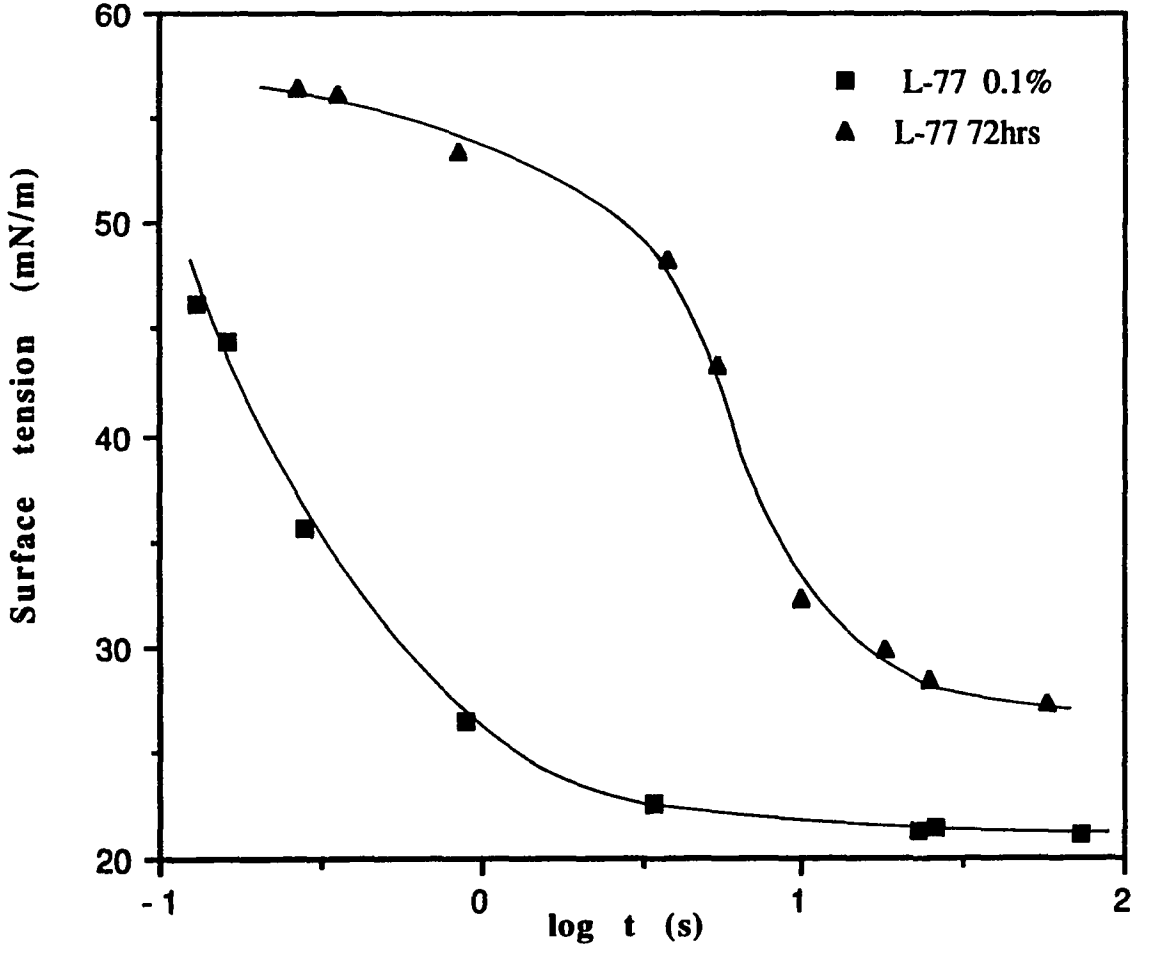

Figure 35 Spreading factor vs. % of aerosol series in L-77 22°C total concentration:0.1%(w/w)-showing synergism

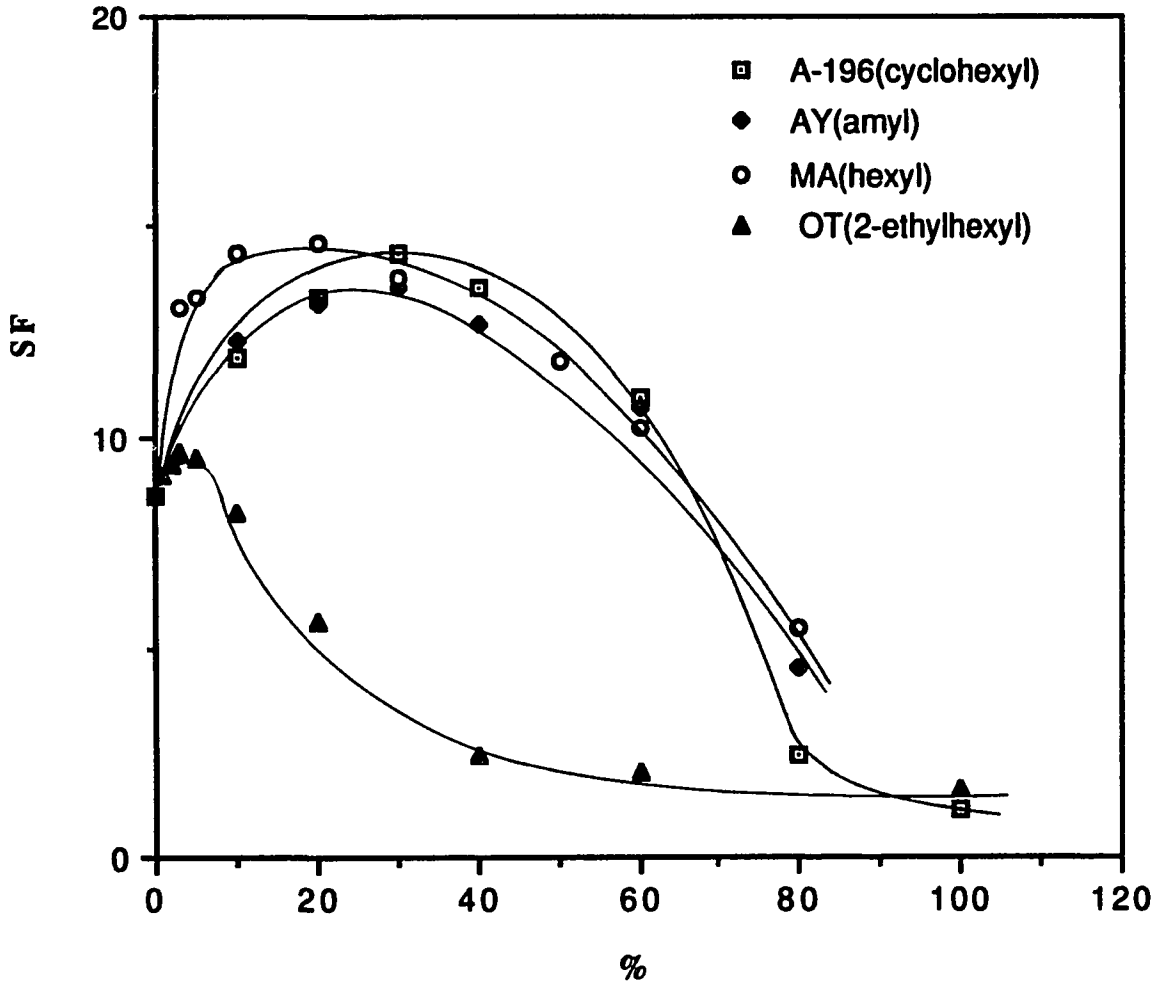

Figure 36 Spreading factor vs. % of N-alkyl pyrrolidone series in L-77 total concentration: 0.1(w/w) at 22°C-showing synergism

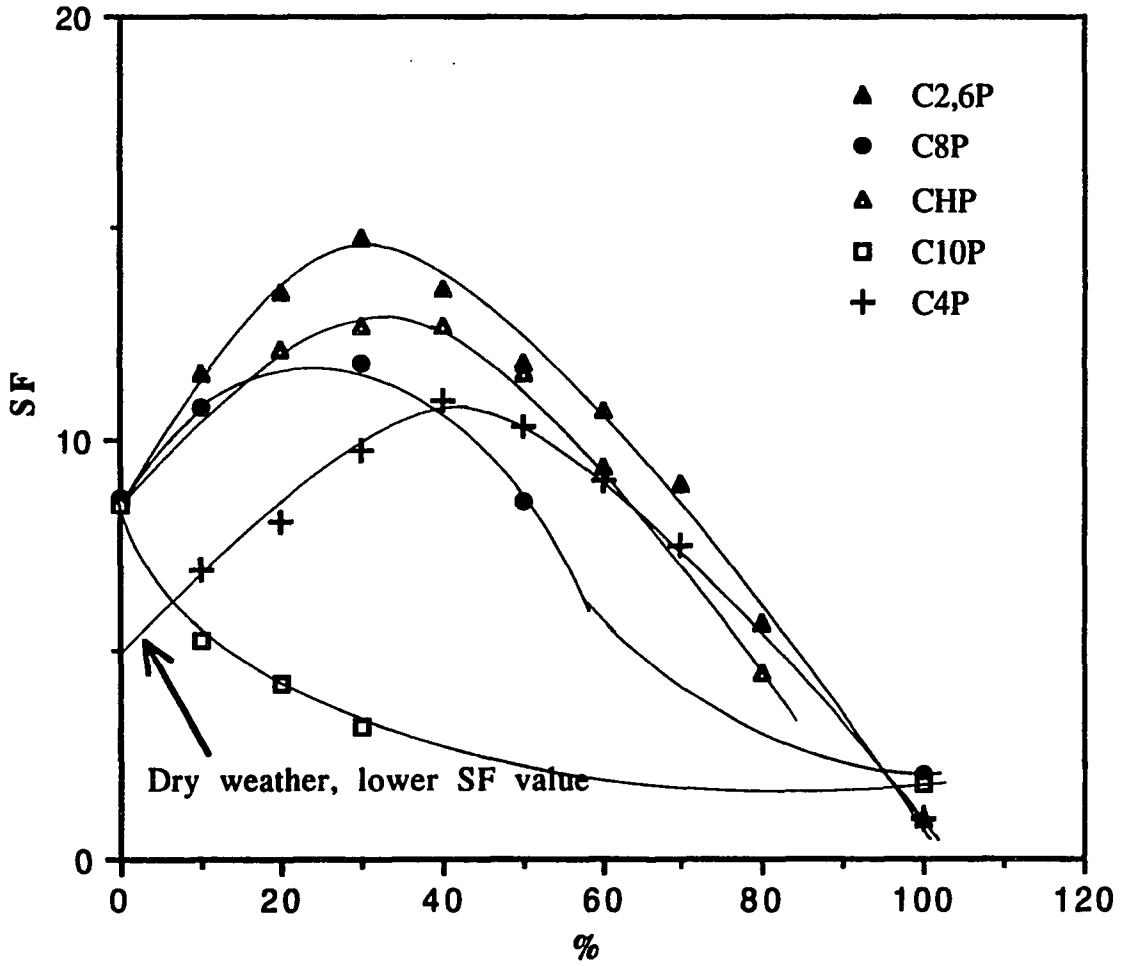

Fig. 37 Spreading factor vs. % of short chain alchohols in L-77 22°C total concentration: 0.1% (w/w) - showing synergism

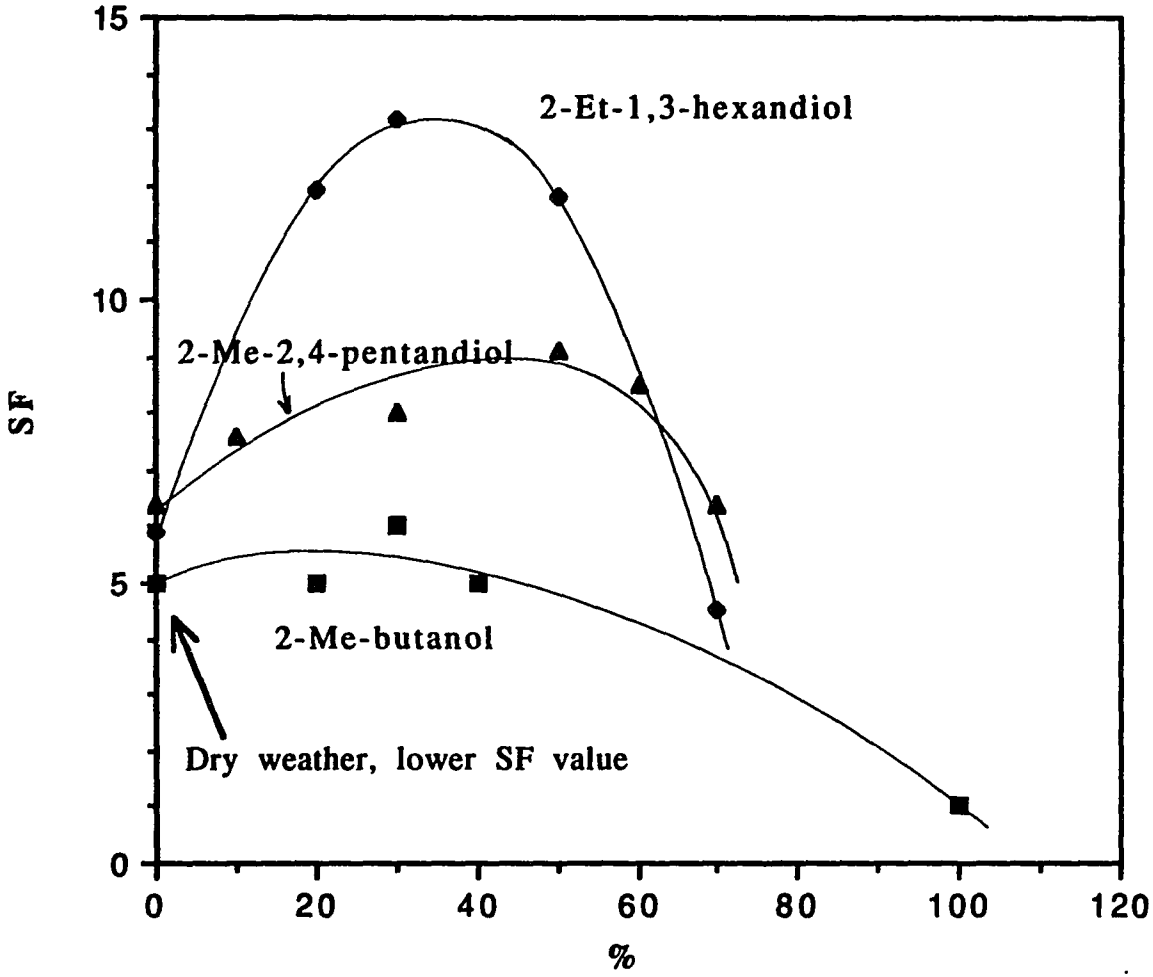

Figure 38 Spreading factor vs. % of cationic surfactants in L-77 22°C, total concentration: 0.1% (w/w) - showing synergism (0.1w/w)

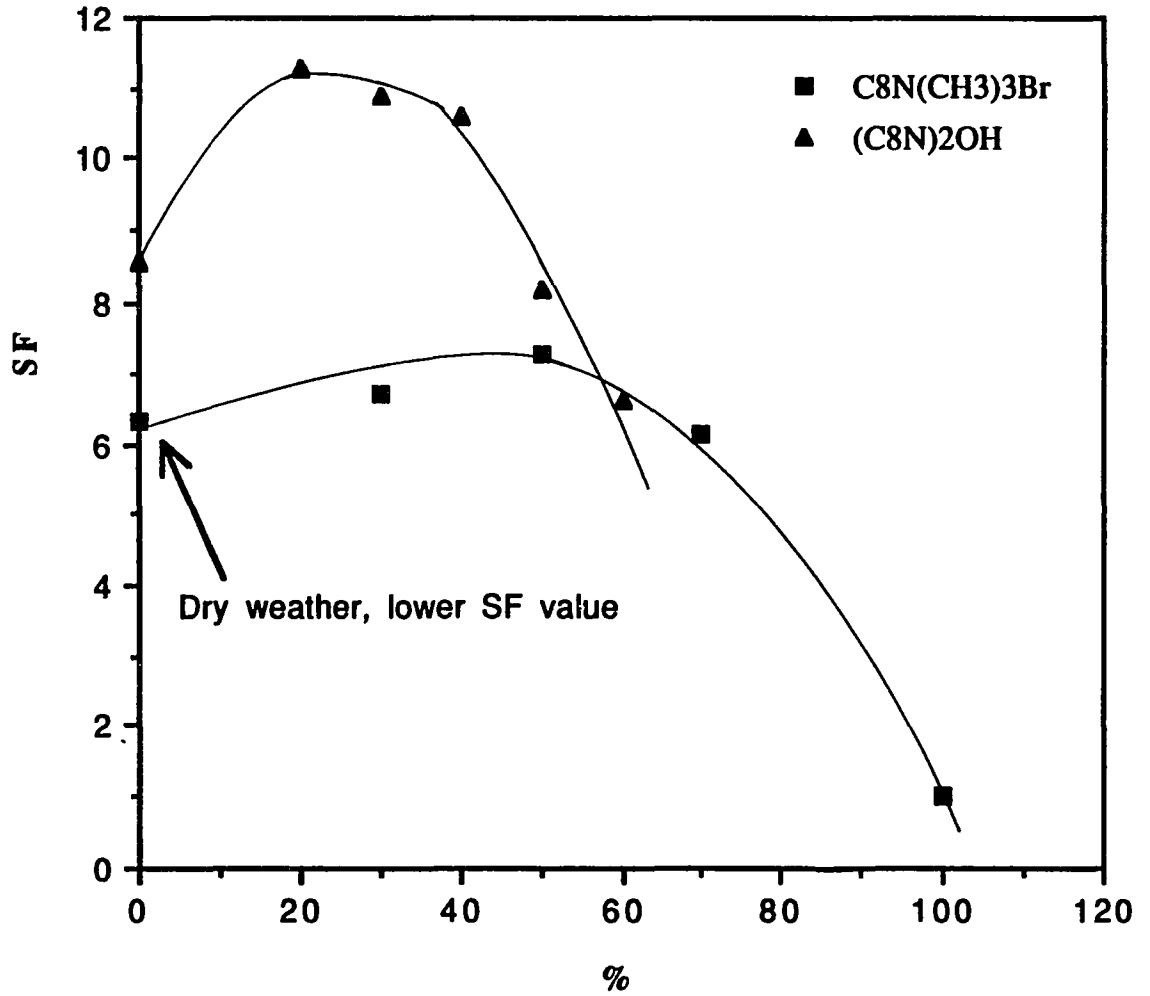

Figure 39 Spreading factor vs. time of L-77 with additives 22°C total concentration: 0.1%(w/w) - showing synergism

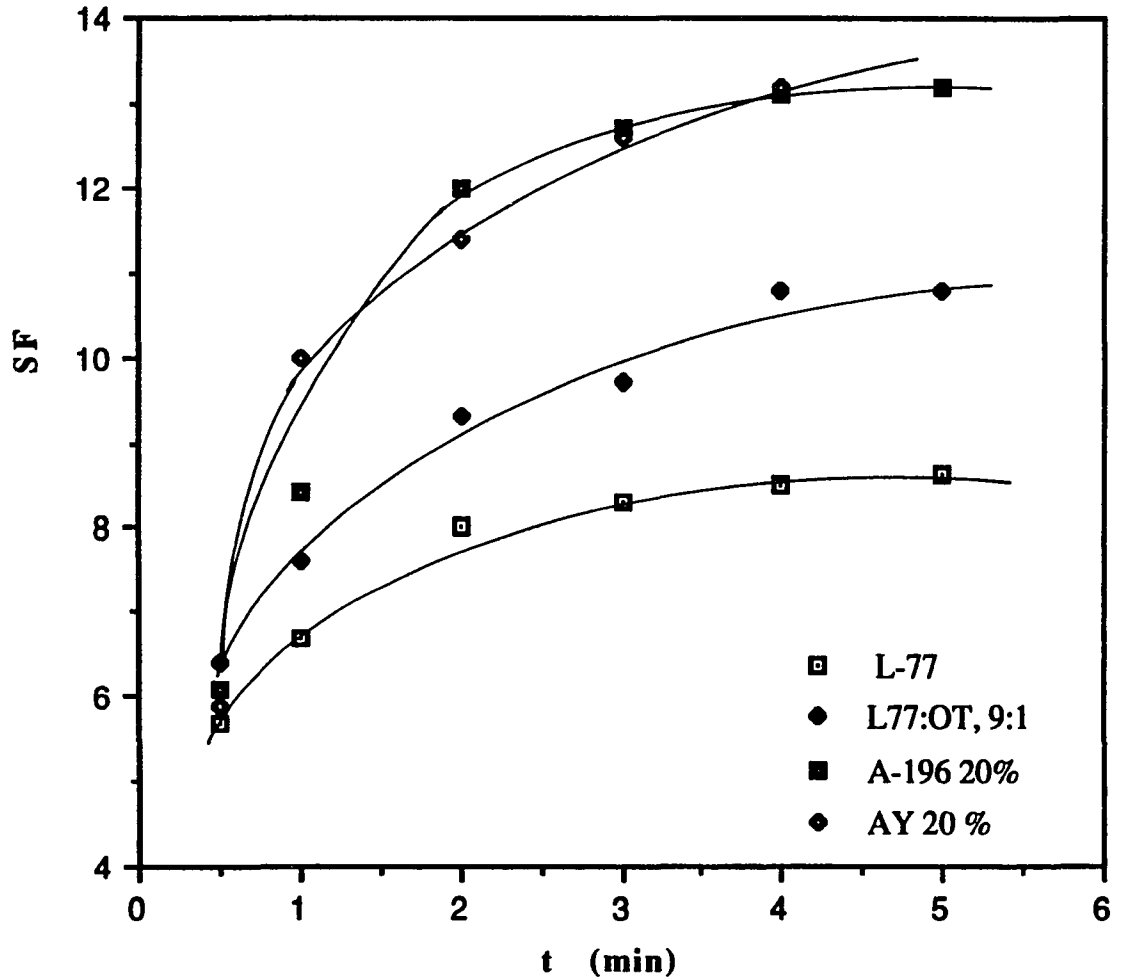

Table A-1 Equilibrium Surface Tension of $C_{10}C_1C_{10}$ in 0.1 N NaCl at 25 °C

-log C (M)	surface tension (mN/m)
4.22	39.35
4.62	39.43
4.92	39.30
5.32	41.41
5.62	44.17
5.92	48.08

Table A-2 Equilibrium Surface Tension of of $C_{12}H_{25}SO_3Na$ in 0.1 N NaCl at 25 °C

-log C (M)	surface tension (mN/m)
2.30	34.75
2.48	34.75
2.74	36.67
2.99	42.05
3.24	46.67

Table A-3 Equilibrium Surface Tension of Mixture of $C_{10}C_1C_{10}$ - $C_{12}H_{25}SO_3Na$ in 0.1 N NaCl at 25 °C, α=0.11, pH=5.8

-log C (M)	surface tension (mN/m)
4.17	37.63
4.59	37.63
5.00	38.40
5.42	40.32
5.59	44.74
5.83	48.27
6.25	53.57

Table A-4 Equilibrium Surface Tension of Mixture of $C_{10}C_1C_{10}$ - $C_{12}H_{25}SO_3Na$ in 0.1 N NaCl at 25 °C, α=0.11, pH=2.9

-log C (M)	surface tension (mN/m)
3.16	34.72
3.41	35.69
4.02	36.80
4.37	38.58
4.79	42.44

Table A-5 Equilibrium Surface Tension of $C_{12}EO_8$ in 0.1 N NaCl at 25 °C

-log C (M)	surface tension (mN/m)
3.80	34.00
3.98	34.00
4.23	37.80
4.45	41.00
4.75	44.80
5.05	49.00

Table A-6 Equilibrium Surface Tension of $C_{10}C_1O_{10}$ - $C_{12}EO_8$ in 0.1 N NaCl α = 0.16 at 25 °C

-log C (M)	surface tension (mN/m)
3.61	35.72
3.91	35.88
4.21	36.73
4.51	37.46
5.21	41.37
5.40	44.01
5.61	48.90

Table A-7 Equilibrium Surface Tension of $C_{12}EO_7$ in 0.1 N NaCl at 25 °C

-log C (M)	surface tension (mN/m)
3.76	33.4
3.98	33.4
4.46	39.4
4.96	47.4
5.50	55.5

Table A-8 Equilibrium Surface Tension of $C_{10}C_1O_{10}$ - $C_{12}EO_7$ in 0.1 N NaCl $\alpha = 0.16$ at 25 °C

-log C (M)	surface tension (mN/m)
3.62	34.10
3.86	34.50
4.12	35.12
4.82	39.60
5.25	45.40
5.38	47.60

Table A-9 Equilibrium Surface Tension of $C_{14}N(CH_3)_2O$ in 0.1 N NaCl at 25 °C

-log C (M)	surface tension (mN/m)
3.73	29.50
4.00	29.50
4.30	35.30
4.60	40.90
4.90	46.80

3.68	26.94
3.98	27.03
4.28	27.40
4.68	29.87
4.91	35.18
5.18	42.53

Table A-10 Equilibrium Surface Tension of $C_{10}C_1O_{10}$-$C_{14}N(CH_3)_2O$ in 0.1 N NaCl α = 0.19 at 25 °C, pH=2.9

-log C (M)	surface tension (mN/m)
3.69	29.38
3.81	30.15
4.51	31.51
4.92	33.02
5.30	35.84
5.59	39.82
5.71	42.33
6.03	45.35
4.00	27.69
4.30	28.14
4.70	27.77
5.00	28.10
5.60	32.20
6.00	35.00
6.14	35.80
6.53	39.10

Table A-11 Equilibrium Surface Tension of $C_{10}C_8O_{10}$ - $C_{12}EO_7$ in 0.1 N NaCl $\alpha = 0.17$ at 25 °C

-log C (M)	surface tension (mN/m)
3.89	31.89
4.30	31.49
4.72	31.68
5.13	33.45
5.50	38.25
5.91	43.62

Table A-12 Equilibrium Surface Tension of $C_{10}C_8O_{10}$ - $C_{12}EO_7$ in 0.1 N NaCl $\alpha = 0.029$ at 25 °C

-log C (M)	surface tension (mN/m)
3.80	32.00
4.36	38.10
4.65	34.40
5.00	39.40
5.40	45.10

Table A-13 Equilibrium Surface Tension of $C_{10}C_8O_{10}$ - $C_{14}N(CH_3)_2O$ in 0.1 N NaCl $\alpha = 0.18$ at 25 °C, pH = 5.8

-log C (M)	surface tension (mN/m)
3.60	28.59
3.85	28.82
4.55	31.71
4.97	34.07
5.38	39.43

Table A-14 Equilibrium Surface Tension of $C_{10}C_8O_{10}$ - $C_{14}N(CH_3)_2O$ in 0.1 N NaCl α = 0.05 at 25 °C, pH = 5.8

-log C (M)	surface tension (mN/m)
3.90	27.21
4.56	27.20
4.98	37.56
5.26	46.10
5.58	55.12

Table A-15 Equilibrium Surface Tension of $C_{10}C_8O_{10}$ - $C_{14}N(CH_3)_2O$ in 0.1 N NaCl α = 0.034 at 25 °C, pH = 5.8

-log C (M)	surface tension (mN/m)
3.54	27.20
3.84	27.10
4.36	37.38
4.72	31.56
5.12	41.00
5.56	55.60

Table A-16 Equilibrium Surface Tension of $C_{10}C_8O_{10}$ - $C_{14}N(CH_3)_2O$ in 0.1 N NaCl α = 0.034 at 25 °C, pH = 7.2

-log C (M)	surface tension (mN/m)
3.54	28.94
3.94	29.39
4.24	30.03
4.54	32.98
4.94	39.49
5.24	46.33

Table A-17 Equilibrium Surface Tension of $C_{10}C_8O_{10}$ - $C_{12}EO_8$ in 0.1 N NaCl
α = 0.011 at 25 °C

-log C (M)	surface tension (mN/m)
4.00	33.40
4.50	33.25
5.05	37.69
5.40	47.20
5.80	57.41

Table A-18 Equilibrium Surface Tension of $C_{10}C_8O_{10}$ - $C_{12}EO_8$ in 0.1 N NaCl
α = 0.18 at 25 °C

-log C (M)	surface tension (mN/m)
3.90	29.70
4.20	29.60
4.80	29.79
5.20	30.16
5.50	31.81
5.90	36.92
6.30	41.74

Table A-19 Equilibrium Surface Tension of $C_{10}C_8O_{10}$ - $C_{12}EO_8$ in 0.1 N NaCl
α = 0.26 at 25 °C

-log C (M)	surface tension (mN/m)
4.15	28.26
4.46	28.26
4.57	28.72
5.46	31.51
5.85	36.28
6.15	39.43

Table A-20 Equilibrium Surface Tension of $(C_8N)_2Ar$ in H_2O at 25 °C

-log C (M)	surface tension (mN/m)
1.42	37.21
1.88	45.38
1.92	45.60
2.22	50.40
2.52	56.50
2.83	59.90

Table A-21 Equilibrium Surface Tension of $(C_8N)_2Ar$ in H_2O at 50 °C

-log C (M)	surface tension (mN/m)
1.93	49.50
2.45	59.52
3.24	66.20
3.88	67.20
4.17	66.60

Table A-22 Equilibrium Surface Tension of $(C_8N)_2Ar$ in 0.1 N NaBr at 25 °C

-log C (M)	surface tension (mN/m)
1.50	38.38
1.75	38.40
2.06	40.80
2.22	43.12
2.50	47.51

Table A-23 Equilibrium Surface Tension of $(C_8N)_2Ar$ in 0.01 N NaCl at 50 °C

-log C (M)	surface tension (mN/m)
1.24	40.22
1.37	40.25
1.60	42.11
1.90	48.30
2.20	54.50

Table A-24 Equilibrium Surface Tension of $(C_8N)_2Ar$ in 0.1 N NaCl at 50 °C

-log C (M)	surface tension (mN/m)
1.50	42.20
1.68	42.20
1.90	45.11
2.20	49.22
2.44	52.52

Table A-25 Equilibrium Surface Tension of $(C_{10}N)_2Ar$ in H_2O at 25 °C

-log C (M)	surface tension (mN/m)
1.88	38.42
2.32	43.00
2.53	44.72
2.66	47.70
3.96	58.70
4.36	59.80
4.62	59.80

Table A-26 Equilibrium Surface Tension of $(C_{10}N)_2Ar$ in 0.1 N NaBr at 25 °C

-log C (M)	surface tension (mN/m)
3.12	36.82
3.24	37.02
3.40	38.83
4.10	45.65
4.35	48.38
5.40	60.02

Table A-27 Equilibrium Surface Tension of $(C_{10}N)_2Ar$ in 0.01 N NaCl at 50 °C

-log C (M)	surface tension (mN/m)
1.72	40.30
1.90	40.42
2.30	41.52
2.50	45.11
2.76	49.80

Table A-28 Equilibrium Surface Tension of $(C_{10}N)_2Ar$ in 0.1 N NaCl at 50 °C

-log C (M)	surface tension (mN/m)
1.66	40.78
1.80	40.80
2.20	44.38
2.67	50.40
2.97	54.38

Table A-29 Equilibrium Surface Tension of $(C_{12}N)_2Ar$ in H_2O at 50 °C

-log C (M)	surface tension (mN/m)
2.62	39.20
2.88	39.22
3.26	47.18
3.48	52.98
3.65	57.12

Table A-30 Equilibrium Surface Tension of $(C_{12}N)_2Ar$ in 0.1 N NaCl at 25°C

-log C (M)	surface tension (mN/m)
3.95	39.58
4.16	39.65
4.66	41.80
4.96	44.82
5.17	47.03

Table A-31 Equilibrium Surface Tension of $(C_{12}N)_2Ar$ in 0.01 N NaCl at 50°C

-log C (M)	surface tension (mN/m)
2.95	39.42
3.00	39.83
3.15	40.20
3.55	43.03
3.70	45.40
3.96	48.42
4.28	52.20
4.56	54.80

Table A-32 Equilibrium Surface Tension of $(C_{12}N)_2Ar$ in 0.1 N NaCl at 50°C

-log C (M)	surface tension (mN/m)
2.75	37.81
3.00	37.60
3.88	38.20
4.32	38.32
4.58	41.20
4.84	44.43
5.24	50.64

Table A-33 Equilibrium Surface Tension of $(C_{14}N)_2Ar$ in H_2O at 50°C

-log C (M)	surface tension (mN/m)
2.72	37.21
2.92	37.84
3.42	39.46
3.72	42.63
4.10	52.10
4.56	62.62
4.98	66.38
5.24	67.00

Table A-34 Equilibrium Surface Tension of $(C_{14}N)_2Ar$ in 0.01 N NaCl at 50°C

-log C (M)	surface tension (mN/m)
3.83	38.92
4.13	39.32
4.49	39.50
4.83	40.20
5.13	43.32
5.33	46.66
5.63	50.76

Table A-35 Equilibrium Surface Tension of $(C_{14}N)_2Ar$ in 0.1 N NaCl at 50°C

-log C (M)	surface tension (mN/m)
4.13	36.20
4.43	36.42
4.83	37.40
5.13	38.22
5.25	40.30
5.42	43.80
5.98	47.90

Table A-36 Equilibrium Surface Tension of $(C_{16}N)_2Ar$ in H_2O at 50°C

-log C (M)	surface tension (mN/m)
2.93	36.41
3.28	37.60
3.87	39.80
4.34	46.00
4.64	52.00
4.92	58.00
5.22	63.22

Table A-37 Equilibrium Surface Tension of $(C_{16}N)_2Ar$ in 0.01 N NaCl at 50°C

-log C (M)	surface tension (mN/m)
4.40	37.62
4.70	38.00
5.00	38.41
5.28	40.78
5.44	42.61
5.60	44.00
5.66	44.60
5.76	47.72

Table A-38 Equilibrium Surface Tension of $(C_{16}N)_2Ar$ in 0.1 N NaCl at 50°C

-log C (M)	surface tension (mN/m)
3.93	34.88
4.28	35.20
4.52	36.00
4.66	36.42
4.90	36.72
5.44	41.41
5.57	44.46
5.72	47.80

Table A-39 Equilibrium Surface Tension of $(C_{18}N)_2Ar$ in H_2O at 50°C

-log C (M)	surface tension (mN/m)
2.77	44.00
3.50	44.51
4.58	46.00
4.80	45.80
5.17	46.20
5.53	47.72
5.87	49.92
6.00	54.00
6.08	57.20
6.20	61.22
6.33	66.02

Table A-40 Equilibrium Surface Tension of $(C_{18}N)_2Ar$ in 0.01 N NaCl at 50°C

-log C (M)	surface tension (mN/m)
2.82	40.71
3.51	41.10
3.80	41.20
4.46	42.20
4.82	42.62
5.34	44.40
5.47	44.00
5.62	47.80
5.74	51.20
5.94	55.80

Table A-41 Equilibrium Surface Tension of $(C_{18}N)_2Ar$ in 0.1 N NaCl at 50°C

-log C (M)	surface tension (mN/m)
2.92	32.80
3.30	32.76
3.62	32.92
3.82	33.20
3.98	32.78
4.12	33.42
4.32	38.21
4.52	41.32
4.78	43.00
5.06	42.86
5.22	43.10
5.66	43.20
5.80	47.21
6.02	53.00

Table A-42 Equilibrium Surface Tension of $(C_8N)_2OH$ in 0.1 N NaCl at 25°C

-log C (M)	surface tension (mN/m)
1.50	38.2
1.80	38.2
2.08	39.0
2.39	43.2
2.78	48.2

Table A-43 Equilibrium Surface Tension of $(C_{10}N)_2OH$ in 0.1 N NaCl at 25°C

-log C (M)	surface tension (mN/m)
2.52	36.00
3.00	35.98
3.37	35.98
3.70	40.00
4.04	44.60
4.19	46.60
4.33	47.60
4.74	53.60

Table A-44 Equilibrium Surface Tension of $(C_{12}N)_2OH$ in 0.1 N NaCl at 25°C

-log C (M)	surface tension (mN/m)
3.56	33.20
4.62	33.20
4.96	32.82
5.36	39.40
5.66	44.72
5.82	49.01

Table A-45 Equilibrium Surface Tension of $(C_{14}N)_2OH$ in 0.1 N NaCl at 25°C

-log C (M)	surface tension (mN/m)
4.22	32.62
4.80	32.62
5.40	39.00
5.63	43.02
5.93	47.45

Table A-46 Equilibrium Surface Tension of $(C_{16}N)_2OH$ in 0.1 N NaCl at 25°C

-log C (M)	surface tension (mN/m)
3.98	41.76
4.43	41.50
4.69	44.20
5.00	50.20
5.42	58.32

Table A-47 Equilibrium Surface Tension of $(C_8N)_2OH$ in 0.1 N NaCl at 50°C

-log C (M)	surface tension (mN/m)
1.40	36.00
1.80	36.00
2.10	38.12
2.38	43.32
2.78	48.03

Table A-48 Equilibrium Surface Tension of $(C_{10}N)_2OH$ in 0.1 N NaCl at 50°C

-log C (M)	surface tension (mN/m)
2.60	34.00
2.92	34.00
3.54	38.80
3.90	44.40
4.30	50.00

Table A-49 Equilibrium Surface Tension of $(C_{12}N)_2OH$ in 0.1 N NaCl at 50°C

-log C (M)	surface tension (mN/m)
3.54	31.62
3.96	32.00
4.26	32.23
4.58	32.31
4.96	37.60
5.26	42.40
5.50	45.00

Table A-50 Equilibrium Surface Tension of $(C_{14}N)_2OH$ in 0.1 N NaCl at 50°C

-log C (M)	surface tension (mN/m)
4.35	28.89
4.64	29.56
4.99	31.42
5.36	36.40
5.62	40.43
5.92	43.02

Table A-51 Equilibrium Surface Tension of $(C_{16}N)_2OH$ in 0.1 N NaCl at 50°C

-log C (M)	surface tension (mN/m)
4.30	36.82
5.00	36.81
5.42	40.20
5.72	43.58
6.00	48.20

Table A-52 Equilibrium Surface Tension of $C_{12}EO_2S$ in 0.1 N NaCl at 25°C

-log C (M)	surface tension (mN/m)
3.10	35.73
3.54	35.80
3.82	41.23
4.12	47.26
4.36	52.38

Table A-53 Equilibrium Surface Tension of $C_{12}EO_2S$-$(C_8N)_2OH$ in 0.1 N NaCl at 25°C, α= 0.17

-log C (M)	surface tension (mN/m)
3.82	28.65
4.08	29.40
4.46	34.62
4.76	41.63
5.07	49.02

Table A-54 Equilibrium Surface Tension of $C_{12}EO_2S$-$(C_{10}N)_2OH$ in 0.1 N NaCl at 25°C, α= 0.17

-log C (M)	surface tension (mN/m)
4.10	28.80
4.40	28.93
4.80	30.02
5.10	34.60
5.52	40.32

Table A-55 Equilibrium Surface Tension of $(C_{12}N)_2OH$-$C_{12}EO_2S$ in 0.1 N NaCl at 25°C, α= 0.17

-log C (M)	surface tension (mN/m)
3.95	34.40
4.26	34.73
4.56	35.20
4.92	37.00
5.16	40.00
5.44	43.80

Table A-56 Equilibrium Surface Tension of $C_{12}EO_2S$-$(C_{10}N)_2Ar$ in 0.1 N NaCl at 25°C, α= 0.17

-log C (M)	surface tension (mN/m)
4.10	29.60
4.49	29.58
4.88	32.00
5.12	36.59
5.42	43.20

Table A-57 Dynamic Surface Tension of $(C_8N)_2Ar$ in H_2O, at 25°C,

t (s) (bubble interval)	γ_t(mN/m)
C=2.40x10^{-2}M	
0.17	50.35
0.12	50.35
0.23	50.70
0.65	50.00
1.95	49.56
4.90	49.05
12.50	48.56
41.30	47.69
65.13	47.31
C=7.30x10^{-3}M	
0.13	60.49
0.33	60.00
0.75	59.62
1.15	59.60
2.50	59.56
6.85	59.10
40.60	57.65
170.00	56.63
258.40	56.34

Table A-58 Dynamic Surface Tension of $(C_8N)_2Ar$ in 0.1N NaBr, at 25°C,

t (s) (bubble interval)	γ_t(mN/m)
C=7.30x10^{-3}M	
0.27	52.79
0.30	52.55

1.78	51.84
3.50	51.49
21.60	49.81
25.50	49.54
89.00	48.12
C=3.65x10^{-3}M	
0.17	56.10
0.41	55.69
0.97	55.51
3.20	54.86
22.00	53.50
50.00	52.43
149.00	51.31
C=3.32x10^{-4}M	
0.49	65.79
0.75	65.25
2.75	64.84
8.60	64.37
18.70	64.01
84.00	63.07
360.00	61.89

Table A-59 Dynamic Surface Tension of $(C_{10}N)_2Ar$ in H_2O, at 25°C,

t (s) (bubble interval)	γ_t(mN/m)
C=7.30x10^{-3}M	
0.10	43.08
0.24	42.13
0.75	41.78
2.35	41.43
7.50	41.14

23.30	40.80
45.50	40.73
50.50	40.62
C=6.64x10^{-4}M	
0.11	52.74
0.38	51.28
1.45	50.61
6.90	50.12
14.50	49.68
100.00	48.69

Table A-60 Dynamic Surface Tension of $(C_{10}N)_2Ar$ in 0.1N NaBr, at 25°C,

t (s) (bubble interval)	γ_t (mN/m)
C=3.93x10^{-4}M	
0.09	60.94
0.19	50.69
0.31	48.46
0.55	46.53
1.78	44.81
5.30	43.93
31.00	42.86
47.00	42.67
117.00	42.15
C=1.96x10^{-4}M	
0.15	69.04
0.21	66.56
0.30	58.46
0.88	52.08
1.40	50.60
2.30	49.33

5.10	47.95
9.10	47.27
20.40	46.35
43.00	46.05
70.00	45.58
360.00	44.81
C=6.24x10^{-5}M	
0.18	70.78
0.33	70.40
0.71	69.51
1.76	65.58
3.75	60.55
8.50	56.60
34.00	52.61
60.00	51.58
97.5	51.31
C=3.93x10^{-5}M	
0.17	72.01
0.38	71.44
0.56	71.32
1.09	70.97
5.00	68.31
11.30	61.70
21.30	58.96
59.00	55.45
101.00	54.47
C=1.12x10^{-5}M	
0.46	70.87
1.16	70.87
6.50	70.51
11.90	69.10
21.80	65.67
63.00	59.25
99.00	58.54
173.00	57.31

Table A-61 Dynamic Surface Tension of $(C_{10}N)_2Ar$ in 0.1N NaCl, at 25°C,

t (s) (bubble interval)	γ_t (mN/m)
C=1.27x10^{-4}M	
0.14	69.45
0.16	68.98
0.32	65.43
0.64	61.65
3.00	58.58
10.40	57.40
39.00	56.34
42.00	56.45
236.00	54.74
C=3.93x10^{-5}M	
0.15	72.00
0.28	71.25
1.00	68.98
2.05	67.44
3.80	65.43
6.90	63.07
25.30	61.30
44.00	60.59
70.00	59.70
205.00	59.41
C=1.12x10^{-5}M	
0.26	72.13
0.57	71.98
1.20	71.86
9.97	70.11
16.45	69.99
32.14	68.46
77.48	66.82
85.63	65.38
115.58	64.95

Table A-62 Dynamic Surface Tension of $(C_{12}N)_2Ar$ in H_2O at 25°C

t (s) (bubble interval)	γ_t (mN/m)
C = 6.64x10^{-4} M	
0.37	51.47
0.57	50.09
1.28	48.59
3.60	47.21
7.40	46.76
11.20	46.47
25.00	45.94
127.00	44.75

Table A-63 Dynamic Surface Tension of $(C_{12}N)_2Ar$ in H_2Oat 50°C

t (s) (bubble interval)	γ_t (mN/m)
C = 2.03x10^{-3} M	
0.63	40.70
1.93	40.39
4.30	40.25
9.00	40.31
9.30	40.02
12.60	39.93
21.00	40.62
67.50	40.39
C = 5.79x10^{-4} M	
2.90	49.47
5.60	49.09
12.00	48.32
27.00	47.94
67.50	47.18

C = 3.38x10^{-4} M	
20.20	54.42
36.00	54.05
99.00	53.67
102.00	53.28

Table A-64 Dynamic Surface Tension of $(C_{12}N)_2Ar$ in 0.1 N NaBr at 25°C

t (s) (bubble interval)	γ_t (mN/m)
C = 1.12x10^{-5} M	
1.04	71.89
3.30	71.79
11.10	71.77
139.50	70.87

Table A-65 Dynamic Surface Tension of $(C_{12}N)_2Ar$ in 0.1 N NaCl at 25°C

t (s) (bubble interval)	γ_t (mN/m)
C = 3.93x10^{-5} M	
0.16	71.89
0.21	71.44
0.35	70.85
0.66	69.25
1.74	67.41
2.70	64.39
5.70	55.80
15.50	49.00
45.00	45.59
73.00	44.07
131.00	42.90
244.00	42.49

C = 1.12x10^{-5} M	
0.21	72.24
0.41	72.22
0.95	72.10
7.60	70.69
19.00	68.11
28.00	61.66
57.00	54.08
111.00	50.70
181.00	49.64
C = 8.62x10^{-6} M	
1.05	71.92
2.50	71.56
3.60	71.48
4.00	71.16
9.00	70.40
16.00	70.78
26.83	63.94
40.00	59.76
44.00	59.00
60.00	54.83
66.00	53.68
74.00	52.92
164.00	49.69
420.00	48.36

Table A-66 Dynamic Surface Tension of $(C_{12}N)_2Ar$ in 0.1 N NaCl at 50°C

t (s) (bubble interval)	**γ_t (mN/m)**
C = 1.27x10^{-4} M	
0.14	64.27
0.17	62.86
0.21	58.50
0.40	50.87

0.43	50.35
0.74	45.24
1.17	43.20
1.93	41.84
4.80	40.67
26.00	39.38
84.00	38.67
86.00	38.67

Table A-67 Dynamic Surface Tension of $(C_{14}N)_2Ar$ in H_2O at 50°C

t (s) (bubble interval)	γ_t (mN/m)
C = $1.27x10^{-4}$M	
0.16	64.56
0.39	64.59
0.93	63.77
3.35	56.03
23.00	49.82
68.00	48.34

Table A-68 Dynamic Surface Tension of $(C_{16}N)_2Ar$ in H_2O at 25°C

t (s) (bubble interval)	γ_t (mN/m)
C = $6.35x10^{-5}$M	
0.18	71.25
0.21	71.37
0.64	71.52
30.00	71.58
177.00	70.25

Table A-69 Dynamic Surface Tension of $(C_{16}1N)_2Ar$ in H_2O at 50°C

t (s) (bubble interval)	γ_t (mN/m)
C = 6.35x10^{-4}M	
46.00	48.86
60.00	46.03
101.00	42.09
161.00	40.82
C = 1.27x10^{-4}M	
0.34	66.24
0.88	66.35
2.00	66.35
7.00	66.00
26.50	62.91
44.50	57.50
56.00	55.33
76.00	51.14
157.00	46.30
237.00	45.12
C = 2.44x10^{-5}M	
25.70	64.81
29.00	64.04
49.00	55.29
50.50	55.00
59.00	52.14
137.00	46.16
147.00	45.46
C = 1.27x10^{-5}M	
4.00	67.40
11.30	67.28
69.00	60.28
113.00	54.04
130.00	50.10

Table A-70 Dynamic Surface Tension of $(C_{16}N)_2Ar$ in 0.1 N NaCl at 25°C

t (s) (bubble interval)	γ_t (mN/m)
C = 6.35×10^{-5}M	
0.34	71.58
1.28	71.81
4.50	71.25
33.00	70.63
75.00	70.04
218.00	62.89
274.00	58.74
C = 1.12×10^{-5}M	
0.16	72.11
0.29	71.34
0.46	71.81
1.45	71.83
7.60	71.69
31.00	71.17
168.00	70.72

Table A-71 Dynamic Surface Tension of $(C_{16}N)_2Ar$ in 0.1 N NaCl at 50°C

t (s) (bubble interval)	γ_t (mN/m)
C = 1.27×10^{-4}M	
0.19	67.06
0.52	67.06
0.54	66.88
2.40	66.88
10.20	66.71
21.00	64.01
50.50	50.67
65.00	43.13
129.00	38.42
239.00	36.80

C = 6.35x10^{-5}M	
0.16	68.31
0.41	68.07
1.46	67.76
1.73	67.06
3.20	66.94
7.50	66.82
22.20	64.95
35.00	60.41
71.00	51.34
84.00	43.48
219.00	38.26
C = 5.90x10^{-5}M	
1.70	65.81
5.10	65.69
6.50	64.94
20.00	64.90
44.00	59.47

Table A-72 Dynamic Surface Tension of $(C_{18}N)_2Ar$ in 0.1 N NaCl at 50°C

t (s) (bubble interval)	γ_t (mN/m)
C = 1.27x10^{-4} M	
0.33	66.82
0.91	67.17
6.20	67.53
19.00	67.17
40.00	66.28
97.00	58.89
224.00	45.63
266.00	41.43

Table-73 Dynamic Surface Tension of $(C_{10}N)_2OH$ in 0.1 N NaCl at 25°C

t (s) (bubble interval)	γ_t (mN/m)
C = 5.00x10^{-4}M	
0.11	51.37
0.18	46.53
0.36	44.75
0.88	43.22
6.50	41.37
34.00	39.91
87.50	39.67
C = 1.27x10^{-4}M	
0.23	68.93
0.90	61.08
2.56	54.73
11.80	50.75
29.30	49.11
54.00	47.71
C = 3.93x10^{-5}M	
0.41	70.58
2.80	66.82
4.60	63.89
13.80	58.14
47.00	54.27
188.00	52.57
C = 1.12x10^{-5}M	
0.28	71.30
1.60	71.16
5.20	70.28
15.80	68.18
47.00	61.34
92.00	59.43
237.00	56.50

Table-74 Dynamic Surface Tension of $(C_{10}N)_2OH$ in 0.1 N NaCl at 25°C

t (s) (bubble interval)	γ_t (mN/m)
C = 5.00x10^{-4}M	
0.11	51.37
0.18	46.53
0.36	44.75
0.88	43.22
6.50	41.37
34.00	39.91
87.50	39.67
C = 1.27x10^{-4}M	
0.23	68.93
0.90	61.08
2.56	54.73
11.80	50.75
29.30	49.11
54.00	47.71
C = 3.93x10^{-5}M	
0.41	70.58
2.80	66.82
4.60	63.89
13.80	58.14
47.00	54.27
188.00	52.57
C = 1.12x10^{-5}M	
0.28	71.30
1.60	71.16
5.20	70.28
15.80	68.18
47.00	61.34
92.00	59.43
237.00	56.50

Table-75 Dynamic Surface Tension of $(C_{10}N)_2OH$ in 0.1 N NaCl at 25°C

t (s) (bubble interval)	γ_t (mN/m)
C = 5.00x10^{-4}M	
0.11	51.37
0.18	46.53
0.36	44.75
0.88	43.22
6.50	41.37
34.00	39.91
87.50	39.67
C = 1.27x10^{-4}M	
0.23	68.93
0.90	61.08
2.56	54.73
11.80	50.75
29.30	49.11
54.00	47.71
C = 3.93x10^{-5}M	
0.41	70.58
2.80	66.82
4.60	63.89
13.80	58.14
47.00	54.27
188.00	52.57
C = 1.12x10^{-5}M	
0.28	71.30
1.60	71.16
5.20	70.28
15.80	68.18
47.00	61.34
92.00	59.43
237.00	56.50

Table A-76 Dynamic Surface Tension of $(C_{14}N)_2OH$ in 0.1 N NaCl at 25°C

t (s) (bubble interval)	γ_t (mN/m)
C = 1.27x10^{-4}M	
0.15	71.51
0.21	71.22
0.45	70.99
2.00	71.16
4.00	71.02
24.80	70.17
45.00	63.74
73.00	55.84
81.00	47.74
C = 3.93x10^{-5}M	
0.15	71.51
0.26	70.85
0.27	71.12
0.80	71.40
1.03	71.44
17.00	71.20
76.00	70.25
104.00	68.26
108.00	64.71
128.00	57.60
C = 1.12x10^{-5}M	
0.16	71.57
0.17	71.37
0.18	71.16
0.33	71.20
1.39	71.98
3.10	71.90
21.80	71.83
107.00	71.10
274.00	58.49

Table A-77 Dynamic Surface Tension of $(C_{14}N)_2OH$ in 0.1 N NaCl at 50°C

t (s) (bubble interval)	γ_t (mN/m)
C = 1.27x10^{-4}M	
0.40	66.83
1.30	67.14
7.70	60.81
12.60	43.45
18.70	42.26
21.50	39.73
23.40	38.30
47.00	34.10
53.00	33.75

Table A-78 Dynamic Surface Tension of $(C_{16}N)_2OH$ in 0.1 N NaCl at 25°C

t (s) (bubble interval)	γ_t (mN/m)
C = 1.27x10^{-4}M	
0.15	71.19
0.18	70.52
2.34	70.62
6.20	71.51
27.00	71.63
124.00	71.21
C = 1.15x10^{-5} M	
0.18	69.45
0.40	71.25
0.90	71.44
3.20	71.79
33.00	71.43
190.00	71.20

Table A-79 Dynamic Surface Tension of $(C_{16}N)_2OH$ in 0.1 N NaCl at 50°C

t (s) (bubble interval)	γ_t (mN/m)
C = 2.52x10^{-4} M	
0.15	66.76
0.26	66.59
3.40	67.29
25.00	66.32
31.00	66.06
58.00	59.00
84.00	55.13
141.00	46.74
C = 2.52x10^{-4} M	
1.05	67.06
5.50	67.45
35.00	67.06
87.00	59.16
130.00	55.25
153.00	50.29

Table A-80 Melting Points of Synthesized Cationic Gemini Surfactants

Surfactant	Melting Point °C
$(C_{12}N)_2OH$	78~80
$(C_{14}N)_2OH$	84~85
$(C_{18}N)_2OH$	84~85
$(C_8N)_2Ar$	222~223
$(C_{10}N)_2Ar$	227~228
$(C_{12}N)_2Ar$	228~229
$(C_{14}N)_2Ar$	227~228
$(C_{16}N)_2Ar$	229~230
$(C_{18}N)_2Ar$	229~230

Bibliography:

(1) M. J. Rosen, "Surfactants and Interfacial Phenomena", 2nd Edn; Wiley, New York, (1989), (a) p.1; (b) p.66; (c) p.70; (d) p.34; (e) p.136; (f) p.398

(2) M. Okahara, A. Masuyama, Y. Sumida, Y. P. Zhu, J. Jpn. Oil Chem. Soc. (Yukagaku), 37, 746, (1988).

(3) Y. P. Zhu, A. Masuyama, M. Okahara, J. Amer. Oil Chem. Soc. , 67, 459, (1990).

(4) Y. P. Zhu, A. Masuyama, T. Nagata, M. Okahara, J. Jpn. Oil Chem. Soc. (Yukagaku), 40, 473, (1991).

(5) Y. P. Zhu, A. Masuyama, M. Okahara, J. Amer. Oil Chem. Soc. 68, 268, (1991).

(6) A. Masuyama, T. Hirono, Y. P. Zhu, M. Okahara, M. J. Rosen, J. Jpn. Oil Chem. Soc. (Yukagaku), 41, 301, (1992).

(7) Y. P. Zhu, A. Masuyama, Y. I. Kinito, M. Okahara, and M. J. Rosen, ibid, 37, 69, (1992).

(8) Y. P. Zhu, A. Masuyama, Y. Kirito, and M. Okahara, J. Amer. Oil Chem. Soc. , 68, 539, (1991).

(9) Y. P. Zhu, A. Masuyama, Y.Kirito, M.Okahara, and M. J. Rosen, J. Am. Oil Chem. Soc. 69, 626, (1992).

(10) Y. P. Zhu, A. Masuyama, Y. Kobata, Y. Nakatsuji, M. Okahara, and M. J. Rosen, J. Colloid Interface Sci. 158, 40, (1993).

(11) A. Masuyama, Y. Yocota, Y. P. Zhu, T.Kida, and Y. Nakatsuji, J. Chem. Soc. Commun. 1435, (1994).

(12) M. J. Rosen, Z. H. Zhu, and X. Y. Hua, J. Am. Oil Chem. Soc. 69, 30, (1992).

(13) F. Devinsky, I. Lacko, F. Bittererova, and L. Tomeckova, J. Colloid and Interface Sci. 114, 314, (1986).

(14) F. Devinsky, I. Lacko, and T. Imam, J. Colloid and Interface Sci. 143, 336, (1991).

(15) F. Devinsky, I. Lacko, and T. Imam, ACTA Facultaties Pharmaceuticae Tom, XLIV, 103, (1990).

(16) F. Devinsky and I. Lacko, Tenside Surf. Det. 27, 344 (1990).

(17) F. Devinsky, I. Lacko, F. Bittererova, and L. Tomeckova, J. Colloid and Interface Sci. 114, 314, (1986).

(18) R. Zana, M. Benrraou, and R. Rueff, Langmuir 7, 1072, (1991).

(19) F. Kern, F. Lequeux, R. Zana, and S. J. Candau, Langmuir 10, 1714, (1994).

(20) R. Zana and Y. Talmon, Nature 362, 228, (1993).

(21) S. Karaborni, K. Esselink, P. A. J. Hilbers, B. Smit, J. Karthauser, N. M. van Os, and R. Zana, Science 226, 254, (1994).

(22) D. Damino, Y. Talmon, H. Levy, G. Beinert, and R. Zana,

Science, 269, 1420, (1995).

(23) H. Diamant and D. Andelman, Langmuir, 10, 2910, (1994).

(24) F. M. Menger and C. A. Littau, J. Am. Chem. Soc. 115, 10083, (1993).

(25) F. M. Menger and C. A. Littau, J. Am. Chem. Soc. 113, 1451, (1991).

(26) M. J. Rosen, H. Z. Zhu, and T. Gao, J. Colloid Interface Sci. 157, 254, (1993).

(27) R. S. Gregorian, Text. Chem. Color., 19, 13, (1987).

(28) K. L. Mysels, Colloids and Surfaces, 43, 241, (1990).

(29) T. Gao and M. J. Rosen, J. Am. Oil Chem. Sci. 71, 771, (1994).

(30) J. W. Gibbs, The Collected Works of J. W. Gibbs, Longmans, Green, London, Vol. I. 119, (1928).

(31) M. J. Rosen and S. Aronson, Colloids Surf. 3, 201, (1981).

(32) P. Debye and E. Hüchkle, Phys. Z. 24, 185, (1923).

(33) H. B. Klevens, J. Am. Oil Chem. Sci. 30, 74, (1953).

(34) B. Lindman, "Structural Aspects of Surfactant Micellar System", in "Surfactants", Ed. by Th. F. Tadros, Academic Press, (1983), p.90,

(35) P. Mukerjee, Adv. Colloid Interface Sci. 1, 241, (1967).

(36) T. Nakagaki and N. Handa in "Structure/Performance Relationships in Surfactants", Ed. by M. J. Rosen, ACS symp.

series 253, Amer. Chem. Soc., Washington, D. C. (1984), p. 78

(37) D. N. Rubingh in "Solution Chemistry of Surfactant Solutions", K. L. Mittal, Ed., Plenum, New York, 1979, Vol. I, p.337.

(38) M. J. Rosen and X. Y. Hua, J. Colloid Interface Sci. 86, 164, (1982).

(39) A. F. H. Ward and L. Tordai, J. Chem. Phys. 14, 453, (1946).

(40) P. Joos, J. P. Fang, and G. Serrien, J. Colloid and Interface Sci. 151, 180, (1992).

(41) P. Joos, J. P. Fang, and G. Serrien, J. Colloid Interface Sci. 151, 144, (1992).

(42) F. Ravera, L. Liggieri, and A. Steinchen, J. Colloid Interface Sci. 156, 109, (1993).

(43) X. Y. Hua and M. J. Rosen, J. Colloid and Interface Sci. 124, 652, (1988).

(44) T. Gao and M. J. Rosen, J. Colloid Interface Sci. 172, 242, (1995).

(45) J. T. Davies and E. K. Rideal, in "Interfacial Phenomena", 2nd. edn., Academic Press, New York, (1963), p.230.

(46) X. Y. Hua and M. J. Rosen, J. Colloid Interface Sci. 141, 180, (1991).

(47) P. S. de Laplace, "Mechanique Celeste", Supplement to Book 10, (1806).

(48) E. H. Crook, D. B. Fordyce, and G. F. Trebbi, J. Phys. Chem. 67, 1987, (1963).

(49) M. J. Rosen, Chemtech 23, 30, (1993).

(50) Y. S. Lee and K. W. Woo, J. Colloid Interface Sci. 169, 34, (1995).

(51) U. R. K.Rao, C. Manohar, B. S. Valaulikar, and R. M. Iyer, J. Phys. Chem. 97, 3286, (1987).

(52) C. Treiner and A. Makayssi, Langmuir, 8, 794, (1992).

(53) J. F. Rathman, Langmuir, 6, 391, (1990).

(54) E. S. Lower, Soap, Perf. Cosmet, 33:1201, 1313, (1960.).

(55) M. J. Rosen, T. Gao, Y. Nakatsuji and A. Masuyama, Colloids Surfaces A: Phys. Chem. Eng. Aspects, 88, 1, (1994).

(56) M. J. Rosen and X. Y. Hua, J. Amer. Oil Chem. Sci. 86, 582, (1982).

(57) M. J. Rosen and F. J. Zhao, J. Colloid Interface. Sci. 95, 443, (1983).

(58) M. J. Rosen and B. Y. Zhu, J. Colloid Interface. Sci. 99, 427, (1984).

(59) B. Y. Zhu and M. J. Rosen, J. Colloid Interface. Sci. 99, 435, (1984).

(60) M. J. Rosen and D. J. Murphy, J. Colloid Interface. Sci. 110, 224, (1986).

(61) X. Y. Hua and M. J. Rosen, J. Colloid Interface Sci. 141, No.1, 180, (1991).

(62) L. Liu and M. J. Rosen J. Colloid Interface Sci. in press.

(63) I. Levine, "Physical Chemistry", 4th edn., McGraw-Hill Inc. (1995), p.469.

(64) M. Konche, H. Tamura, and M. J. Bukovac, J. Ag. FoodChem. 39, 202, (1991).

(65) J. A. Zabkiewicz and R. E. Gaskin, in "Adjuvants and Agrochemicals", Vol. I: Model of Action and Physiological Activity; N. P. Chow, C. A. Grant, A. M. Hinshalwood, E. Simundsson, CRC Press: Boca Raton. FL, (1989), p142.

(66) A. W. Adamson, "Physical Chemistry of Surfaces", 5th edn., John Wiley & Sons, Inc. (1990), p494.

(67) C. Z. Draves and Am. Dyestuff Rep. 28, 425, (1939).

(68) K. P. Ananthapadmanabhan, E. D. Goddard, and P. Chandar, Colloids Surfaces, 44, 281, (1990).

(69) E. Kissa, "Fluorinated Surfactants", Marcel Dekker, Inc. New York, (1993), p.2.

(70) N. H. Anderson, D. J. Hall, Adjuvants Agrochem. 2, 51, (1989).

(71) Z. Lin, M. He, H. T. Davis, L. E. Scriven, and S. A. Snow, J. Phys. Chem. 97, 3571, (1993).

(72) M. He, R. M. Hill, Z. Lin, H. T. Davis, and L. E. Scriven, J. Phys. Chem. 97, 8820, (1993).

(73) Z. Lin, R. M. Hill, H. T. Davis, and M. D. Ward, Langmuir, 10, 4060, (1994).

(74) S. Zhu, W. G. Miller, L. E. Scriven, and H. T. Davis, Colloids Surfaces A, Physicochem. & Eng. Aspects 63-78, (1994).

(75) H. W. Fox and W. A. Zisman, J. Colloid Sci. 5, 514, (1950).

(76) W. A. Zisman, Advances in Chemistry, No. 43, American Chemical Society, Washington, DC. (1964).

(77) E. F. Hane, E. G. Shafrin, and W. A. Zisman, J. Phys. Chem. 58, 236, (1954).

(78) T. Young, Miscellaneous Works, Vol. 1, G. Peacock, Ed., Murray, London, (1855), p.418.

(79) C. Z. Draves and R. G. Clarkson, Amer. Dyest. Rep. 20:20, (1931).

(80) M. J. Rosen and Z. H. Zhu, J. Amer. Oil Chem. Soc. 70, 65, (1993).

(81) N. M. van Os, J. R. Haak, and L. A. M. Rupert, in "Physical-Chemical Properties of Selected Anionic, Cationic, and Nonionic Surfactants" Elsevier, (1993), p111.

(82) E. Matijevic and B. A. Pethica, Trans. Faraday Soc. 54, 1382, 1390, 1400 (1958).